Influence of Al Foil Layers on Thermal Conductivity and Flexural Strength of Glass Fiber Core VIPs

Nie Lili, Chen Zhaofeng*

Super Insulation Composite Laboratory, College of Materials Science and Technology,
Nanjing University of Aeronautics and Astronautics, Nanjing, 210016, P. R. China

Abstract

Vacuum insulation panels (VIPs) are regarded as the most promising high-performance thermal insulation products on the market today. A high and stable vacuum state within VIP enclosure provides a durable service life for VIP. Its core is typically made of laminated glass fiber (GF) due to its low thermal conductivity, high modulus, high toughness, light weight and non-combustible property. However, fiber-bridging significantly exist under the low-pressure condition inside VIP, resulting in solid heat conduction intensified between the layers. Also, the VIP with pure GF core is comparatively soft. In this paper, aluminum foils were orderly arranged in 30 cascading layers of GF core, 10 different new structural VIPs with "1－10GF＋1Al" were got to compare with the pure 30GF core VIP. The influence of different layers of Al foil on the thermal conductivity and flexural strength of VIPs were discussed. Thermal conductivities of the as-prepared VIPs with proportion of 490mm×210mm were evaluated by the heat flow meter thermal conductivity instrumentation Netzsch HFM 436. Flexural strength was compared between the different samples by electronic universal testing machine. Results showed that Al foil layers laminated in the core can make a contribution to the flexural strength of VIP. The thermal conductivity of the pure 30GF core VIP was 2.278 mW/(m·K), while the data of "1－8GF＋1Al" structure were higher than 2.278 mW/(m·K). The thermal conductivity of "9GF＋Al" and "10GF＋Al" structure were 2.330 mW/(m·K) and 2.146 mW/(m·K) respectively. Theoretical and experimental analysis showed that the optimum layers of Al foil for 30GF core are 2, and the structure is "10GF＋1Al".

Keywords VIP, glass fiber, Al foil, thermal conductivity, flexural strength

1. Introduction

Vacuum insulation panels (VIP) are regarded as one of the most upcoming high performance thermal insulation solutions. At delivery, thermal conductivity for a VIP can be as low as 0.002～0.004 W/(m·K) depending on the core material[1]. The purpose of the core material is to provide the VIP's insulating and mechanical properties. Hence, there is a lot of focus on the core material, as this is important for a VIP to attain the highest possible thermal resistance. To optimize the conditions of the VIPs, the core needs to fulfil certain requirements. These are described in a comprehensive review by Baetens et al. [2]. Several different materials are being tested for use as core materials in VIPs, such as fiber-powder composites [3], polycarbonates [4], phenolic foam [5] and ultrafine glass fibers [6]. Different core materials have different advantages and drawbacks.

The laminated glass fiber (GF) is a typical core material of VIP developed in Asia due to its low thermal conductivity, high modulus, high toughness, light weight and non-combustible property. However, fiber-bridging significantly exist under the low-pressure condition inside VIP, resulting in solid heat conduction intensified between the layers. Also, the VIP with pure GF core is comparatively soft. In this paper, aluminum foil were orderly arranged in 30 cascading layers of GF

* Corresponding author, Tel: 86－25－52112909, E-mail: zhaofeng_chen@163.com

core, 10 different new structural VIPs with "1—10GF+1Al" were got to compare with the pure 30GF core VIP. The influence of different layers of Al foil on the thermal conductivity and flexural strength of VIPs were discussed to obtain the optimum layers of Al foil in 30GF core material. These provide a new way of improving the VIP's flexural strength and heat-insulating property, resulting in a great significance for exploiting the use level and application market of glass fiber core VIPs.

2. Experimental details

Raw materials, including core materials, aluminum foils, envelope materials and getters used in this study were provided by Suzhou V. I. P. New Material Co., Ltd. (Taicang City, P. R. China). Glass fiber core material layers with dimensions of 490mm×210mm×0.4mm were fabricated by wet method. The wet method included the following steps: ①Providing slurry of glass fibers; ②Dewatering the slurry to form a wet-laid mat; ③Drying the mat; ④Cutting the mat to form the finished glass fiber core material layers [7,8]. VIP core materials were made up of 30 pieces of as-prepared glass fiber core material layers and aluminum foils with dimensions of 490mm × 210mm × 0.007mm were orderly added in the 30 cascading GF layers.

The layered core material samples were dried at 150℃ for 1 hour. VIPs with core materials which were structured at different layered conditions (In Tab. 1) were produced after the same vacuum process. The barrier membrane with one side aluminum foil and the other side aluminum plating film were used. The used getter was smart combo getter from Italy SAES Company. The initial thermal conductivities of VIP samples were evaluated by EKO thermal conductivity detector HC - 120 quickly. And the accurate measurements of thermal conductivities were evaluated by the heat flow meter thermal conductivity instrumentation Netzsch HFM 436.

Flexural strength was compared between the different samples by electronic universal testing machine CTM 2200, according to GB/T 1456—2005 standard [9]. Flexural strength tests were carried out using rectangular samples with proportion of 490mm × 210mm, while the span and velocity of the machine grips were 490 mm and 2 mm/min, respectively. Surface morphology of the core materials was observed by scanning electron microscopy (SEM, Model SU8010).

Tab. 1 VIPs with core materials which were structured at different layered conditions

Sample No.	Structural Units	Total GF layers	Total Al layers
1	Pure GF	30	0
2	10GF+1Al	30	2
3	9GF+1Al	30	3
4	8GF+1Al	30	3
5	7GF+1Al	30	4
6	6GF+1Al	30	4
7	5GF+1Al	30	5
8	4GF+1Al	30	7
9	3GF+1Al	30	9
10	2GF+1Al	30	14
11	1GF+1Al	30	29

3. Results and discussions

3.1 Experimental results of thermal conductivity

The EKO thermal conductivity detector HC-120 was used to quickly eliminate the nonconforming products. Then, the thermal conductivities of effective samples 1～11 were evaluated and the data were shown in Fig. 1. Sample 1 represents the pure 30GF core VIP, its initial thermal conductivity tested 3 days after production was 2.278mW/(m·K). The data of sample 3, 5～11 were much larger, which were 2.330mW/(m·K), 2.340mW/(m·K), 2.343mW/(m·K), 2.409mW/(m·K), 2.667mW/(m·K), 2.589mW/(m·K), 2.864mW/(m·K) and 3.908mW/(m·K), respectively. While sample 2 with the structural unit "10GF + 1Al" had the lowest thermal conductivity 2.146mW/(m·K), sample 4 with the structural unit "8GF + 1Al" second, its thermal conductivity was 2.283 mW/(m·K). The curve of the test data 25 days after production demonstrated the same trend.

Centre of panel thermal conductivity (λ_{cop} of a VIP core) is a summation of the solid conductivity, gaseous conductivity and radiative conductivity and can be expressed using Eq. (1) [10].

$$\lambda_{cop}=\lambda_S+\lambda_R+\lambda_G+\lambda_{coup} \quad (1)$$

Where λ_S is the solid thermal conductivity, λ_R is the

radiative thermal conductivity and λ_G is the gaseous conductivity. Here λ_{coup} is the thermal conductivity caused by a complex interaction between gas and laminated construction in the composite. This term, λ_{coup} rises exponentially at higher pressures. However, at low pressure this term can be negligible. Solid conduction takes place through the structure of core material where heat is transmitted through the physical contact of fibers of core material. Solid conductivity is a material property and its value depends upon material structure, density and external pressure on the core. Materials with low density are preferred for achieving low solid conduction. Thermal conductivity in VIP core can be lowered by restricting the gaseous and radiative conductivities [11].

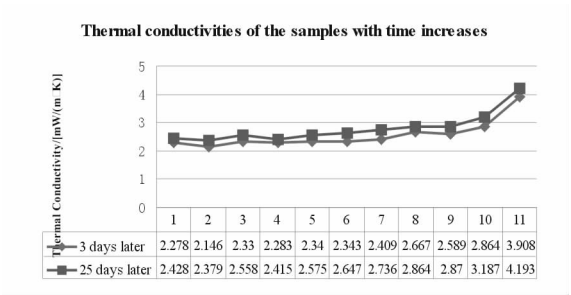

Fig. 1 Thermal conductivities of the 1～11 samples evaluated at 3 days and 25 days after production

Glass fiber, owing to its very small aperture size and low bulk density has a low solid conduction, but suffers from a lower resistance to radiative heat transfer. Aluminum foil can be added effectively to restrict the gaseous and radiative conductivities. Nonetheless, caution has to be exercised when using aluminum as these typically have high solid thermal conductivity which means higher content of aluminum will lead to a higher solid thermal conductivity offsetting any benefit it provides by reducing the radiative conductivity; on the other hand, an insufficient amount of aluminum in a VIP core will lead to a higher radiative conductivity. Hence, an optimum mass proportion of a given aluminum needs to be identified to achieve a minimum radiative conductivity in VIP cores. Experimental results showed that the optimum layers of Al foil for 30GF core are 2, and the structural unit is "10GF+1Al".

3.2 Microstructure and microstructural model of core material

The properties of VIP core material are closely related to their structure, which depends on the preparation method, the microstructure, chemical composition, and the phase of VIP core materials [12]. The SEM micrographs of VIP core material were shown in Fig. 2. As seen in Fig. 2(a), fiberglassVIP core material consisted of a mass of randomly oriented, super-cooled glossy fibers of varying lengths and diameters. The average diameter of the fiberglass was about 2～6 mm [13]. As shown in Fig. 2(b), the VIP core material was made up of continuous fiber layers which were parallel to each other. These horizontally oriented fiber layer faces were perpendicular to the direction of heat flux. Thus, the thermal conductivity of VIP core material could decrease [14, 15].

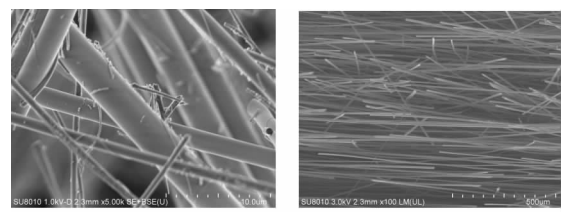

Fig. 2 SEM micrograph of VIP core materials

(a) Fibers of varying lengths and diameters;

(b) Horizontal oriented fiber layers

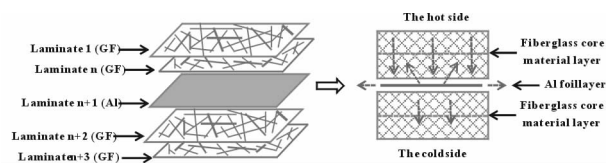

Fig. 3 Microstructural model of laminated core material

Fig. 3 shows the microstructural model of core material. Each core material layers consisted of continuous parallel fibers and aluminum foil laminates. The real morphology of core material could be described by a simplified model [16], i. e., multiphase medium model [17]. Representative elemental volume [18, 19] in the model at microscopic level consisted of solid phase (i. e. glass fibers), gas phase (i. e. air, water vapor and other gases), and impurity phase (small water droplets and specially introduced additions). Gas phase filled in the voids among solid phases while the impurity phase

attached to the surface of solid phase.

Aluminum foils have low emissivity and density, commonly used as the reflector screen in multi-layer insulation and outer protective structure for thermal insulation. Hence, adding aluminum foil laminates artificially to block vertical thermal bridge is an effective way to restrict the gaseous and radiative conductivities between GF layers. But the laminates are not the more the better, there are an optimum laminates of Al foil in the core as mentioned in 3.1. This is because vacuum resistance and solid thermal conductivity increases with the layer and density, resulting in an increase in thermal conductivity of residual gas.

3.3 Measured results of flexural strength

According to the charts, the flexure strength of sample 1, 2 and 11 is 3MPa, 3MPa and 4MPa, respectively. As shown in Fig. 4 (a), the bending force increases gradually with displacement, the resistance distribution is relatively uniform, and is consistent with the structure characteristics of pure glass fiber core material. Two obvious turning points (tag in red circle) can be found in the force-displacement curve of Fig. 4 (b), each turn represents the resistance of aluminum foil layer, which is also consistent with the structural characteristic of "10GF + 1Al" sample. Due to the alternating layers of aluminum foil and glass fiber, there are a lot of twists and turns in the curve of Fig. 4(c), the first turn (tag in red circle) represents the resistance of the VIP's barrier membrane. These suggest that the core material of aluminum foil may increase the bending strength of VIP.

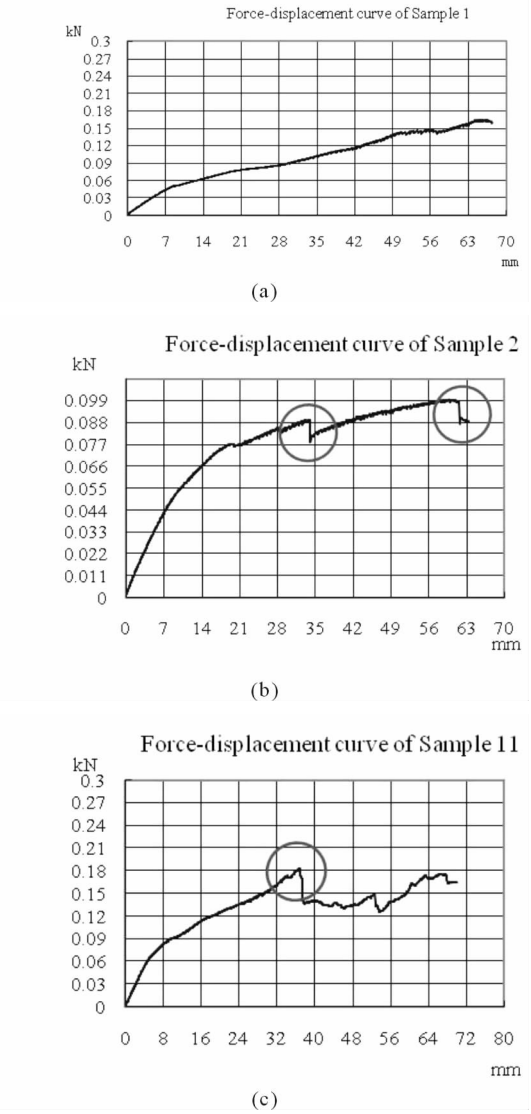

Fig. 4 Force-displacement curve of sample 1, 2 and 11

(a) Force-displacement curve of Sample 1;

(b) Force-displacement curve of Sample 2;

(c) Force-displacement curve of Sample 11

4. Conclusions and outlook

Al foil layers properly laminated in the core can make a contribution to the insulating performance and flexural strength of VIP. To balance solid, residual gas and heat conductivity, there is an optimum number of laminates of Al foil in the core, for instance, the optimum Al layers for 30GF core are 2, and the structure is "10GF+1Al". This provides a new way to increase the stiffness and the service life of GF core VIP, further promoting GF VIPs' application in the top field like aerospace and navigation.

Acknowledgements

The authors would like to express their gratitude to the Suzhou V. I. P. New Material Co., Ltd. for the facilities provided during the experiments and all their valuable support. This work was carried out with the scientific research innovation projects for ordinary university graduate students in Jiangsu Province (No. SJLX_0126) and the Jiangsu Project BA2013097 and National Project 2015DFI53000.

References

[1] Kalnæs, S. E. and B. P. Jelle. Vacuum insulation panel products: A state-of-the-art review and future research

pathways. Applied Energy, 116(2014):355 - 375.

[2] Baetens R, Jelle BP, Thue JV, et al. Vacuum insulation panels for building applications: a review and beyond. Energy Build, 42 (2010):147 - 72.

[3] Mukhopadhyaya P, Kumaran K, Normandin N, et al. fiber-powdercomposite as core material for vacuum insulation panels. In: Proceedings of the 9th international vacuum insulation symposium (IVIS - 2009), London, UK; 17 - 18 September, 2009.

[4] Kwon JS, Jung H, Yeo IS, et al. Outgassing characteristics of a polycarbonatecore material for vacuum insulation panels. Vacuum, 85 (2011):839 - 46.

[5] Kim J, Lee JH, Song TH. Vacuum insulation properties of phenolic foam. International Journal of Heat and Mass Transfer55 (2012):5343 - 5349.

[6] Di X, Gao Y, Bao C, Hu Y, et al. Optimization of glass fiber based core materialsfor vacuum insulation panels with laminated aluminum foils as envelopes. Vacuum, 97 (2013):55 - 59.

[7] Takeuchi N, Okada K, Konishi T. Wet process for manufacturing nonwovenfabric and apparatus therefor. United States Patent, US006058583A,1999.

[8] Helwig, GS, Hendrik J, Paul G. Wet-laid nonwoven mat and a process formaking same. United States Patent, US006267843B1,1998.

[9] GB/T1456 - 2005. Test method for flexural properties of sand wich constructions. China:The People's Republic of China's National Standardization Management Committee, 2005.

[10] J. Fricke, Materials research for the optimization of thermal insulations. HighTemperatures-High Pressures, 25 (1993): 379 - 390.

[11] M. Alam, H. Singh, S. Brunner, et al. Experimental characterization and evaluation of the thermo-physicalproperties of expanded perlite — Fumed silica composite for effectivevacuum insulation panel (VIP) core. Energy and Buildings, 69 (2014): 442 - 450.

[12] Mroginski, J. L., Rado, H. A. D., Beneyto, P. A., et al. A finiteelement approach for multiphase fluid flow in porous media. Mathematics and Computers in Simulation, 81 (2010): 76 - 91.

[13] Cheng-Dong Li,Zhao-Feng Chen, Fred Edmond Boafo, et al. Determination of Optimum Drying Condition of VIPCore Material by Wet Method. Technology: An International Journal, 31(2013): 1084 - 1090.

[14] Veiseh, S., Hakkaki-Fard, A., Kowsary, F. Determination of the airfiber conductivity of mineral wool insulations in building applicationsusing nonlinear estimation methods. Journal of Building Physics, 32 (2009): 243 - 260.

[15] Lei, L. X., Jing, S.; Walton, R. I., Xin, X. Q., et al. Investigation ofthe solid state reaction of Fe $SO_4 \cdot 7H_2O$ with 1, 10 - phenanthroline. Journal of the Chemical Society, Dalton Transactions 2002: 3471 - 3476.

[16] Wang ZC, Kan AK. The applications of vacuum drying technology in the VIPcore material' pre-treatment. Advanced Materials Research, 472 - 475 (2012):649 - 652.

[17] Cheng-Dong Li, Zheng-CaiDuan, Qing Chen, et al. The effect of drying condition of glassfiber core material on the thermalconductivity of vacuum insulation panel. Materials and Design, 50 (2013): 1030 - 1037.

[18] Leskovšek U, Medved S. Heat and moisture transfer in fibrous thermalinsulation with tight boundaries and a dynamical boundary temperature. International Journal of Heat and Mass Transfer, 54(2011):4333 - 4340.

[19] Zhao SY, Zhang BM, Du SY. An inverse analysis to determine conductive andradiative properties of a fibrous medium. Journal of Quantitative Spectroscopy and Radiative Transfer,110(2009):1111 - 1123.

Effect of the Number of Core Material Layers on the Interior Pressure and Thermal Conductivity of Glass Fiber Vacuum Insulation Panel

Li Chengdong, Chen Zhaofeng*, Guan Shengnan

Super Insulation Composites Laboratory, College of Materials Science and Technology, Nanjing University of Aeronautics and Astronautics, Nanjing, 210016, P. R. China

Abstract

Compared with other types of vacuum insulation panels (VIPs), glass fiber VIPs (GF - VIPs) have better initial thermal insulating properties and lower price but need a higher vacuum to ensure their durable service life. In this paper, the core materials for GF - VIPs were made up of 8, 16, 24 and 32 pieces of 1mm-thickness core material layers (CMLs). The microstructure and compression ratio of each core material was recorded. The interior pressure of the as-prepared GF - VIPs possessing 8 pieces of CMLs rose rapidly from initial 6.1 Pa to 10.2 Pa in 10.5 hours while that possessing 16 and 24 pieces of CMLs almost grew linearly from original 1.4 Pa to 10.2 Pa in 120 hours and from incipient 1.3 Pa to 10.4 Pa in 409 hours, respectively. Conversely, GF - VIPs possessing 32 pieces of CMLs had an excellent pressure holding ability, having maintained at a low interior pressure of less than 5 Pa for 300 hours. Thermal conductivity of GF - VIPs with 8 pieces of CMLs was at among the highest while that of GF - VIPs with 16, 24 and 32 pieces of CMLs increased with the thickness of the core. In order to obtain high-quality GF - VIPs with long-term service life and low thermal conductivity, the number of CMLs in a GF - VIP should be between 16 and 32.

Keywords vacuum insulation panel, core material layers, interior pressure, thermal conductivity

1. Introduction

In recent decades, energy-saving technology has been widely investigated in order to mitigate climate change triggered by the increase of CO_2 emissions [1]. A superior thermal insulation system called vacuum insulation panels (VIPs), which have about 5 to 10 times higher thermal resistance than the conventional insulators such as polystyrene or polyurethane foams, provides alternative solution for the worldwide problem [2]. Compared with other types of VIPs such as fumed silica VIPs, glass fiber VIPs (GF - VIPs) exhibits a distinguished low thermal conductivity of less than 0.004 W/(m · K) and become an ideal thermal insulation materials in refrigeration and cryogenics [3, 4].

Generally speaking, the core material for GF - VIPs (GF - CM) consist of several or dozens of parallel glass fiber core material layers (CMLs). It was reported that the thermal conductivity of GF - VIPs greatly increases with the interior pressure when the interior pressure is higher than 10Pa. An extremely low and stable interior pressure of less than 100Pa is the prerequisite for high-quality GF - VIPs with low thermal conductivity. Due to the specific characteristics of the GF - CM, both the structures of the overlay core material and the single CML affects the thermal insulation properties of the GF - VIPs. Kim et al. [5] studied the relationship between pore size of GF - CM and density and the thermal insulation performance of GF - VIPs under variable pressing load and vacuum level. Di et al. [6] investigated the dependence of thermal conductivity of two different types of GF - VIPs on gas pressure theoretically and experimentally while Li

* Corresponding author, Tel: 86 - 25 - 52112909, Fax: 86 - 25 - 52112626, E-mail: zhaofeng_chen@163.com

et al. [7] explored the mass transfer within GF－VIP enclosure in a vacuum and the influence of pressure holding time of extraction process on thermal conductivity of the GF－VIPs. Although vacuum-pumping system can reduce the interior pressure within VIP enclosure to a minimum, it is difficult to achieve a high vacuum between all layers in the GF－CM [8]. Moreover, the gases in the surrounding environment may slowly permeate into the GF－VIPs, resulting in an increase in interior pressure of GF－VIPs. The gases within VIP enclosure may desorb on the warm side and adsorb on the cool side in the closed system and aid on an increase in thermal conductivity of the GF－VIPs. Glass fibers may function as a wick and block the movement of the gases within VIPs and thus suppress the thermal conductivity. However, to the best of the authors' knowledge, few literatures analyzed the dependence of thermal conductivity of GF－VIPs on the microstructure of core material. Again, there are few literatures that have analyzed the effect of the number of CMLs on the thermal conductivity of GF－VIPs.

In this paper, the GF－CMs were composed of different numbers of CMLs. The cross-sectional morphologies, pore parameters and compression ratios of the GF－CMs were investigated. The changes in the interior pressure of GF－VIPs with time were recorded and the thermal conductivity of each GF－VIP was compared. The aim of this paper is to obtain a high-vacuum-state and long-term GF－VIPs.

2. Experimental

Raw materials, including GF－CMs, envelope materials and getters used in this study were provided by Suzhou V. I. P. New Material Co., Ltd. (Taicang, P. R. China). Among them, GF－CMs, consisting of 70% centrifuged glass wool and 30% flame attenuated glass wool, were produced by wet method (described in Ref. [7]). The length, width, and thickness of each CMLs was 410mm, 290mm, and 1mm, respectively. The GF－CMs were composed of 8, 16, 24 and 32 pieces of 1mm-thickness CMLs. The envelope materials were made up of four layered film with an overall thickness of 95 μm, i.e., polyamide film (PA, 15μm), polyethylene terephthalate film (PET, 12μm), aluminum film (Al, 7 μm) and polyethylene film (PE, 55 μm). Firstly, the GF－CMs were dried at 150℃ for 60 mins, and then bagged in envelope materials. Afterwards, the GF－VIPs were produced by vacuum process.

The cross-sectional morphologies and the pore parameters of GF－CMs were analyzed by scanning electron microscopy (SEM, JEOL JSM－6360) and mercury injection apparatus (AutoPore IV 9510), respectively. The as-prepared GF－VIPs were placed in a closed room at 35℃ and 37% R. H. The interior pressure and thermal conductivity of each GF－VIP were measured by convection vacuum gauges (CVM201 Super Bee TM) and heat flow meter (Netzsch HFM 436), respectively.

3. Results and discussion

3.1 Microstructure

Fig. 1 shows the cross-sectional morphology of the GF－CMs. At the macroscopic level (see Fig. 1(a)), the GF－CM was made up of continuous CMLs which were parallel and in contact with each other. The CMLs were flat, thin, rough, and flexible, but could not be coiled beyond a certain limit because of low strength. There was nearly a straight small space called "interlayer interface" between two CMLs. At the microscopic level (see Fig. 1(b)), each CML possesses a stable structure. Glass fibers within each CML were randomly oriented. There were also some parallel micro-spaces called "interlaminate interface" existing in each CML. Actually, each CML was touched at isolated microcontacts which were interspersed with gaps; and the real contact area between two CMLs was the sum of these microcontacts. The limited number and size of the microcontacts resulted in an actual contact area which was significantly smaller than the apparent contact area.

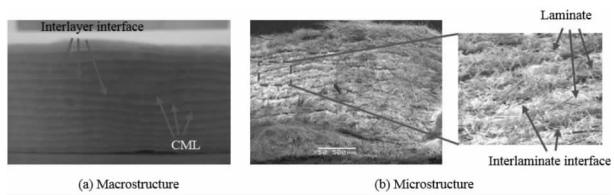

Fig. 1 Cross-sectional morphology of the GF－CMs

Fig. 2 shows the pore diameter distribution of the CMLs. Most of pores diameter concentrated between

5 μm and 30μm while only a small amount of macro pores of over 50 μm existed in the CMLs. Tab. 1 shows the pore parameters and bulk density of the CMLs. The total pore area, average pore diameter, porosity, and bulk density of the CML were 1.446 m^2/g, 20.2211 μm, 87.858 4%, and 120.2 kg/m^3, respectively, while the total intrusion volume was 7.311 5 mL/g. The low density (120.2 kg/m^3) of the CML implied that the fibrous network delicately provided limited pathways for solid-to-solid thermal conduction in the GF－CM.

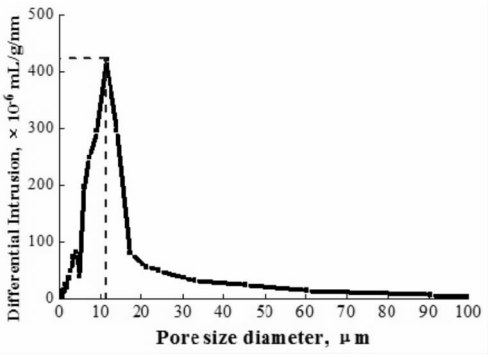

Fig. 2 Pore diameter distribution of the CMLs

3.2 Changes in interior pressure with time

The thermal conductivity of GF－VIPs remains at a low and stable value when the interior pressure of the GF－VIP is lower than 10Pa while that increases exponentially when the interior pressure of the GF－VIP is higher than 100 Pa [9]. Hence, in order to behave best in the thermal insulation performance, the interior pressure of GF－VIPs should be strictly controlled below 10 Pa. Fig. 3 shows the development of interior pressure of GF－VIPs with time. The interior pressure of the as-prepared GF－VIPs possessing 8 pieces of CMLs rose rapidly from initial 6.1 Pa to 10.2 Pa in 10.5 hours while that possessing 16 and 24 pieces of CMLs almost grew linearly from original 1.4 Pa to 10.2 Pa in 120 hours and from incipient 1.3 Pa to 10.4 Pa in 409 hours, respectively. Conversely, GF－VIPs possessing 32 pieces of CMLs had an excellent pressure holding ability, having maintained at a low interior pressure of less than 5 Pa for 300 hours. Therefore, GF－VIPs with more pieces of CMLs had better holding capacity in the interior pressure.

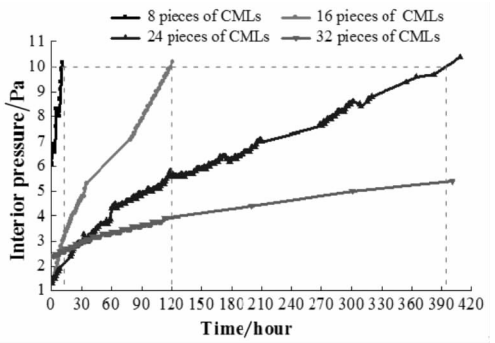

Fig. 3 Development of interior pressure of GF－VIPs with time

3.3 Compression ratio of GF－CMs

As glass wool was highly porous and soft, they could be easily deformed when pressing load was exerted. The thickness of the GF－CM achieved a stable value after vacuum process as a stable atmospheric pressure was loaded on the surface of the GF－VIP. The compression ratio of the GF－CMs ω could be described as following relation:

$$\omega = \frac{d_0 - d_1}{d_0} \tag{1}$$

where d_0 and d_1 are the thickness of GF－CM before and after vacuum process, respectively. Tab. 1 shows the thickness and compression ratio of GF－CM. All of the thickness of the GF－CM reduced greatly after vacuum process. The ω reached a maximum of 39.9% when the GF－CM was composed of 8 pieces of CMLs and decreased with the number of CMLs.

Tab. 1 Thickness and compression ratio of GF－CM

Number of CMLs	Thickness before vacuum process/mm	Thickness after vacuum process/mm	Compresion ratio/(%)
8	8	4.81	39.9
16	16	10.20	36.3
24	24	16.64	30.7
32	32	22.83	28.7

3.4 Thermal conductivity of GF－VIPs

Fig. 4 shows the thermal conductivity of GF－VIPs possessing 8, 16, 24 and 32 pieces of CMLs with different interior pressure. The thermal conductivity of GF－VIPs possessing 8, 16, 24 and 32 pieces of CMLs was marked as λ_1, λ_2, λ_3 and λ_4, respectively. It was observed that the thermal conductivity of the GF－VIPs slightly increased with increasing interior pressure.

Moreover, at the same interior pressure, thermal conduction of GF – VIPs slightly increased with the number of CMLs except for the one with 8 pieces of CMLs (always maximum), i. e. , $\lambda_2 < \lambda_3 < \lambda_4 < \lambda_1$.

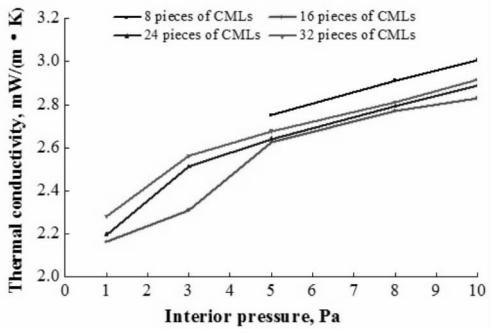

Fig. 4 Thermal conductivity of GF – VIPs possessing 8, 16, 24 and 32 pieces of CMLs with different interior pressure

Fig. 5 shows the heat flow transfer mechanism for vacuum-evacuated fibrous materials. The fiber-to-fiber solid thermal conduction took up the great mass of heat transfer through the GF – CMs and was greatly affected by the solid volume fraction (SVF), fiber diameter (FD), and fibers' through-plane orientations (FTO) [10, 11]. Although there is no difference in the SVF, FD and FTO among CMLs, the internal microstructures of the GF – CM were different due to the difference in the compression ratio of the GF – CM. A mass of glass fibers was planished under the pressing load of 1 atmosphere and arranged in different behavior compared with the status without pressing load. Compared with GF – CMs with low compression ratio, the fibers parallelism for GF – CMs with high compression ratio was higher. And the heat transfer path for the GF – CMs with high compression ratio was much longer than that with low compression ratio. The heat flow path for GF – CMs with high compression ratio thus extended. As a result, fiber-to-fiber solid thermal conduction decreased. At the same interior pressure of less than 10 Pa, the contribution from the gas was the same. Therefore, $\lambda_2 < \lambda_3 < \lambda_4$. The reason for the thermal conductivity of GF – VIPs with 8 pieces of CMLs was that the movement of gases, which coustituted the maximum within the VIP enclosure, was not sufficiently restricted due to too few numbers of CMLs. The residual gases might flow relative freely through the edge of the GF – CM and thus the gas thermal conductivity increased. In order to obtain high-quality GF – VIPs with long-term service life and low thermal conductivity, the number of CMLs in a GF – VIP should be between 16 and 32.

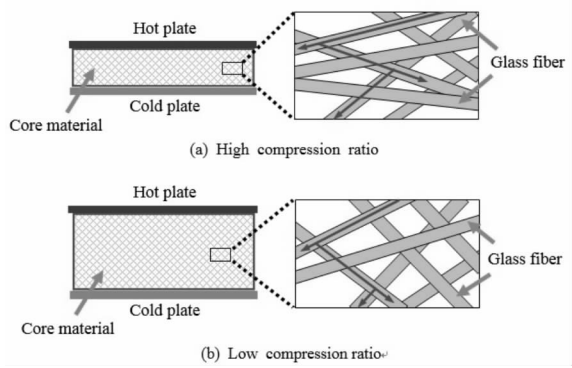

Fig. 5 Heat flow transfer mechanism for vacuum-evacuated fibrous materials

4. Conclusions

GF – VIPs possessing more pieces of CMLs required a more rigorous vacuum process. GF – VIPs with high number of CMLs have better ability to maintain the interior pressure in a low value but possessed a higher thermal conductivity. In order to obtain high-quality GF – VIPs with long-term service life and low thermal conductivity, the number of CMLs in a GF – VIP should be between 16 and 32.

Acknowledgments

This work was supported by Funding for Outstanding Doctoral Dissertation in NUAA (BCXJ13 – 10), Funding of Jiangsu Innovation Program for Graduate Education (the Fundamental Research Funds for the Central Universities, CXLX13_149), Project Funded by the Priority Academic Program Development of Jiangsu Higher Education Institutions, the Jiangsu Project BA2013097 and National Project 2015DFI53000.

References

[1] X. Wang, N. Walliman, R. Ogden, C. Kendrick, VIP and their applications in buildings: a review, Proceedings of the institution of civil engineers: construction materials. 160 (2007) 145 – 153.

[2] B. P. Jelle, Traditional, state-of-the-art and future thermal building insulation materials and solutions – Properties, requirements and possibilities, Energ Buildings. 43 (2011) 2549 – 2563.

[3] K. Araki, D. Kamoto, S. Matsuoka, Optimization about multilayer laminated film and getter device materials of vacuum insulation panel for using at high temperature, J Mater Process Tech. 209 (2009) 271－282.

[4] C. D. Li, Z. C. Duan, Q. Chen, Z. F. Chen, F. E. Boafo, W. P. Wu, J. M. Zhou, The effect of drying condition of glassfiber core material on the thermal conductivity of vacuum insulation panel, Mater Design. 50 (2013) 1030－1037.

[5] J. Kim, T. Song, Vacuum insulation properties of glass wool and opacified fumed silica under variable pressing load and vacuum level, Int J Heat Mass Tran. 64 (2013) 783－791.

[6] X. Di, Y. Gao, C. Bao, Y. Hu, Z. Xie, Optimization of glass fiber based core materials for vacuum insulation panels with laminated aluminum foils as envelopes, Vacuum. 97 (2013) 55－59.

[7] C. D. Li, Z. F. Chen, F. E. Boafo, T. Z. Xu, L. Wang, Effect of pressure holding time of extraction process on thermal conductivity of glassfiber VIPs, J Mater Process Tech. 214 (2014) 539－543.

[8] J. E. Fesmire, S. D. Augustynowicz, B. E. Scholtens, Robust multilayer insulation for cryogenic systems, American Institute of Physics. 53 (2008) 1359－1366.

[9] H. Simmler, S. Brunner, U. Heinemann, H. Schwab, K. Kumaran, Mukhopadhyaya, D. Quenard, H. Sallee, K. Noller, E. Kucukpinar-Niarchos, C. Stramm, M. J. Tenpierik, J. J. M. Cauberg, M. Erb, Vacuum insulation panels：Study on VIP components and panels for service life prediction in building applications (Subtask A), (2005)

[10] R. Arambakam, H. V. Tafreshi, B. Pourdeyhimi, A simple simulation method for designing fibrous insulation materials, Materials and Design. 44 (2013) 99－106.

[11] S. S. Woo, I. Shalev, R. L. Barker, Heat and Moisture Transfer Through Nonwoven Fabrics Part I：Heat Transfer, Text Res J. 64 (1994) 149－162.

Research on the Biological Solubility of Ultra-fine Glass Fibers

Sha Lili, Chen Zhaofeng*, Chen Zhou

Super Insulation Composite Laboratory, College of Material Science and Technology,
Nanjing University of Aeronautics and Astronautics, Nanjing, 210016, P.R. China

Abstract

Ultra-fine glass fibers have many excellent properties, such as good insulation, low thermal conductivity and high acoustic property, et al. However, traditional mineral fibers usually form a lot of dusts when they are produced or used. It is easy to be inhaled into human body, but hardly to be degraded, which must do a great harm to human health. In this paper, we design an experiment putting glass fibers into continuously updated simulated lung fluid for different cycles. Glass fibers are produced by centrifugal blowing system. Diameters and the surface morphology of fibers are measured by optical microscope and scanning electron morphology, respectively. The results show that the simulated lung fluid absorb various metal ions and non-metallic ions when fibers gradually dissolve. The results from inductively coupled plasma atomic emission spectroscopy test further shows that silicon, boron, calcium and magnesium ions can easily be absorbed, which consume the hydrogen ion of the simulated lung fluid leading to an increase of the pH value of the fluid. However, it is difficult for Aluminum ion to dissolve in the fluid. By this experiment, the proportion of different ions can be controlled to obtain fibers with good biocompatibility.

Keywords glass fiber, gamble solution, biological solubility, fiber diameter

1. Introduction

Glass fibers have excellent insulation property, such as low thermal conductivity, good thermal shock resistance and high mechanical strength. In many developed countries, glass fibers have been widely used in high-tech fields, such as military field, cabin and cockpit of aircraft, man-made earth satellite and shipbuilding [1 - 3]. In China, glass fibers are widely used in appliance, house partition and refrigerated containers. For traditional glass fibers, which are rich in silicon and aluminum and lack of boron. It is easy to form lots of dusts when they are produced or used. Once these dusts are inhaled into the lungs leading to a series of gradual biochemical reactions with human cells. It means that the insoluble fibers will endanger human body health. Nowadays, people draw great attention to personal health and are devoted to developing and using non-polluting environmentally-friendly materials. So it is significant to study the solubility of ultra-fine glass fiber.

There are two important indexes that can help divide the fibers. One is European index (KNB), the other is KI index.

$$KNB=[Na_2O+K_2O+CaO+MgO+BaO]\times 100 \quad (1)$$

The value of metallic oxide represents the mass percentage of the oxide in the fiber. The larger the value of KNB is, the less carcinogenicity the fiber may have.

$$KI=[(Na_2O+K_2O+CaO+MgO+BaO+B_2O_3)2\times(Al_2O_3)]\times 100 \quad (2)$$

The value of metallic oxide represents the mass percentage of the oxide in the fiber. If the value of KI is more than 40, the fiber can be considered as safe material.

Part of man-made mineral fibers can be inhaled into

* Corresponding author, Tel:86 - 25 - 52112909, E-mail: zhaofeng_chen@163.com

the human lungs, but some can not be inhaled. Different chemical component, different chemical structure and different manufacture technology making the fibers show different chemical and physical properties [4 - 5]. The effect of fibers on human health is decided by many factors. When the fiber diameter is more than 6 μm, the fiber will not be inhaled into lungs. When the diameters of fibers are 3～6 μm, the fibers can be inhaled into nostril and oral cavity but then they will be filtered by mucus from nostril and oral cavity. Only when the fiber diameter is less than 3μm, the fibers will easily be inhaled into lungs and can hardly be cleared from the lungs. Once mineral fibers enter human body, macrophages in lungs will start to attack the foreign material (mineral fiber). Some short fibers (the length is less than 20μm) can be cleared from lungs by macrophages. However, for the long fibers (the length is more than 20 μm), they will be surrounded by acid medium provided by macrophages and then be corroded gradually. Long fibers will break into many short fibers and this process can be called fiber dissolution.

Bio-soluble fiber is a kind of mineral materials with high degradability in human lungs, which can be dissolved in simulated human lung fluid after some time. Researchers mainly focus on two points to study the bio-soluble fibers, one is the research on biocompatibility and biological activity of soluble fibers and the other is the concrete metabolic mechanism soluble fibers in human bodies. Experimental methods mainly include two parts. One is the biological performance test conducted in the body of laboratory rats. The other is in-vitro test, during which solutions with certain pH are chosen to simulate lung fluid, then fibers are put in the solution. The mass loss, surface structure, leaching components and phase composition of the materials are observed. Nowadays in-vitro tests are widely used in researches on bio-solubility. Researches are mainly based on biological soluble ceramic fibers. However, the researches on glass fibers are limited.

2. Experiment

2.1 Preparation of glass fibers

Plate glass, quartz sand, soda, borax, dolomite fines, feldspar and limestone are used to prepare glass fiber. These raw material are mixed according to a certain proportion and then be sent to glass kiln. $Na_2O-CaO-SiO_2-B_2O_3$ series can be produced by melting at a high temperature. At last, the glass fibers are produced by centrifugal blowing system. Composition of the fibers is shown in Tab. 1.

Tab. 1 Composition of glass fibers

Component	SiO_2	K_2O_3	Na_2O	CaO
Composition/(%)	67.1	0.8	15.44	5.9
Component	MgO	Al_2O_3	B_2O_3	
Composition/(%)	2.7	3.13	4.25	

2.2 Bio-solubility experiment invitro

Gamble solution is usually used to simulate the lung fluid in many researches. Metabolism and lung fluid of human body are gradually updated so that an electronic peristaltic pump is necessary in our experiment in order to simulate the renewal of lung fluid accurately. The glass fibers which we prepare are put in a certain vessel. The electronic peristaltic pump will transport some Gamble solution from a beaker with plastic wrap on the top to the certain vessel at a low rate. At the same time, redundant solution will return to the beaker. Glass fibers are dissolved in circulating solutions rather than a stable solution. The flow rate is 15 milliliters per hour. Composition of the Gamble solution is shown in Tab. 2.

Tab. 2 Composition of the Gamble solution per litre

Chemical name	Weight/g
NaCl	6.415
$NaHCO_3$	2.703
$MgCl_2 \cdot 6H_2O$	0.212
Na_2HPO_4	0.148
$CaCl_2 \cdot 2H_2O$	0.318
$Na_2SO_4 \cdot 2H_2O$	0.179
Sodium tartrate	0.180
Sodium citrate	0.186
Sodium lactate	0.175
Sodium pyruvate	0.172
Glycine	0.118

In this experiment, four samples (glass fibers) were prepared. The weight of each sample is 0.3 g, which was measured by analytical balance. Then they were stored in circulating Gamble solutions for 0 day, 1 day, 2 days and 3 days, respectively. Glass fibers were collected respectively after being dried. Four pieces of solutions with 30 ml from the beaker were also collected, respectively. Surface topography of the fibers were observed by SEM (Scanning Electron Microscope) and the dissolution rate of different elements were got from ICP - OES (Inductively Coupled Plasma Optical Emission Spectroscopy).

3. Results and discussion

3.1 Morphology of glass fibers

The diameters of 100 original fibers are measured by OM (optics microscope) and the average diameter is 3.0067μm. As is shown in Fig. 1(a), all the glass fibers distribute disorderly in three-dimensional direction. Smooth surface of a single fiber can be observed in Fig. 1(b).

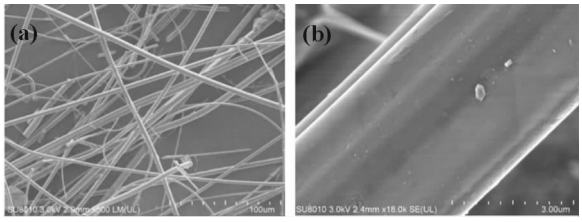

Fig. 1 Morphology of glass fibers without dissolving
(a) fiber distribution; (b) surface of glass fiber

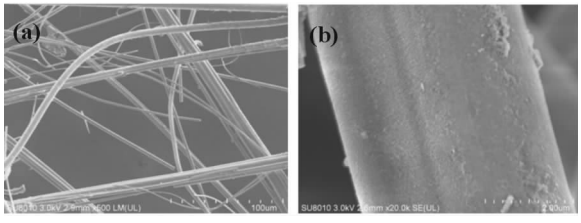

Fig. 2 Morphology of the glass fibers after dissolving for 1 day
(a) fiber length; (b) surface of glass fiber

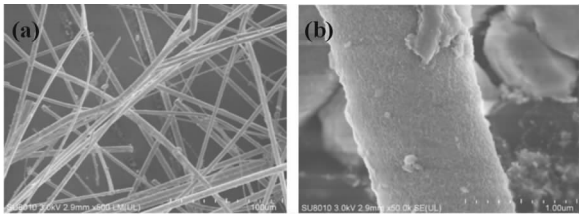

Fig. 3 Morphology of the glass fiber after dissolving for 2 days
(a) fiber length; (b) surface of glass fiber

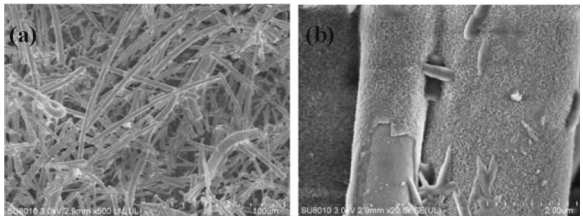

Fig. 4 Morphology of the glass fiber after dissolving for 3 days
(a) fiber length; (b) surface of glass fiber

The average diameters of glass fibers after dissolving 1 day, 2 days and 3 days are 3.0147μm, 2.976μm and 2.968μm, respectively. It indicate that the diameter of glass fibers reduced with the increase of storing time in Gamble solutions, i.e., fiber dissolved. From the Fig. 2(a), Fig. 3(a) and Fig. 4(a), it can be seen that the original long fibers were gradually broken into short fibers. The longer the storing time was, the shorter the fiber lengths were. The surface of the original fibers were smooth and compact with no spots and no signs of corrosion. After one day's dissolution, the surface of glass fibers were rougher than that without dissolving. Some little fibrous granular dusts which came from the fracture corrosion of the extreme fiber tend to reunite in few area of the fiber surface, as shown in Fig. 2(b). We can see that the surface became more and more rougher with the increase of dissolution time from 1～3 days with the increment of 1, as shown in Fig. 3(b) and Fig. 4(b). The improvement of the specific surface area can increase the dissolution rate. From the Fig. 3(b), it was observed that glass fibers have been corroded. Some parts of the extreme fiber even fell off from the surface so that the diameter reduces gradually, as shown in Fig. 4(b).

3.2 Analysis of the results of ICP - OES test

With the increase of storing time in Gamble solution, the silicon ion concentration in solutions increased, this phenomenon can be explained from Tab. 3 and Fig. 5. Usually, silica has three coordination compounds with different electric charges and the pH value in Gamble solution is over 7. Once fibers were put into Gamble solution, the coordination compounds would hydrolyze and the surface of the fiber became negative. Positive ions in Gamble solution combined with the negative charges of the surface to break the structure of the extreme fiber. The Si - O - Si bond in

the solution also increased so the dissolution rate rose at the same time. Besides this, the original organic substances in Gamble solution such as Sodium tartrate, Sodium citrate, Sodium lactate, Sodium pyruvate and Glycine interacted with silica to produce hydroxide, which also results in the dissolution.

Tab. 3 The content of microelements in the series of experiments

No.	Si mg/L	Ca mg/L	Mg mg/L	B mg/L	Al mg/L
0	0	81.55	33.28	0	0
1	3.22	82.88	33.36	0.12	0
2	6.7	82.72	34.57	0.2	0
3	9.42	83.65	34.78	0.24	0

The Calcium ion concentration in solutions rose slowly with the increase of dissolving time. Calcium silicate in fibers is amorphous which has great instability leading to Calcium silicate to dissolve. However, Magnesium ion concentration in solutions rises more slowly. Magnesium silicate of vitreous state is a single link structure, which has a certain solubility in Gamble solutions. As for boron, it can only leach a little in the solution and the Aluminum can hardly leach in the solution.

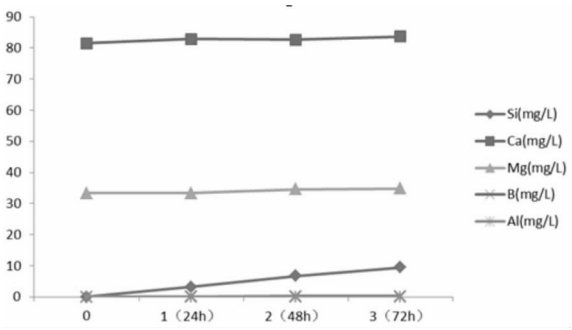

Fig. 5 The content of microelements in different storing times in Gamble solution

4. Conclusions

Glass fiber of $Na_2O-CaO-SiO_2-B_2O_3$ series will dissolve in continually circulating Gamble solutions, starting from the surface. The surface will become more and more rougher due to the dissolution time increases. Silicon ion, Calcium ion, Magnesium ion and Boron ion can be leached in the solution at different rates, however, aluminum can hardly leach in the solution. Controlling the proportion of different ions according to the dissolution rates, we can obtain biological soluble glass fiber.

Acknowledgements

The authors would like to express their gratitude to the Suzhou V. I. P. New Material Co., Ltd. for the facilities provided during the experiments and all their valuable support. The authors would like to thank the Jiangsu Project BA2013097 and National Project 2015DFI53000.

References

[1] Y. Z. Liu. Studies on process optimisation of multistage atomization, Materials Science and Technology, 18 (2002) 929－934.

[2] N. Marheineke, J. liljo, J. Mohring, J. Schnebele, R. Wegener. Multiphysics and multimethods of rotational glass fiber melt-spinning. International journal of numerical analysis and modeling, series B, 2012, 3(3): 330－344.

[3] W. Arne, N. Marheineke, J. Schnebele, R. Wegener. Fluid-fiber-interactions in rotational spinning process of glass wool production. Journal of Mathematics in Industry, 2 (2011), 26－52.

[4] F. Millot, V. Sarou-Kanian, J. C. Rifflet, et al. The surface tension of liquid silicon at high temperature, Materials Science and Engineering A, 495 (2008) 8－13.

[5] F. Aqra, A. Ayyad. Theoretical temperature-dependence surface tension of pure liquid gold. Materials Letters, 65 (2011) 2124－2126.

Research on Dry Process for Making Glass Fiber Core Material of Vacuum Insulation Panel

Yang Yong, Chen Zhaofeng*, Li Yufang, Fu Renli

College of Material Science and Technology, Nanjing University of Aeronautics and Astronautics, Nanjing, 210016, P. R. China

Abstract

Vacuum insulation panel (VIP) is a high performance thermal insulation material composed of an evacuated core material encapsulated in an envelope and supplemented with a desiccant. In this paper, dry process, structure, fiber arrangement and thermal conductivity of VIP were discussed. Core material was fabricated by centrifugal-spinneret-blow, and swing cylinder was designed as a uniform process with non-uniformity being less than 5%. The uniformity and fiber orientation had an important effect on the thermal insulation performance of VIP, and the thermal conductivity of core material with fibers being in 2D distribution was better than that in 3D distribution. Most fibers with two-dimensional distribution laid in the same plane, and directional fiber was superior to the random fiber. VIP produced by wet process with thermal conductivity 21～23mW/(m·K) was compared with that by dry process, with thermal conductivity within the range of 17～19mW/(m·K). Lastly, the heat-transfer mechanism of VIPs by different processes was explained.

Keywords vacuum insulation panel (VIP), dry process, glass fiber core material

* Corresponding author, Tel: 86-25-52112909, E-mail: zhaofeng_chen@163.com

New Organic Fiber-Based Core Material for Vacuum Thermal Insulation

Vincenc Nemanič*, Marko Žumer

Jožef Stefan Institute, Jamova cesta 39, 1000 Ljubljana, Slovenia

Abstract

Today, inorganic fibers are applied as the fibrous core in vacuum thermal insulation panels exclusively as none of the organic candidates could match required physical and chemical properties. Our recent studies reveal that melamine-formaldehyde fibers with high thermal stability and small fiber diameter below 5μm may well compete with glass fibers. The fibers were synthesized from a meltable pre-polymer of etherified melamine-formaldehyde in a form of a low density fleece, subsequently cured at 200℃ and post-heated at 260℃.

Two most crucial core properties, thermal conductivity and outgassing rate, were investigated in thin-walled stainless steel envelopes in the shape of vacuum panels, enabling thermal processing combined with a pump-out procedure and subsequent testing. A base thermal conductivity of $\sim$ 2.3 mW $\cdot$ m^{-1} $\cdot$ K^{-1} was achieved with randomly oriented fibers at a density of $\sim$250 kg $\cdot$ m^{-3}. The long-term pressure-rise measurements revealed extremely low outgassing rates, $q \approx 10^{-15}$ mbar L $\cdot$ s^{-1} $\cdot$ cm^{-2}. These low values could be measured, as the background outgassing of the stainless steel envelope was previously substantially reduced. Additional measurements of thermal conductivity in a wide pressure range indicate that these fibers could be the first organic candidates applied as the core material in vacuum insulating panels with an adequate service lifetime. Their performance is comparable to selected inorganic core materials like glass fibers.

Keywords vacuum insulation panel (VIP), novel core material for VIP, melamine-formaldehyde fibers, extremely low outgassing rate

* Corresponding author, Tel: 386 - 1 - 4773 409, E - mail: vincenc. nemanic@ijs. si

The Thermal Conductivity of Basalt Fiber at High Temperature

Wang Fei, Chen Zhaofeng*, Guan Shengnan

College of Materials Science and Technology, Nanjing University of Aeronautics and Astronautics, Nanjing, 210016, P. R. China

Abstract

Basalt fiber is an important high-powered material which draws much attention just as carbon fiber and glass fiber. The basalt fiber was processed at high temperature in 100 ~ 700 ℃ temperature range. The thermal conductivity of the fiber processed in different temperature were measured and compared with measurement at normal temperature. The results indicate that the thermal conductivity of basalt fiber increases as the temperature, especially when it's over 500℃.

Keywords basalt fiber, high temperature, thermal conductivity

1. Introduction

Basalt belongs to the volcanic rock, one of the most widely distributed minerals [1]. The broken basalt was added to furnace and melted between 1450 ℃ and 1500 ℃, and made to basalt fiber through platinum rhodium wire-drawing bushing. Basalt fiber belongs to silicon aluminate system, and SiO_2 is the most major component of it [2 - 3].

The structure and performance of basalt fiber is similar to the glass fiber, but basalt fiber has better high temperature resistance, corrosion resistance, heat and sound insulation [4 - 5]. The working temperature of basalt fiber can reach 600～700 ℃, while the glass fiber doesn't exceed 400 ℃ in the same conditions. The thermal conductivity of basalt fiber is very low even at high temperature. Besides, it will not release toxic substances in air and water, and becomes a soil parent material after degradation, so it's pretty friendly to the environment. It is usually applied in friction materials, heat insulators, filtration materials and cement base composite materials, etc [6 - 8].

2. Experiment

The samples used in the experiment are super fine basalt fibers, which are manufactured in the form of layered wool. For measurements, pieces of wool were cut into flat rectangular felt in the size of 10 cm × 10 cm. Then one of the samples was placed in thermal conductivity measuring instrument, and its thermal conductivity at room temperature was measured. The other samples were put into electric oven and heated for an hour at temperature from 100 ℃ to 700 ℃. The thermal conductivity of the samples processed in different temperature were measured and compared with the measurement at normal temperature. The relation curve of thermal conductivity of basalt fibers changing with temperature was made. The crystal structure of every sample was analyzed by X - ray diffraction.

3. Results and Discussions

The effect of temperature on the thermal conductivity of basalt fiber is shown in Fig. 1.

Apparently, as the treatment temperature increases, the thermal conductivity of the samples becomes higher and higher. When the temperature is below 500℃, the thermal conductivity increases slightly and keeps in a pretty low level. The relationship between temperature and thermal conductivity is linear. However, when the temperature exceeds 500 ℃, the thermal conductivity increases abruptly and even reach over five times of that at normal temperature.

* Corresponding author, Tel: 86 - 25 - 52112909, E-mail: zhaofeng_chen@163.com

The increase of thermal conductivity of basalt fiber is mainly caused by thermal radiation. The capacity of heat transmission is proportional to radiation coefficient of the fibers, temperature difference between fibers and the third power of absolute temperature. Besides, as the temperature rises, the thermal motion of molecule is more severe and the amount of heat conducted becomes more. As a result, the thermal conductivity becomes higher accordingly.

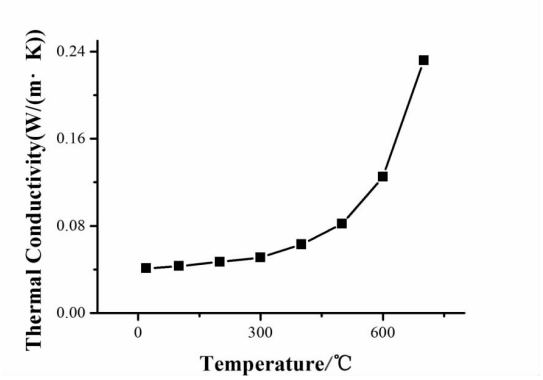

Fig. 1 Effect of temperature on the thermal conductivity of basalt fiber

In general, the thermal conductivity of crystal materials is higher than that of amorphous materials. There is no obvious diffraction peak in X-ray diffraction pattern of basalt fiber at normal temperature, which indicates that the bulk structure of the fiber is non-crystal with short range order structure. The diffraction peak of samples gradually becomes sharp with the increase of heat treatment temperature. It shows that the degree of crystallization has improved, which can also improve the thermal conductivity of basalt fibers.

4. Conclusions

The following conclusions are made from the study:

1) The thermal conductivity of basalt fiber increases as the temperature, especially when it's over 500℃.

2) The increase of thermal conductivity of basalt fiber is because of thermal radiation, thermal motion of molecule and the improvement of degree of crystallization.

Acknowledgements

The authors would like to thank the funds from Jiangsu Project BA2013097 and National Project 2015DFI53000.

References

[1] R. J. Sweeneyf. Geology of the Sabie River Basalt Formation in the Southern Kruger National Park[J]. Koedoe, 1986, 29: 105-116.

[2] Huijun Wu, Jing Zhao, Zhongchang Wang. Study on Micro-structure and Durability of Fiber Concrete[J]. Research Journal of Applied Sciences, Engineering and Technology, 2013, 5(2): 659-664.

[3] A. Todic, D. Cikara, V. Lazic, et al. Examination of Wear Resistance of Polymer-Basalt Composites[J]. Tribology in Industry, 2013, 35(1): 36-41.

[4] T. Deak, T. Czigany, P. Tamas, et al. Enhancement of interfacial properties of basalt fiber reinforced nylon 6 matrix composites with silane coupling agents[J]. Express Polymer Letters, 2010, 4(10): 590-598.

[5] S. Ezhil Vannan, S. Paul Vizhian. Microstructure and Mechanical Properties of as Cast Aluminium Alloy 7075/Basalt Dispersed Metal Matrix Composites[J]. Journal of Minerals and Materials Characterization and Engineering, 2012, 2: 182-193.

[6] Sergey K. Nikoghosyan, Aram A. Sahakyan, Vasak B. Gavalyan, et al. Electro-Physical Properties of Super-Thin Basalt Fiber Chemically Modified by Hydrochloric or Sulphuric Acid[J]. Journal of Modern Physics, 2011, 2: 1450-1454.

[7] S. Ezhil Vannan. Experimental Investigations on Electroless Deposition of Copper on Basalt Fibers[J]. Journal of Minerals and Materials Characterization and Engineering, 2015, 3: 289-297.

[8] M. Cocic, M. Logar, B. Matovic, V. Poharc-Logar. Glass-Ceramics Obtained by the Crystallization of Basalt [J]. Science of Sintering, 2010, 42: 383-388.

Effect of Sepiolite Powders on the Thermal Conductivity of VIP Using Glass Wool as Core Materials

Deniz Eren Erişen, Chen Zhaofeng*, Chen Lihe

College of Material Science and Technology, Nanjing University of Aeronautics and Astronautics, Nanjing, 210016, P. R. China

Abstract

There are few alternatives as core materials for vacuum insulation panels. Developing new or hybrid core materials are important to invent new vacuum insulation applications. It calls for experimental works about some other materials which exist and are available for application. Some minerals with high porosities look promising as an alternative. In this study, sepiolite powder and asbestos like natural fibers are used as core material additives to invent a new hybrid core materials. Investigations were performed to improve existing core material with sepiolite addition and also find out the possibilities of using natural mineral fibers as core materials. Sepiolite is a Magnesium Hydroxyl Silicate mineral with fiber like structure and inner porosities. It sustains a low solid conductivity as glass fiber and it has good water absorption properties. These properties make it a good candidate for producing new hybrid core materials. Micro size fiber sepiolite can be used as core materials and nano size sepiolite can be used as filler or additives for glass fiber and fume silica core materials. Sepiolite is also available to produce insulation boards. This paper gives a basic method to produce hybrid core material with sepiolite mineral and it's insulation and ageing performance.

Keywords vacuum insulation panels, sepiolite, fiber, clay, thermal insulation, desiccant

1. Introduction

Sepiolite is a fibrous clay mineral which consist of Magnesium Silicate and Hydroxide lattices. Sepiolite has structural tunnels along the fibrous with 0.4 nm^2 cross-sectional area [1,2].

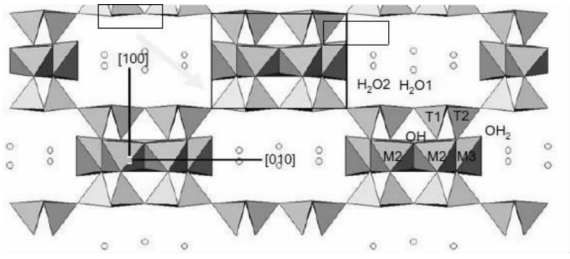

Fig. 1 Lattice of sepiolite crystal structure in cross-sectional sectional views along sepiolite fiber

Sepiolite has high surface area and fibrous structure It shows many micropores and mesopores at different structure levels. And it's fibrous structure can exhibit different variables due to the source. Some sources in Turkey show few nanometer size fibrous with agglomerated as particles, on the other hand, some sources in China show few micro and millimeter long fibers. Also, texture of agglomerated fibers or bundles can be varied depending on its source [3,4]. Texture affects porosity of sepiolite samples. There are so many methods that can change this texture of agglomerated particles and bundled fibers. There are acid, base, amine and thermal treatments. But some of the treatments also change structural porosity. Especially some strong acids can damage structural tunnels. On the other hand, these strong acids can get rid of some calcium ions from surface. Defibering of sepiolite bundles can be performed with some special heat treatments without any other structural damages [4-7]. Chinese sepiolite, within millimetre size fibrous structure can be called asbestos-like clay mineral. But this cannot be likened to the same carcinogenic effect on

* Corresponding author, Tel: 86-25-52112909, Fax: 86-25-52112626, E-mail: zhaofeng_chen@163.com, deerisen@anadolu.edu.tr

mammals' biology [8].

fiber structured materials are usually used as insulation materials [9 - 11]. There are still potentials to invent new core material using locally available fibers or powders which are available for insulating [12]. Sepiolite is used in many insulation applications and it has recent researches in literature [1,13]. So, it should be an interesting area to investigate using sepiolite in vacuum insulation applications. This study is the initial work for vacuum insulation application of sepiolite.

In addition, absorption of moisture which has permeated into core material is important thing. Moisture can easily be diffused through envelope to enter core material during ageing. Sepiolite can absorb this moisture as well. Therefore it can play a role as a desiccant [14 - 16].

2. Material and methods

Different kinds of sepiolite fiber samples found at different sources; one is ESKISEHIR (ESK) region in Turkey. Another one is from HENAN (HEN) region in China. Observation and Scanning Electron Microscope images show that each of them possess different properties. Sepiolite ESK has more short and nano sized fibers, they are agglomerated as fine powders. It is observed like powder samples at beginning without SEM images. But SEM images of the ESK sepiolite shows that it has nano size fibers which mostly agglomerated. These fibers are also short because of grinding conditions. Sepiolite HEN have long fibers, they stick them together as micron and millimetre size bundles. It looks like microns size fibers at beginning without SEM images. But SEM images of the HEN sepiolite show that it has nanometer thickness and micron and millimeter long fibers which constituent 9 microns size thickness fiber bundles.

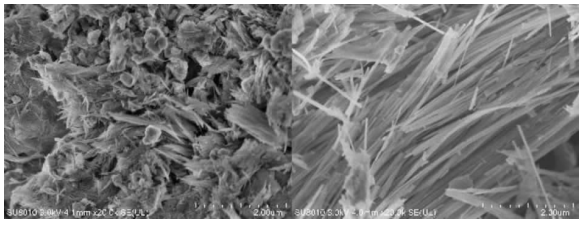

Fig. 2 ×20k SEM images (above) of the ESK (left) and HEN (right) sepiolite. 2.0 μm scales; ESK is just pictured as some small agglomerates and thick fiber bundles; HEN is pictured as long fibers

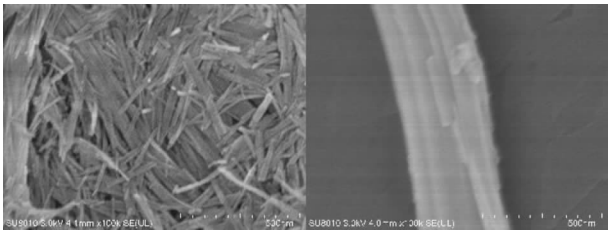

Fig. 3 ×200k SEM images(above) of the ESK(left) and HEN(right) sepiolites. 500nm scales; ESK is pictured as nanosized and short fibers and bundles; HEN is pictured as big bundles which constituent nano size thickness fibers

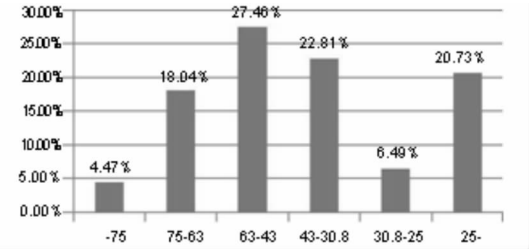

Fig. 4 Graph particle size distribution of ESK sepiolite sample

To prepare hybrid core material; layered with powder and glass fiber core material method is opted. It is a simplified method to understand sepiolite-glass fiber core material's abstracted details. ESK sepiolite powders which are dried at 100℃ and Suzhou VIP New Materials Co.'s glass fiber nonwovens are used. With various sepiolite addition to 24 layer nonwovens ; 250mm × 250mm panels are prepared. [Illustration 1] And they dried at 250℃ oven as 3 hours then evacuated at production line of Suzhou VIP New Materials Co.

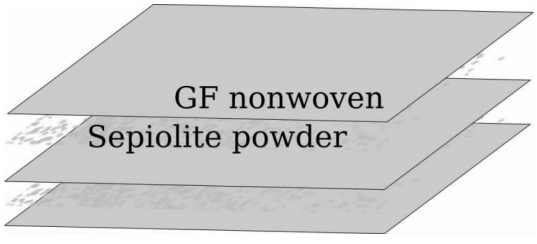

Fig. 5 Illustration of model structure of powder and nonwoven composite core material

Measuring first thermal conductivity values (k_0) of panels were done by Netzsch HFM 436 and inner pressure test was done by Superbee test kit at Suzhou VIP. Other tests were done by Hanita Israel´s laboratories.

3. Results and discussions

The first thermal conduction values were measured. High sepiolite content show worse insulation properties. A control specimen without sepiolite addition was showing 2.165 mW • m^{-1} • K^{-1}. When 32 gr sepiolite added specimen show 2.8 mW • m^{-1} • K^{-1}.

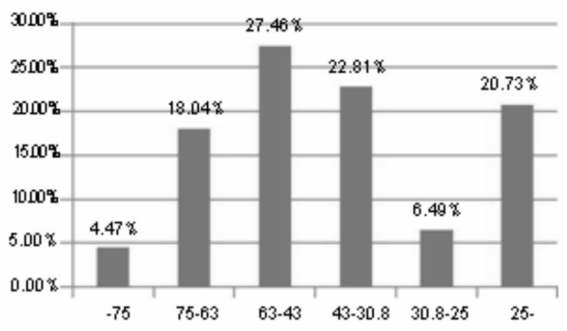

Fig. 6 Graph of conductivity versus sepiolite content

The result can be accounted for considenring two causes, One of them is sepiolite addition as pristine clay with small particle size would increase the density of core material. ESK sepiolite have very small fiber size, it can agglomerate easily and can role as any clay powder. This density increase can make bridging inside core material. On the other hand, lack of drying conditions can affect the insulation properties negatively. Because sepiolite is tended to absorb water molecule inside with many mechanisms (chemical and physical), this can increase conductivity of core material.

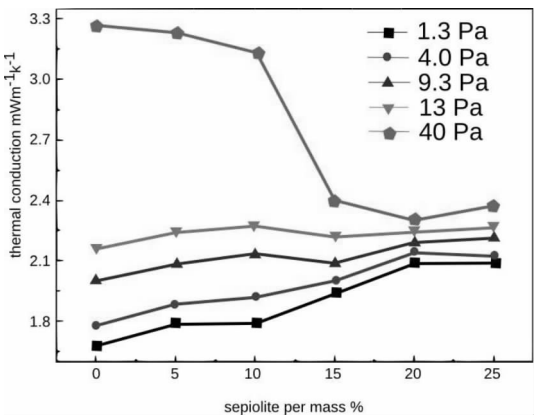

Fig. 7 Graph of thermal conduction values of panels at several inner pressure conditions

All work show sepiolite addition changes critical inner pressure of core material. This outcome can be negligible because addition of any silicate powder will fill big pores and can decrease convection at lower vacuum conditions. Due to result of Hanita Israel Laboratories. A control specimen without sepiolite addition have shown 5.4mbar critical pressure, when 32 gr sepiolite added specimen was showing 5.7 mbar critical pressure.

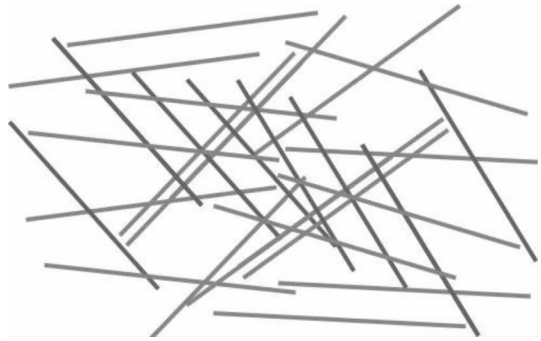

Fig. 8 Illustration of glass fiber structure with empty spaces

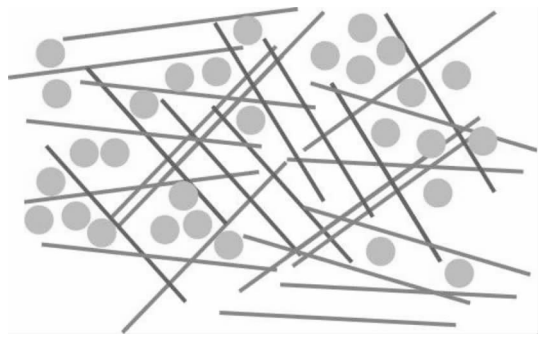

Fig. 9 Illustration of glass fiber structure with filled by nano sepiolite fiber or rode agglomerates

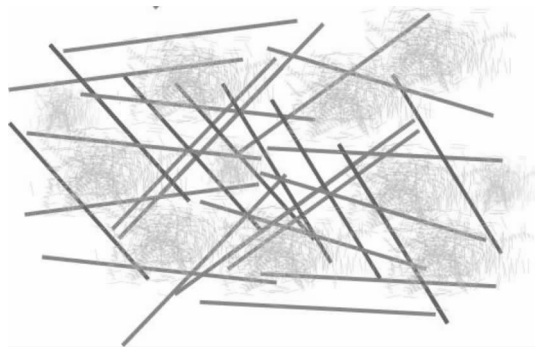

Fig. 10 Illustration of glass fiber structure with fine distributed nano sepiolite fibers or rods

As show in Fig. 2～4, glass fiber nonwoven core material has big pores, that is why it has satisfied insulation properties just at high vacuum conditions. These pores can be filled by any powders. But this will increase the density of core materials. Hence, it will decrease insulation properties at high vacuum. As the

last illustration, this pores can be filled by more small fibers. So this will increase insulation properties both at high vacuum and low vacuum.

4. Conclusions and outlook

Pristine sepiolite from ESKISEHIR region (Turkey) is used for this study, any raw operation except drying is not applied on material. The basic method to produce hybrid core material is chosen, layering powder on glass nonwovens.

It is arduous to see yet advantages about insulation properties via adding sepiolite particle inside core material. Results are observed as it just increases critical inner pressure due to filling bigger pores of glass fiber nonwovens.

Reason of some failures can be abstracted as lack of pre-treatment of sepiolite; doubtfulness on process of panels in the view of drying and absorbing conditions of sepiolite; using less fiber-like sepiolite samples; using the basic processes to create hybrid core material.

Further study can be performed on some treatment on sepiolite to distribute sepiolite fibers and increase density of powder. Therefore sepiolite can be used in wet-laid processes of nonwovens. Moreover, variation of sepiolite clay should be examined by repeating the same methods.

On the other hand, ageing with thermal conduction evaluation test could not apply on this work. To understand humidity control mechanism of sepiolite in VIP, ageing test can be applied at further study.

Acknowledgements

The authors would want to thank the support of Suzhou VIP New Material Co, Taicang, China and Hanita Coating, Hanita, Israel. The authors would like to thank the Jiangsu Project BA2013097 and National Project 2015DFI53000.

References

[1] E. Galan, Properties and applications of palygorskite-sepiolite clays, (1996) 443 - 453.

[2] E. Ruiz-Hitzky, Molecular access to intracrystalline tunnels of sepiolite, J. Mater. Chem. 11 (2001) 86 - doi:10.1039/b003197f.

[3] M. Suárez, E. García-Romero, Variability of the surface properties of sepiolite, Appl. Clay Sci. 67 - 68 (2012) 72 - 82. doi:10.1016/j.clay.2012.06.003.

[4] E. Sabah, Interaction of Original and Heat-Treated Sepiolites with Quaternary Amines, (2001) 747.

[5] A. Miura, K. Nakazawa, T. Takei, N. Kumada, N. Kinomura, R. Ohki, et al., Acid-, base-, and heat-induced degradation behavior of Chinese sepiolite, Ceram. Int. 38 (2012) 4677 - 4684. doi:10.1016/j.ceramint.2012.02.050.

[6] Y. Turhan, P. Turan, M. Dog, Characterization and Adsorption Properties of Chemically Modified Sepiolite, (2008) 1883 - 1895.

[7] L. Lescano, L. Castillo, S. Marfil, S. Barbosa, P. Maiza, Alternative methodologies for sepiolite defibering, Appl. Clay Sci. 95 (2014) 378 - 382. doi:10.1016/j.clay.2014.05.001.

[8] B. Bellmann, H. Muhle, H. Ernst, Investigations on health-related properties of two sepiolite samples., Environ. Health Perspect. 105 Suppl (1997) 1049 - 1052. doi:10.1289/ehp.97105s51049.

[9] Natural fiber and fiber composite materials for insulation in buildings 9, (2010). doi:10.1033/9781845699277.2.229.

[10] Inorganic mineral materials for insulation in buildings, (2010). doi:10.1033/9781845699277.2.193.

[11] Thermal insulation material for building equipment, (2010) 274 - 304. doi:10.1033/9781845699277.2.274.

[12] T. Officer, fiber-powder composite as core material for vacuum insulation panel, (2009).

[13] M. Alam, H. Singh, S. Brunner, C. Naziris, Experimental characterisation and evaluation of the thermo-physical properties of expanded perlite Fumed silica composite for effective vacuum insulation panel (VIP) core, Energy Build. 69 (2014) 442 - 450. doi:10.1016/j.enbuild.2013.11.027.

[14] A. Singer and E. Galan, eds. Palygorskite-Sepiolite. Occurrences, Genesis and Uses, Developments in Sedimentology 37, Elsevier, Amsterdam, 253 - 287.

[15] Ekici S, Isikver Y, Saraydam D. Poly(acrylamide-sepiolite) composite hydrogels: preparation, swelling and dye adsorptionproperties. Polymer Bulletin 2006, 57:231 - 241.

[16] Yang HL, Peng ZQ, Zhou Y, Zhao F, Zhang J, Cao XY, Hu ZW. Preparation and performance of a novel intelligent humidity control composite material. Energy and Building 2011,43:386 - 392.

Pillar-supported Core Structure for Vacuum Insulation Panel

Bongsu Choi, Tae-Ho Song*

School of Mechanical, Aerospace and System Engineering, Korea Advanced Institute of Science and Technology, Daehak-ro 291, Yuseong-gu, Daejeon, Korea

Abstract

Vacuum insulation panels (VIPs) have outstanding insulation performance. It is about 5 to 10 times higher than that of the conventional insulators such as polyurethane foam and glass wool. The filler material of VIP has a great effect on this insulation performance, and it is known that its thermal conductivity is roughly proportional to the density [1]. Thus, if the external pressure on the filler material is released, insulation performance can be enhanced. A pillar-supported core structure proposed in this paper consists of a support structure and a filler material to achieve this object. The support structure sustains the atmospheric pressure instead of the filler material and it is composed of the top and bottom cover plates with pillars inserted between them. For this reason, the support structure is designed considering the mechanical stability and the heat transfer mechanism. A specimen is fabricated using cover plates made of stainless steels, pillars with multi-path supports (MPS) and a filler material. The MPS has a relatively long heat conduction path and the filler material is multi-layered with glass wool sheets and Al-metallized radiation shields. The thermal conductivity measured with a vacuum guarded hot plate (VGHP) is 1.18 mW/(m·K), which is about half of the current VIP thermal conductivities.

Keywords vacuum insulation panels, insulation performance, support structure, filler material, pillar

1. Introduction

Vacuum insulation panels (VIPs) are one of the most promising solutions to improve energy efficiency in buildings and refrigerators. Their insulation performance is about 5 to 10 times higher than that of the conventional insulators such as polyurethane foam, glass wool and expanded polystyrene because the air, which is main cause of heat transfer, is evacuated [2]. A VIP is generally composed of an envelope to maintain the inner vacuum level and a filler material to sustain the atmospheric pressure. Because the inside of VIP is highly evacuated, the filler material has a great effect on the initial insulation performance of VIP. For this reason, there are many researches for the various filler materials such as glass wool, fumed silica, polycarbonate staggered beam and phenolic foam [3-5]. Among them, glass wool and fumed silica are mostly used as the filler materials due to their low thermal conductivity and excellent productivity. Their thermal conductivities are about 2 mW/(m·K) and 4 mW/(m·K) respectively at the atmospheric pressure. For better insulation performance, parallel arrangement of glass fiber and addition of opacifier to fumed silica are applied.

Meanwhile, Kim and Song found that the thermal conductivity of the filler material depends on the external pressing load [1]. Their results show that the thermal conductivities of the glass wool and fumed silica increase with the density. This means that the insulation performance can be enhanced by releasing the external pressure on the filler material. However, because the general VIPs are always compressed by the atmospheric pressure, the performance of VIP is limited.

In this study, a pillar-supported core structure is

* Corresponding author, Tel:82-42-350-3032, Fax:82-42-350-3210, E-mail: thsong@kaist.ac.kr

proposed as a new type ofcore material. It is composed of a support structure and multi-layered filler material. The better insulation performance can be achieved because the support structure sustains the atmospheric pressure instead of the multi-layered filler material.

2. Pillar-supported core structure

The pillar-supported core structure is composed of two cover plates, pillars and a filler material as shown in Fig. 1.

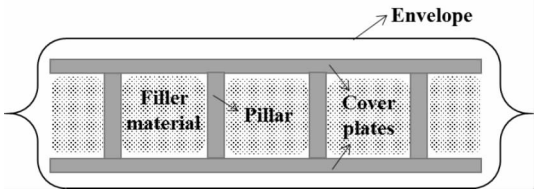

Fig. 1 Schematic of VIP with pillar-supported core structure

The cover plates and pillars are the support structure. When the atmospheric pressure is exerted on the cover plates, the pillars arranged with uniform span W_p withstand the compression force between the two plates. Therefore, not only heat conduction but also mechanical stability has to be considered in designing the support structure. The maximum deflection of cover plates and the permanent deformation of the pillar are main criteria. The maximum deflection δ_{max} occurs at the center of the plates and it is given by [6]

$$\delta_{max} = 0.00581\frac{P_{atm}W_p^4}{\gamma}, \quad \left(\gamma = \frac{E_{cp}t_{cp}^3}{12(1-\nu_{cp}^2)}\right) \quad (1)$$

where

P_{atm} = atmospheric pressure,

W_p = span size of pillars,

γ = flexural rigidity of cover plate,

E_{cp} = Young's modulus of cover plate,

t_{cp} = thickness of cover plate,

ν_{cp} = Poisson's ratio.

For the simple cylindrical pillar, the permanent deformation can be prevented by the following condition [7]

$$P_{atm}W_p^2 < \sigma_{YS}\frac{\pi d_p^4}{4} \quad (2)$$

where

σ_{YS} = yield strength of pillar,

d_p = diameter of pillar.

From Eqs. (1) and (2), it is better to use thick cover plates and pillars for mechanical stability. On the other hand, it results in poor insulation performance because more heat is transferred through thicker pillars. Therefore, optimal dimension is required by considering heat conduction through this structure. The effective thermal conductivity of the pillar-supported core structure k_{eff} can be obtained using electrical analogy as [8]

$$k_{eff} = \frac{h_p + 2t_{cp}}{W_p^2}\left(\frac{2t_{cp}}{k_{cp}W_p^2} + \frac{h_p}{k_{fm}\left(W_p^2 - \frac{\pi}{4}d_p^2\right) + k_p\left(\frac{\pi}{4}d_p^2\right)}\right)^{-1} \quad (3)$$

where

h_p = height of pillar,

k_{fm} = thermal conductivity of filler material,

k_{cp} = thermal conductivity of cover plate,

k_p = thermal conductivity of pillar.

The span size is much larger than the diameter of pillar, i.e., $W_p^2 - \frac{\pi}{4}d_p^2 \approx W_p^2$. Also, substituting Eq. (3) into Eq. (2) leads to

$$k_{eff} \geqslant \frac{h_p + 2t_{cp}}{h_p}\left(k_{fm} + \frac{k_p P_{atm}}{\sigma_{YS}}\right) \quad (4)$$

As shown in Eq. (4), material properties of the pillar have large influence in k_{eff}. The ratio of the thermal conductivity to the yield strength of pillar has to be small for better performance. Polymers are appropriate for this condition. Especially, polycarbonate has a small thermal conductivity and a large yield strength compared with other polymers. Besides selecting the proper material of pillar, its heat conduction can be further reduced by modifying the shape. In the simple cylindrical pillar, heat is transferred directly from hot to cold. Multi-path support (MPS), in the meanwhile, has a complicate heat transfer path as its cross-section shown in Fig. 2.

The MPS has 3 parts; innercircular rod, cup-shaped holder and outer hollow rod. Inner and outer rods are made of polycarbonate. The middle holder is made of stainless steels because relatively high stress is concentrated at the holder. Although total height of MPS, h_p, is equal to that of the simple cylindrical pillar, the effective heat transfer path of MPS, h_{eff_MPS}, is about 2 times longer. As a result, the second term at the right-had side of Eq. 4 is reduced to the ratio of

h_p/h_{eff_MPS}. The effective heat transfer path of the MPS is obtained by numerical simulation using the well-known commercial software FLUENT®. Radiation as well as conduction is simulated together which occurs among the surfaces of the two rods and the holder.

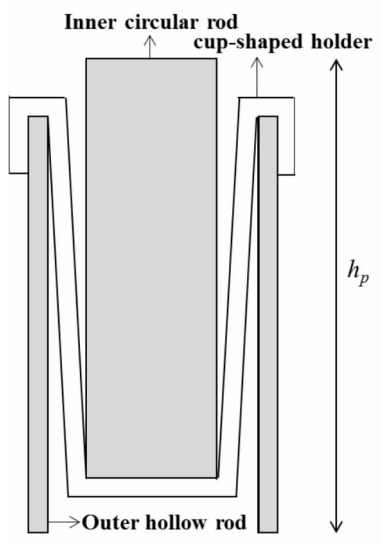

Fig. 2 Cross-section of multi-path support

From Eq. (4), it is found that the thermal conductivity of filler material also has an effect on the insulation performance. Its thermal conductivity is smaller than that of the general VIP filler material. It can be further reduced by using a multi-layered filler material. Multi-layered filler material is made using the glass wool sheets inserting the several radiation shields with high reflectivity. The radiative thermal conductivity k_r of the filler material is also affected by the number of radiation shields N as

$$k_r = \frac{4\sigma T_m^4 h_p}{\frac{3\beta h_p}{4} + N\left(\frac{2}{\varepsilon_{RS}} - 1\right)} \quad (5)$$

where

σ = Stefan-Boltzmann's constant,

T_m mean temperature,

β= extinction coefficient of filler material,

ε_{RS} =emissivity of radiation shield.

Fig. 3 shows the schematic of the MPS/multi-layer VIP.

3. Experiments

MPS-supported VIP (Fig. 3) was fabricated to test its performance. First, thermal conductivity of the pillar-supported core structure is measured by vacuum guarded hot plate (VGHP); a GHP is installed in a vacuum chamber with components to control inner pressure and pressing load. Thus, the thermal conductivity can be measured in variable surrounding pressure and external pressing load. The uncertainty of this apparatus mainly comes from supplied electric power and this error increases with decreasing power. In other words, the smaller the thermal conductivity of sample is, the bigger the uncertainty. For the thermal conductivity of 1 mW/(m · K), the uncertainty is approximately 8%.

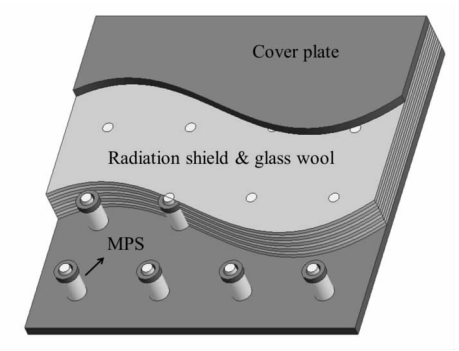

Fig. 3 Schematic of VIP with MPS-supported core structure

Tab. 1 shows the specifications of pillar-supported core structure sample. The total height of the structure is 15 mm. The cover plates are made of stainless steel to reduce the maximum deflection with a small thickness. Al-metallized film is used as the radiation shield, whose emissivity is equal to 0.11. The glass wool has an extinction coefficient of 8565 m^{-1} when it is un-pressed.

Tab. 1 Specifications of pillar-supported core structure

Pillar (MPS)	material	polycarbonate stainless steel
	height	12.6 mm
	arrangement	4× 4
Cover plate	material	stainless steel
	thickness	1.2 mm
	area	280× 280 mm^2
	span of pillar	70 mm
	maximum deflection	0.5 mm
Multi-layered filler material	material	glass wool Al-metallized film
	number of layers	16 layers

4. Results and discussions

The effective thermal conductivity of pillar-supported core structure is measured and compared withthe estimated value from Eq. (4). The measured value using the aforementioned multi-layered filler is 1.18 mW/(m • K). When only glass wool is used as the filler material without pillars, the measured value is 2.08 mW/(m • K). The thermal conductivity of proposed structure is thus about half of current glass wool-based VIP. The insulation performance is increased by 76%. This result shows that the pillar-supported core structure exhibits a high insulation performance although its production cost may be more expensive.

The estimated value of effective thermal conductivity of pillar-supported core structure is obtained from Eq. 4. It is sum of the thermal conductivity of multi-layered filler material and support structure. The first one is estimated to be 0.61 mW/(m • K). The second one is 0.47 mW/(m • K) with the simple cylindrical pillar, whereas it is 0.39 mW/(m • K) with the MPS. The ratio h_p/h_{eff_MPS} calculated by numerical simulation is equal to 0.84. The total effective thermal conductivity of pillar-supported core structure with MPS is estimated to be 1.0 mW/(m • K). The relative error between measured and calculated values is 15.2%. This error results from uncertainty of material properties and measuring equipment.

The insulation performance of support structure can be further enhanced by reducing radiation in MPS. Polycarbonate generally has the emissivity of around 0.8. However, if the surface of the polycarbonate is coated using the metal with low emissivity, the insulation performance can be improved by 35%. Also, if thinner glass wool sheets are prepared, it is possible to stack more layers to reduce the thermal conductivity of filler material.

5. Conclusions and outlook

Vacuum insulation panel with pillar-supported core structure is proposed and investigated. The pillar-supported core structure is composed of two cover plates, pillars and multi-layered filler material. The support structure made of cover plates and pillars sustains the atmospheric pressure instead of the filler material. Thus, thermal conductivity of this un-pressed filler material can be decreased. Multi-layered filler material is glass wool sheets with interlayered radiation shields of low emissivity to decrease radiation. The pillar-supported core structure is designed by considering mechanical stability and heat transfer. After a sample is fabricated, its thermal conductivity is measured using VGHP. The measured value is 1.18 mW/(m • K). This thermal conductivity is about half compared with commercial glass wool VIP.

Acknowledgements

This work was supported by the National Research Foundation of Korea (NRF) grant funded by the Korea government (MEST) (2013R1A2A2A07068924).

References

[1] J. Kim, T. H. Song, Vacuum insulation properties of glass wool and opacified fumed silica under variable pressing load and vacuum level 64 (2013), 783 - 791.

[2] S. E. Kalnæs, B. P. Jelle, Vacuum insulation panel products: A state-of-the-art review and future research pathways, Applied energy 116 (2014) 355 - 375.

[3] B. P. Jelle, Traditional, state-of-art and future thermal building insulation materials and solutions - properties, requirements and possibilities, Energy and Buildings 43 (2011) 2549 - 2563.

[4] J. S. Kwon, C. H. Jang, H. Jung, T. H. Song, Vacuum maintenance in vacuum insulation panels exemplified with a staggered beam VIP, Energy and Buildings 42 (2010) 590 - 597.

[5] J. Kim, J. H. Lee, T. H. Song, Vacuum insulation properties of phenolic foam, International Journal of Heat and Mass Transfer 55 (2012) 5543 - 5549.

[6] A. C. Ugural, Stresses in plates and shells (1981) New York, McGraw-Hill, 88.

[7] W. D. Callister, Materials science and engineering: an introduction (2007) Asia, John Wiley & Sons, 133 - 146.

[8] F. P. Incropera, D. P. Dewitt, T. L. Bergman, A. S. Labine, Introduction to Heat Transfer 5th ed. (2005) John Wiley & Sons, 96 - 101.

The Effect of Rice Husk Ash on the Performance of VIP Core Materials

Guan Shengnan, Chen Zhaofeng*, Li Chengdong

Super Insulation Composite Laboratory, Nanjing University of Aeronautics and Astronautics, Nanjing, 210016, P. R. China

Abstract

The rice husk ash (RHA) contains over 70% of silica in an amorphous form and a lot of applications is being developed for it all over the world. Mixtures with different kinds of powders and fibers can be fabricated into wet-laid mat by wet method and the properties of suspension influences the performance of the resulting wet-laid mat. In this paper, 10wt%, 20wt%, 30wt%, 40wt% and 50wt% addition of RHA were mixed with glass wool with 30% centrifugal glass wool (CGW) and 70% flame attenuated glass wool (FAGW) in cylindrical container and were beaten by 5000 revolutions for uniform distribution. Among them, RAH was used as filler material since it contributes significantly to the reduction of production cost of the VIPs and help to save energy and protect the environment. Beating degree, drainage time and physical stability of the suspension were investigated. In order to evaluate the physical stability of the hybrid suspension, sedimentation of RHA in the suspension was also observed. Experimental results show that the beating degree of hybrid suspension decreased dramatically with the mass fraction of RHA. The addition of RHA resulted in a highly unstable state of the suspension. Physical properties of the wet-laid mat and thermal conductivity of the as-prepared VIP will be analyzed in the coming days.

Keywords rice husk ash, vacuum insulation panel, core materials, thermal conductivity, beating degree

1. Introduction

For several decades, thermal insulation has been the preferred way to improve buildings energy efficiency, and the thermal insulation requirements have increased steadily. As a new insulation method, vacuum insulation panel (VIP) is actively researched recently, as it has very low thermal conductivity reaching to 0.002～0.004W/(m·K) at center of panel[1]. It is generally composed of an envelope and a core. Insulation performance and service-life of VIPs are heavily dependent on the core material. Porous materials are frequently adopted because they can be evacuated easily. Glass wool and fumed silica are typical examples in these days. Insulation foams such as polystyrene and polyurethane foam have been used since the early stage thanks to their low price but they have relatively poor insulation performance and large pore size[2]. Though VIP is a high performance thermal insulation material, it is very expensive. The need of reducing the cost associated to VIP production drove much research towards the study of supplementary materials used in VIP.

Rice husk ash (RHA) is one of the promising materials that can be blended with cement for the production of durable concrete and the reduction of the environmental impact of the cement industry. Commercially available RHA contains 3% or more graphitic carbon which determines the dark pigmentation of the material. Recent studies have led to the production of carbon neutral rice ash named OWRHA (Off-White Rice Husk Ash), with no graphitic carbon, no crystalline SiO_2 and toxic metals, so legitimately considered environmental friendly[3]. The RHA in turn contains around 85%～90% amorphous silica and it is a great environment threat causing damage to the land and the surrounding area in which it is dumped[4,5]. In fact, in the ancient China, Chinese people have already tried to mix RHA with clay in the building to keep the

* Corresponding author, Tel: 86-25-52112909, Fax: 86-25-52112626, E-mail: zhaofeng_chen@163.com

room warm. Now, RHA is added to glass wool to create the novel core materials.

In this paper, 10wt%, 20wt%, 30wt%, 40wt% and 50wt% addition of RHA were mixed with glass wool with 30% centrifugal glass wool (CGW) and 70% flame attenuated glass wool (FAGW). Beating degree and physical stability of the suspension were investigated.

2. Experimental

CGW and FAGW were provided by Suzhou VIP New Material Co., Ltd. (Taicang, PR China). Fig. 1 shows the overview of GBJ - A prototype fiber dissociation device. The fiber dissociation device was primarily made up of one main body, one cylindrical tank, one bar, and three rotational impellers. A total of 2.00 g of glass wool and RHA were mixed in a cylindrical tank for 30 min containing 1000 ml of water and then dispersed by the rotational impellers within the prototype fiber dissociation device. The rotation frequency of the impellers was $48.3 \pm 1.65\ s^{-1}$ while the beating revolutions were 5000r [6]. The addition of RHA were 10wt%, 20wt%, 30wt%, 40wt% and 50wt%, respectively. While the glass wool consisted of 30% CGW and 70% FAGW. 20 ml of the mixture suspension containing RHA and glass wool was fed into a transparent glass bottle. Drainage resistance and drainage time of the mixture suspension was measured by beating freeness tester (PNSDJ100), according to ES ISO 5267 - 1: 2012 standard. Fiber and RHA distribution of the mixture suspension was observed after 0min, 30min, 90min, 150min, 5h, 10h and 24h, respectively.

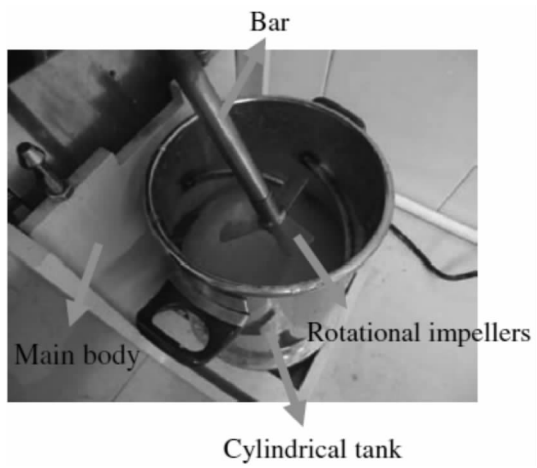

Fig. 1 The overview of GBJ - A prototype fiber dissociation device

3. Results and discussion

3.1 Drainage resistance and drainage time of the mixture suspension

In general, papermaking process is a rapid water removal operation. One of the most important factors characterizing the performance of fiber suspension filtration is its drain ability, because it determines the filtration rate of water in the fiber suspension. The drainage resistance of glass wool suspension depends on the fiber aspect ratio and concentration of the suspension [7]. Fig. 2 shows the drainage resistance and drainage time of the mixture suspension after beaten with additional RHA of 10wt%, 20wt%, 30wt%, 40wt% and 50wt%. The drainage time-RHA content curve could be divided into there stages. At stage I, from 0 to 10wt%, the drainage time of the mixture suspension sharply decreased from 29s (with no RHA) to 27.57s (with 10wt%). At stage II, from 10wt% to 40wt%, the drainage time of the suspension gradually decreased to 26.7s (with 40wt%). At stage III, from 40wt% to 50wt%, the drainage time of the suspension sharply decreased to 25.6s. It was also found that the drainage resistance gradually decreased from 27 °SR (with no RHA) to 17 °SR (with 50wt%). The drain ability of suspensions is mainly affected by fibers. RHA can't attach to fibers, they can't block the channels made by fibers. The addition of RHA resulted in the reduction of glass fiber content, which finally caused the decrease of drainage time and drainage resistance.

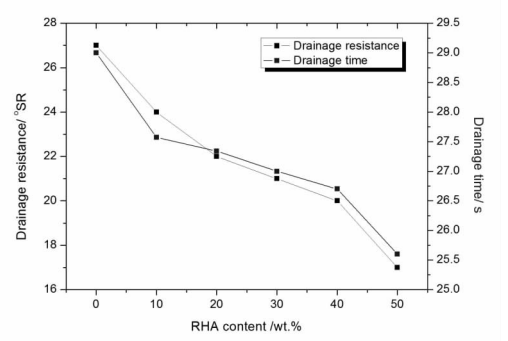

Fig. 2 Change in the drainage resistance and drainage time of the mixture suspension with addition of RHA

3.2 Fiber and RHA distribution in the mixture suspension

Glass fiber distribution under wet condition was

affected by both the flow characteristics of the fiber suspension and the interactions with neighboring fibers [8]. Fig. 3 shows fiber and RHA distribution of the mixture suspension after 0min, 30min, 90min, 150min, 5h, 10h and 24h. After the beating process (see Fig. 3 (a)), the layer was obvious, most RHA were at the top of the beaker, while fibers were mainly at the bottom of the beaker and tried to aggregate into fiber clumps. After 30 min (see Fig. 3 (b)), there was no obvious change compared with 0 min situation. But it seemed the fiber clumps at the bottom become bigger. After 90 min (see Fig. 3 (c)), the RHA and sparse glass fibers settled down slowly and RHA tended to distribute uniformly in the fibers. After 150 min (see Fig. 3 (d)), it was interesting that fiber clumps with some RHA occurred at the top of the beaker and sparse fibers with few RHA remained at the bottom. After 5 h (see Fig. 3 (e)), fibers and RHA aggregated slowly at the top of the beaker. After 10 h (see Fig. 3 (f)), the clumps became bigger and muddy. After 24 h (see Fig. 3 (g)), the fiber clumps became compact (compared to Fig. 3 (f)) and RHA distributed evenly. The central part of the beaker were nearly clear water, while at the bottom of the beaker, were few fibers and RHA. The changes of fiber and RHA distribution in the mixture suspension reflected a highly unstable state of the suspension. And it still needs further investigations to know how the RHA affects the suspension.

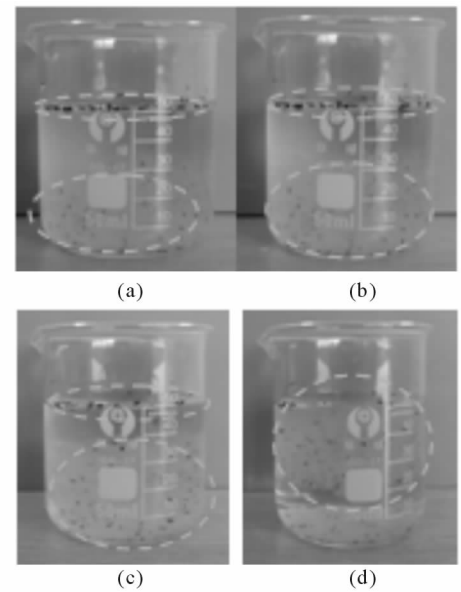

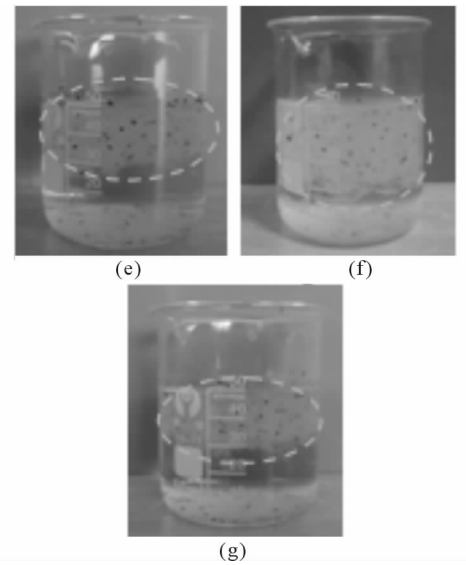

Fig. 3 Fiber and RHA (with 30wt%) distribution in suspension
(a) 0 min; (b) 30 min; (c) 90 min; (d) 150 min; (e) 5 h; (f) 10 h; (g) 24 h

4. Conclusions

Experimental results showed that the drainage resistance and drainage time of hybrid suspension decreased dramatically with the mass fraction of RHA. The addition of RHA resulted in a highly unstable state of the suspension. Further research work is needed to study the influence mechanism of RHA. Also, physical properties of the wet-laid mat and thermal conductivity of the as-prepared VIP are needed to be analyzed in the coming days.

Acknowledgments

The author would like to thank the Jiangsu Project BA2013097 and National Project 2015DF153000.

References

[1] Wegger E, Petter B, Ab J, et al. Accelerated Ageing of Vacuum Insulation Panels (VIPs) [J]. Norsk Informatikkonferanse, 2010.

[2] Wakili K G, Stahl T, Brunner S. Effective thermal conductivity of a staggered double layer of vacuum insulation panels[J]. Energy & Buildings, 2011, 43(6):1241 - 1246.

[3] Ferraro R M, Nanni A. Effect of off-white rice husk ash on strength, porosity, conductivity and corrosion resistance of white concrete[J]. Construction & Building Materials, 2012, 31(6):220 - 225.

[4] Soares L W O, Braga R M, Freitas J C O, et al. The effect of rice husk ash as pozzolan in addition to cement Portland class G for oil well cementing[J]. Journal of Petroleum

Science & Engineering，2015；80－85.

[5] Gon04alves M R F，Bergmann C P. Thermal insulators made with rice husk ashes：Production and correlation between properties and microstructure[J]. Construction & Building Materials，2007，21(12)：2059－2065.

[6] Li C D，Chen Z F. Effect of beating revolution on dispersion of flame attenuated glass wool suspension and tensile strength of associated glass fiber wet-laid mat[J]. Powder Technology，2015，279.

[7] M. A. Hubbe，J. A. Heitmann，Review of factors affecting the release of water from cellulosic fibers during paper manufacture，BioResources 2 (2007) 500－533.

[8] O. J. Rojas，M. A. Hubbe，The dispersion science of papermaking，J. Dispers. Sci. Technol. 25 (2004) 713－732.

Fiber Reinforced Hollow Silica Nanospheres for Thermal Insulation Applications

Gao Tao[a*], Bjørn Petter Jelle[a,b]

a. Norwegian University of Science and Technology (NTNU), Department of Civil and Transport Engineering, NO-7491 Trondheim, Norway
b. SINTEF Building and Infrastructure, Department of Materials and Structures, NO-7465 Trondheim, Norway

Abstract

This study proposes the assembly of robust nano insulation materials (NIM) based on hollow silica nanospheres (HNSN). A special focus is given on fiber reinforced HSNS composites, which can be achieved by mixing the fiber reinforcements with core-shell typed polystyrene-silica nanospheres followed by an annealing treatment to remove the organics. The as-prepared composites show potential as high performance thermal insulation materials, e. g. as core materials for vacuum insulation panels.

Keywords nanomaterial, thermal insulation, hollow silica nanosphere, fiber, reinforcement

1. Introduction

In most European countries, buildings account for approximately 40% of the total energy use and 30% of the greenhouse gas emissions; thus highlighting the importance of improving the energy efficiency in the building sector [1]. In this respect, the application of thermal insulation is very important, which has been regarded as one of the most cost-effective measures to achieve energy efficient buildings [2]. Traditional thermal insulation materials such as cork, mineral wool, cellulose, and polystyrene are capable of preserving energy to certain extents. However, to obtain a desired insulation level would require thicker or multiple layers of these materials due to their relatively large thermal conductivities (typical values around 30 ~ 40 mW/(m·K)). Very thick building envelopes are not feasible with respect to building weight and dimensions, material economy, transport volumes, architectural design, etc. Hence, developing new, high performance thermal insulation materials is a crucial need for the insulation market [2, 3].

Vacuum insulation panels (VIP) and silica aerogels represent probably the best thermal insulation solutions today with respect to their very low thermal conductivity values, i. e. ~ 4 and 15 mW/(m·K) for VIP and silica aerogels, respectively [4, 5]. However, both VIP and silica aerogels are very costly solutions compared to other insulation materials and have also various drawbacks [3]. Several attempts have recently been made to develop novel materials to meet the requirements of super insulation**, and the application of nanotechnology is indeed promising [6-8]. The author has reported the synthesis of nano insulation materials (NIM) by using hollow silica nanospheres (HSNS), as shown in Fig. 1 [6]. The properties of HSNS NIM can be controlled by e. g. tuning the sizes of HSNS (i. e. sphere diameter D and shell thickness L); typical thermal conductivities ranging from 20 to 40 mW/(m·K) can be obtained.

Although promising, it remains a great challenge to turn the conceptual HSNS NIM into a practical

* Corresponding author, Tel: 47-99895405, E-mail: tao.gao@ntnu.no

** Super Insulation Materials (SIM) should have a thermal conductivity below 25 mW/(m·K) if air-filled, below 20 mW/(m·K) if gas-filled, and below 15 mW/(m·K) if evacuated.

building material, and substantial research efforts are obviously required. The objective of this work is to discuss the possibilities of making high performance thermal insulation materials based on HSNS. Monolithic HSNS NIM and HSNS composites are proposed, with emphasis being given to fiber reinforced HSNS composites, which can be used as a mechanically robust thermal insulation material or for other applications, e. g. as core materials for VIP.

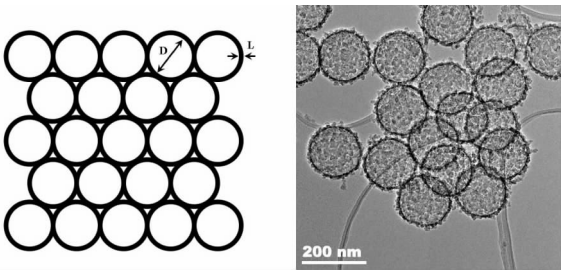

Fig. 1 Schematic drawing and transmission electron microscopy image of a HSNS NIM [6]

2. Monolithic HSNS NIM

Monolithic HSNS NIM can be prepared by binding properly the individual HSNS together, see for example, Fig. 2. However, the intrinsic spherical arrangement (see Fig. 1) endows monolithic HSNS NIM a weak mechanical strength that is not suitable for many practical applications. Therefore, structural enhancement of monolithic HSNS NIM needs to be considered. In this respect, the application of binding media such as crosslink organic molecules seems very promising [9].

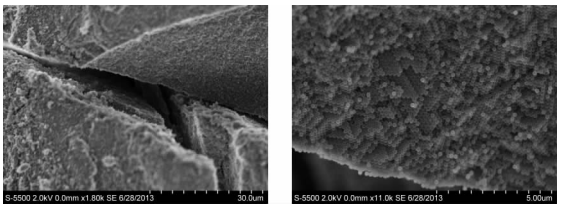

Fig. 2 Monolithic HSNS NIM (scale-bar 30 μm to left and 5 μm to right)

3. HSNS composites

Previous study has indicated that the manufacture cost of HSNS NIM is relatively high [10]. In this regard, forming HSNS composites may provide interesting alternatives for their practical applications. Depending on the performance requirements, the HSNS can be used either as the main phase or as additives of the resulting composites. It is worth noting that forming HSNS composites may also help to reduce the overall thermal conductivities, in particular the radiative thermal transfer by adding thermal absorbers such as TiO_2 or carbon black [11].

Fibrous materials are ideal for structural reinforcement of granular aggregations [12]. Glass wools, for example, have widely been used for thermal insulation purposes; these mineral fibers may also be used as a structural reinforcement for HSNS NIM, see Fig. 3. A preliminary experimental investigation has indicated that the synthesis of glass fiber reinforced HSNS composites is rather straight forward, which can be performed by (1) mixing the fiber reinforcements with core-shell typed polystyrene-silica nanospheres and (2) an annealing treatment at around 550℃ to remove the organics. By varying the dimensions of glass fibers (length and diameter) as well as their concentration, it is possible to assemble a mechanical robust porous material for thermal insulation applications. This is currently an on-going research work.

Fig. 3 Schematic drawing of the synthesis of a fiber reinforced HSNS composite

4. Conclusions and outlook

Hollow silica nanospheres (HSNS) can be used to assemble high performance thermal insulation materials, and forming mechanical robust composites such as fiber reinforced HSNS, represents promising alternatives for their practical applications.

Acknowledgements

This work has been supported by the Research Council of Norway and several partners through "The Research Centre on Zero Emission Buildings" (ZEB)

References

[1] A. J. Marszal, P. Heiselberg, J. S. Bourrelle, E. Musall, K. Voss, I. Sartori, A. Napolitano, Zero Energy

Building — A review of definitions and calculation methodologies, Energy and Buildings 43 (2011) 971 - 979.

[2] B. P. Jelle, A. Gustavsen, R. Baetens, The path to the high performance thermal building insulation materials and solutions of tomorrow, Journal of Building Physics 34 (2010) 99 - 123.

[3] B. P. Jelle, Traditional, state-of-the-art and future thermal building insulation materials and solutions - Properties, requirements and possibilities, Energy and Buildings 43 (2011) 2549 - 2563.

[4] R. Baetens, B. P. Jelle, J. V. Thue, M. J. Tenpierik, S. Grynning, S. Uvsløkk, A. Gustavsen, Vacuum insulation panels for building applications: A review and beyond, Energy and Buildings 42 (2010) 147 -172.

[5] R. Baetens, B. P. Jelle, A. Gustavsen, Aerogel insulation for building applications: A state-of-the-art review, Energy and Buildings 43 (2011) 761 - 769.

[6] T. Gao, B. P. Jelle, L. I. C. Sandborg, A. Gustavsen, Monodisperse hollow silica nanospheres for nano insulation materials: synthesis, characterization, and life cycle assessment, ACS Applied Materials & Interfaces 5 (2013) 761 - 767.

[7] Y. Luo, C. Ye, Using nanocapsules as building blocks to fabricate organic polymer nanofoam with ultra low thermal conductivity and high mechanical strength, Polymer 53 (2012) 5699 - 5705.

[8] B. Wicklein, A. Kocjan, G. Salazar-Alvarez, F. Carosio, G. Camino, M. Antonietti, L. Bergström, Thermally insulating and fire-retardant lightweight anisotropic foams based on nanocellulose and graphene oxide, Nature Nanotechnology 10 (2015) 277 - 283.

[9] L. A. Capadona, M. A. B. Meador, A. Alunni, E. F. Fabrizio, P. Vassilaras, N. Leventis, Flexible, low-density polymer crosslinked silica aerogels, Polymer 47 (2006) 5754 - 5761.

[10] T. Gao, L. I. C. Sandberg, B. P. Jelle, Nano insulation materials: Synthesis and life cycle assessment, Procedia CIRP 15 (2014) 490 - 495.

[11] J. Kuhn, T. Gleissner, M. C. Arduini-Schuster, S. Korder, J. Fricke, Integration of mineral powders into SiO_2 aerogels, Journal of Non-Crystalline Solids 186 (1995) 291 - 295.

[12] Y. Liao, H. Wu, Y. Ding, S. Yin, M. Wang, A. Cao, Engineering thermal and mechanical properties of flexible fiber-reinforced aerogel composites, Journal of Sol-Gel Science and Technology 63 (2012) 445 - 456.

The Influence of Different Cross-sectional Structure of Glass Fiber Felt on Its Thermal Conductivity and Heat Transfer Mechanism

Li Yanming, Chen Zhaofeng*, Yang Yong, Wu Cao

Super Insulation Composite Laboratory, College of Materials Science and Technology, Nanjing University of Aeronautics and Astronautics, Nanjing, 210016, P. R. China

Abstract

Glass fiber felts are getting more and more popular on the market as thermal reduction in the field of building engineering due to the advantages of low thermal conductivity, good insulation properties, stable chemical properties, etc. In this paper, glass fiber felt was produced by flame blowing process, thermal conductivity of different cross-sectional morphology of glass fiber felts such as micro-layer and random was considered. The thermal conductivity were determined by heat flow meter thermal conductivity instrumentation (Netzsch HFM 436), cross-sectional morphology of glass fiber were observed by optical microscope. The results showed that thermal conductivity coefficient of glass fiber felt with similar areal density and thickness was random > micro-layered, and the mean thermal conductivity were 31mW/(m·K) and 36mW/(m·K), respectively. Lastly, the conclusion that using the heat transfer mechanism of the fibrous materialst to explain this phenomenon had also been drawn by experiment.

Keywords glass fiber felt, cross-sectional structure, thermal conductivity, heat transfer mechanism

1. Introduction

Glass fiber felts are used widely as insulations and building sections in commercial and industrial applications. Generally, insulation materials are divided into several types, these being organic, inorganic, combined, and other types, depending on the chemical structures. Organic insulation material are mainly polyurethane foam, polystyrene board, phenolic foam, etc. Inorganic insulation material mainly concentrate on the aerogel felt, glass wool, rock wool, micro-nano insulation board, etc [1].

Glass fiber felts have excellent thermal insulation and sound absorption performance, light weight and stable chemical performance, recognized as the most superior thermal insulation and acoustic materials. Most building insulation projects use glass fiber felts, and they are also used for other applications, such as, aviation, aerospace, thermal insulation and cold areas [2-4]. Thermal conductivity is measured to assess the ability of the heat transfer of materials, one of the main thermal physical properties of thermal insulation materials. The smaller the coefficient of thermal conductivity, the better the performance of thermal insulation material. Generally, thermal properties of a fibrous material depend on: thermal properties of each phase (fiber and air), fiber volume fraction, and fiber size, orientation and mass distribution [5]. The value of the thermal conductivity of heat-insulating materials is affected by their density and kind, the size and location of pores, the chemical composition and molecular structure of hard constituents, the emissivity of surfaces bounding the pores, and the kind and pressure of the gas filling the pores [6].

In this paper, cross-sectional morphologies of glass fiber felts are measured. Effect of cross-sectional morphology of glass fiber felt on thermal conductivity

* Corresponding author. Tel: 86-18952018969, E-mail: zhaofeng_chen@163.com

are explored, and the heat-transfer mechanism is explained. The paper is structured as follows: fabrication approaches and experimental approaches are introduced in Sec. 2. Cross-sectional morphology and experimental results on the thermal conductivity are presented in Sec. 3. Section. 4 concludes the paper.

2. Experiment

2.1 Glass fiber felt preparation

For this study, glass fiber felts were produced by flame blowing process. The preparation process is showed in Fig. 1, and this method include following steps: raw materials; raw materials melting; wire drawing; flame blowing; spray binder; glass fiber felt forming.

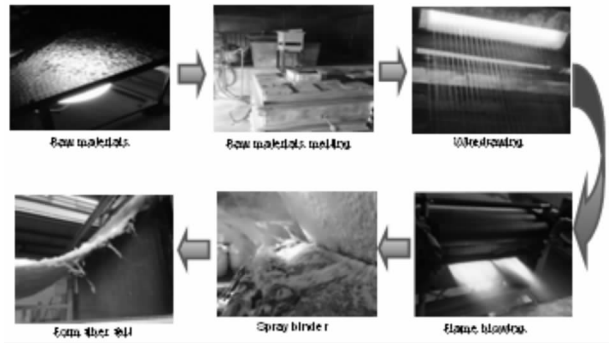

Fig. 1 The processing of glass fiber felt

2.2 Thermal conductivity and morphology measurement

Cross-sectional morphology and thermal conductivities are measured by optical microscope (BD-200) and heat flow meter (Netzsch HFM 436), respectively, as shown in Fig. 2.

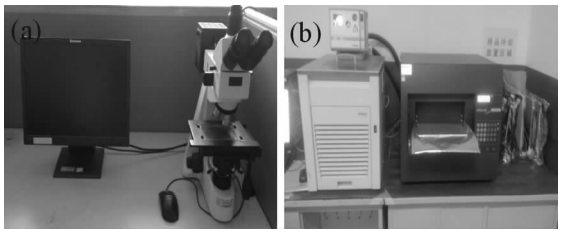

Fig. 2 Experimental device

(a) Photo of optical microscope;

(b) Photo of the coefficient of thermal conductivity test instrument

3. Results and discussion

3.1 Glass fiber felt structure description

Cross-sectional morphologies of glass fiber felts measured by optical microscope are shown in Fig. 3. It was showed that cross-sections of samples exhibited micro-layer and random structure, respectively. For micro-layer structure, the axes of fibers were located on planes parallel to each other with random positions and orientations on these planes. However, random structure provided lots of fibers in 3D structures which were randomly positioned and oriented in space. The internal structure of all samples were investigated in Fig. 4. It indicated that the internal structure of samples were all disordered.

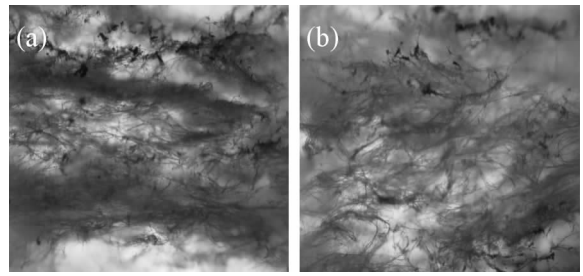

Fig. 3 Cross-sectional morphology of glass fiber felts

(a) micro-layered; (b) random

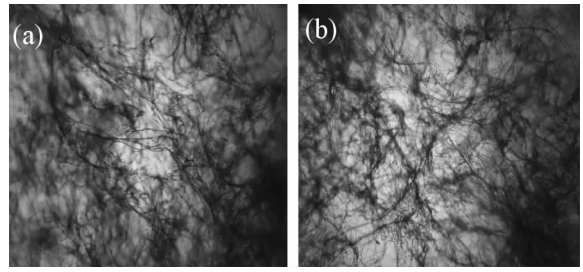

Fig. 4 Internal morphology of glass fiber felts with different cross-section

(a) internal structure of micro-layer;

(b) internal structure of random

3.2 Effect of the cross-sectional morphology of glass fiber felts on thermal conductivity

Thermal conductivities of glass fiber felts with different cross-sectional structure are shown in Fig. 5. For the same density and thickness, thermal conductivity of glass fiber felts was random > micro-layered. It also indicated that with the increase of the density, thermal conductivity of samples would be increased.

This phenomenon would be explained as: firstly, with the increase of layers, thermal resistance of glass fiber felts with micro-layer increased leading to lower thermal conductivity. Compared to micro-layer structure, the axis of fibers in 3D structures were

randomly positioned and oriented in space. 3D distribution led to abundance of interconnected fibers through the thermal-flow direction. The heat conductivity increased leading to the increase of the coefficient of thermal conductivity. Secondly, with the density increasing, thermal conductance through the solid was increased, the pore size and porosity were decreased, both radiation and convection through the pores were in the absence of main factors. Therefore, the results of coefficient of thermal conductivity was increased.

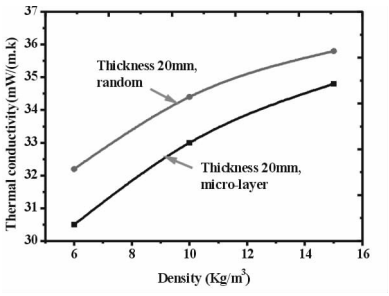

Fig. 5 Thermal conductivity of glass fiber felts with different cross-sectional structure

4. Conclusions

Glass fiber felts were successfully fabricated by flame blowing process. Thermal conductivity of glass fiber felts with similar areal density and thickness. However, different structure were random ＞ micro-layered , and the mean thermal conductivity were 31mW/(m • K) and 36mW/(m • K), respectively.

Acknowledgements

The author would like to thank the financial support of Jiangsu Project BA2013097 and National project 2015DFI53000.

References

[1] A. Karamanos et al. Energy and Buildings 40 (2008) 1402 - 1411.

[2] J. L. Qiu et al. China-Japan Joint Conference on Composite Materials (2012).

[3] Z. X. Sun et al. Journal of Materials Engineering and Performance 22 (2013) 3140 - 3146.

[4] Y. Yang et al. Applied Acoustics 91 (2015) 6 - 11.

[5] Y. Yang et al. Advanced Materials Research 628 (2013) 33 - 36.

[6] J. FRANCL et al. Journal of The American Ceramic Society-Francl and Kingery 37, 99 - 101.

Effective of Density and Thickness of Ultra-fine Glass Wool Felt on Thermal Conductivity Under High Temperature

Ye Xinli, Chen Zhaofeng*

Super Insulation Composite Laboratory, College of Materials Science and Technology, Nanjing University of Aeronautics and Astronautics, Nanjing, 210016, P. R. China

Abstract

Ultra-fine glass wool felt has been used in cryogenic industry such as refrigerators and building field for many years while rarely used under high temperature according to the reported literatures. In this paper, effective thermal conductivity and heat transfer mechanism of ultra-fine glass wool felt under high temperature were investigated. Thermal conductivity was measured by DRS－II under the temperature ranged from 100℃ up to 500℃ with the variation of density from 0.09 g/cm^3 to 0.126 g/cm^3. The results indicated that the thermal conductivity of ultra-fine glass wool felt decreased with the increase of its density under the same high temperature, while when the density was the same, thermal conductivity did not increase with increasing temperature, it initially decreased and then increased because of the heat radiation. Three heat transfer mechanism of ultra-fine glass wool felt were theoretically investigated with special emphasis on the solid conduction due to high temperature. It was concluded in the present paper that using the heat transfer mechanism of the ultra-fine glass wool felt explained this phenomenon had also been drawn by experiment.

Keywords ultra-fine glass wool felt, high temperature, thermal conductivity, heat transfer mechanism

1. Introduction

As modern materials, glass fibers play vital roles both in industrial applications and in everyday life. For example, they are widely used in national defense, military industry, airline and ships, chemical, oil, electric power, smelting, gold and other industrial sectors. It is also the ideal material for the production of sealed lead-acid battery glass fiber adsorption partition or filter paper and the preferred internal filling material of VIP (vacuum insulation panel). There are two different types of glass fibers: continuous and discontinuous fibers. The former, produced by continuously drawing a fiber from melts, are often used for optical communication and reinforcement of materials ranging from plastics to cement, while the latter, obtained by stretching short discontinuous fibers from melts using centrifugal processes, are used for thermal and acoustic insulation [1].

In recent years, thermal insulations have been the subject of great interest and importance to thermal engineers and to the early development of heat transfer technologies and decades of developments in heat transfer and use of thermal insulations in emerging technologies have extended the range of applications from cryogenic temperatures to high temperatures under re-entry conditions into planetary atmospheres. Metallic thermal protection systems (TPS) are an attractive technology to help meet the ambitious goals of future space transportation systems. Its thermal performance is of critical concern. There are many design options that have the potential to improve the thermal performance of metallic TPS. An obvious way to improve the thermal performance of metallic TPS is to develop more efficient non-load-bearing insulation. Ultra-fine glass

* Corresponding author, Tel:86－18952018969, E－mail: zhaofeng_chen@163.com

wool felt becomes the insulation candidate being considered for use in the metallic TPS on reusable launch vehicles, because Ultra-fine glass wool felt is a light qualitative thermal insulation material with small thermal conductivity, good heat and cold resistance, chemical stability [2-3].

For efficient insulation and structural applications, Ultra-fine glass wool felt should possess qualified heat insulation properties especially under high temperatures [4]. To obtain qualified heat insulation properties, one of the most important things is to test the coefficient of thermal conductivity under high temperature. The present paper focuses on the effective of density and thickness of ultra-fine glass wool felt's thermal conductivity under high temperature.

2. Experiment

2.1 The Ultra-fine glass wool felt preparation

The Ultra-fine glass wool felt used in this study was provided by Suzhou V. I. P. New Material Co., Ltd. (Taicang, PR China). Among them, Single-layer glass wool blanket were produced by wet method including following steps: preparing glass fiber slurry; dewatering the slurry to form a wet-laid mat; drying the mat; and cutting the mat to form finished CMLs. The length and width of the Ultra-fine glass wool felt were both 200 mm, while the thickness was 25 mm, 30 mm, 35 mm, respectively. The Single-layer glass wool blanket were horizontally put together to form the Ultra-fine glass wool felt. Table 1 lists the test specimens of fibrous materials acquired for measurements, with their given reference code, density and nominal thickness.

Tab. 1 List of test samples ordered by type, code, and mass densities

Material type	Sample code	Density / g·cm^{-3}	Nominal thickness/mm
fiberglass	FG-1	0.126	25
fiberglass	FG-2	0.105	30
fiberglass	FG-3	0.090	35

2.2 Water flow plate method

The coefficient of thermal conductivity under high temperature of the Ultra-fine glass wool felt was evaluated by water flow tablet tester (DRS-II), as shown in Fig. 1.

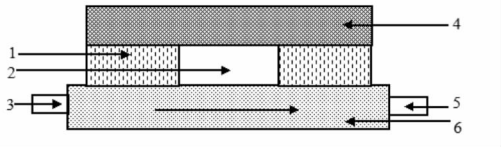

Fig. 1 Schematic of the thermal conductivity apparatus

1—ceramic wool; 2—Ultra-fine glass wool felt; 3—hot side; 4—heating equipment; 5—cold side; 6—Water copper plate

3. Results and discussion

3.1 Test result

The effective thermal conductivity of the Ultra-fine glass wool felt as a function of temperature difference across the samples for an environmental pressure is shown in Fig. 2. There were three different heat transfer mechanism: solid conduction through fibers, gas conduction in the void spaces between fibers, and radiation interchange through participating media in the fibrous insulation and at this pressure, gas conduction was negligible [5], therefore, the effective thermal conductivity comprised of contributions from solid conduction and radiation heat transfer. It was observed that the effective thermal conductivity varied nonlinearly with temperature difference across the sample, increasing rapidly with increasing temperature caused by the nonlinear radiation heat transfer. This effect was more pronounced with the lower density insulation, where radiation heat transfer was more dominant. But at room temperature, effective thermal conductivity decreased with the increase of thickness. This means that the radiation heat transfer was negligible at this temperature and the effective thermal conductivity did due to the solid conduction contribution, which was associated with the density of material. As the density increased, the solid conduction contribution increased, but the radiation heat transfer did not increase obviously, resulting in a gentle decrease in the effective thermal conductivity. Furthermore, the effective thermal conductivity did not appear to vary with sample thickness. But when at high temperature, the radiation heat transfer increased rapidly which was in proportion to the temperature, so the effective thermal conductivity increased rapidly as temperature increased. It also showed

that the Ultra-fine glass wool felt with lower density had a larger the effective thermal conductivity [6].

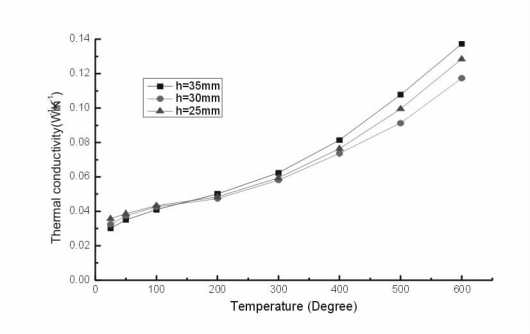

Fig. 2 Thermal conductivity of Ultra-fine glass wool felt with different density and temperature

3.2 The scanning photos of the Ultra-fine glass wool felt

The fiber morphology of the Ultra-fine glass wool felt observed by scanning electron microscope are showed in Fig. 3. The Ultra-fine glass wool felt are made up of a number of single fiber bundle, the diameter of which varies between 5～10 microns, and each single fiber bundle overlaps each other. There are many pores between fibers, the diameter of which varies between 56～65 microns, and the pore size of fiber is normally distributed, these two reasons account for the reason why the coefficient of thermal conductivity of the Ultra-fine glass wool felt is so small. On the one hand, the diameter of fiber is very small. When single fiber bundle overlaps each other by a point contact, the thermal resistance increases greatly because the contact area is very small, which reduces the coefficient of thermal conductivity rapidly. On the other hand, because of the increase of porosity of Ultra-fine glass wool felt, the proportion of solid conduction reduces greatly making the effective thermal conductivity decrease at the same time.

4. Conclusions

The effective thermal conductivity of the Ultra-fine glass wool felt increased with in creasing temperature and there were three different heat transfer mechanism, under low temperature, the solid conduction accounted for the main body which meant the Ultra-fine glass wool felt of lower density had small effective thermal conductivity while at high temperature radiation heat transfer was the most important and the higher one had small effective thermal conductivity.

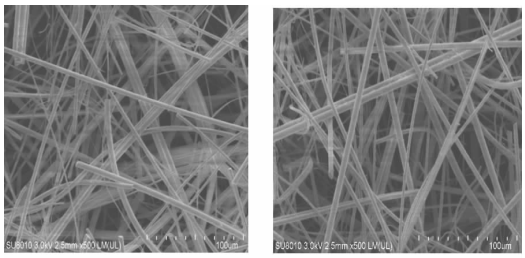

(a) (b)

Fig. 3 The fiber morphology of the Ultra-fine glass wool felt measured by scanning electron microscope

Acknowledgements

The author would like to thank the financial support from Jiangsu Project BA201397 and National Project 2015DFI53000.

References

[1] Stark, C. and J. Fricke, Improved heat-transfer models for fibrous insulations. International Journal of Heat and Mass Transfer, 1993. 36(3): p. 617 - 625.

[2] Yang, C. - L., S. - H. Sheu, and K. - T. Yu, The reliability analysis of a thin-edge blade wear in the glass fiber cutting process. Journal of Materials Processing Technology, 2009. 209(4): p. 1789 - 1795.

[3] Lonnroth, N., et al., Nanoindentation of glass wool fibers. Journal of Non-Crystalline Solids, 2008. 354(32): p. 3887 - 3895.

[4] Lee, S. - C. and G. R. Cunnington, Conduction and Radiation Heat Transfer in High-Porosity Fiber Thermal Insulation. Journal of Thermophysics and Heat Transfer, 2000. 14(2): p. 121 - 136.

[5] Yuen, W. W. and L. W. Wong, Heat Transfer by Conduction and Radiation in a One-Dimensional Absorbing, Emitting and Anisotropically-Scattering Medium. Journal of Heat Transfer, 1980. 102(2): p. 303 - 307.

[6] Daryabeigi, K., Heat Transfer in High-Temperature Fibrous Insulation. Journal of Thermophysics and Heat Transfer, 2003. 17(1): p. 10 - 20.

Effect of Large Pores in Silica Aerogels on the Gaseous Thermal Conductivity of Vacuum Insulation Panels

Yang Hailong*, Hu Zijun, Li Junning, Sun Chencheng, Wu Wenjun

Aerospace Research Institute of Materials & Processing Technology, Beijing, 100076, P. R. China

Abstract

The pore structure of core material has a significant effect on the thermal insulation properties of vacuum insulation panels (VIPs). Silica aerogels are the most promising core material due to their very small pores less than 100 nm. However, this material also consists of many pores larger than 100 nm, and these large pores certainly affect the thermal insulation performance of VIPs. The information on pores less than 100nm of a silica aerogel with a density of 0.15g/cm^3 was derived from nitrogen sorption, and then the effects of size and percentage of large pores in this silica aerogel on the gaseous thermal conductivity and tolerable internal gas pressure of VIPs were quantitatively described by using Kaganer model. The results indicated that the volume of large pores occupied 58% in the total pore volume of the prepared silica aerogel. With decreasing size or percentage of large pores in silica aerogel, the gaseous thermal conductivity of VIPs decreases while the tolerable internal gas pressure increases. Moreover, there is a linear relationship between the tolerable internal gas pressure and the size of large pores in log-log coordinate.

Keywords vacuum insulation panels, silica aerogels, large pore, gaseous thermal conductivity

1. Introduction

It is well known that vacuum insulation panels (VIPs) are one of the most promising high performance thermal insulation materials on the market today. Their thermal resistance is 5～8 times higher than that of conventional thermal insulation materials, so they have great potential applications in many areas. For example, VIPs have been used to reduce energy usage in hot-water applications, cold applications [1] and building applications [2－5]. In principle, VIPs can be described as an evacuated open porous material placed inside a multilayer envelope and their main components are core material, barrier envelope, getters and desiccants. The core material is important for a VIP to attain the highest possible thermal resistant and mechanical properties. Generally, the porous materials such as open porous foams, powders and fibers are used as core material. Previous studies [2, 4] indicate that the pore structure of core material has an important effect on the gaseous thermal conductivity, tolerable internal gas pressure, and the useful life time of a VIP. Now, it is clear that the requirement to sufficiently suppress gaseous thermal conductivity can be fulfilled at a comparatively higher internal gas pressure and the useful life time of VIPs can be extended if the material with small pores is used as core material [2, 5].

Silica aerogels with small pores less than 100 nm are very suitable to be used as core material for VIPs [4, 6]. Unfortunately, the test results of nitrogen sorption reveal that many pores larger than 100 nm may exist in this material because the pore volume determined by this method is commonly less than that calculated by its bulk density and skeletal density [7－15]. These large pores certainly affect the thermal insulation performance of VIPs.

In this paper, the information on pores less than 100 nm for a prepared silica aerogel has been obtained by nitrogen sorption, and then the effect of large pores on

* Corresponding author, Tel: 86－10－68755517, E－mail: yhl20032003@126.com

the gaseous thermal conductivity and tolerable internal gas pressure of VIPs has been discussed.

2. Experiments

2.1 Silica aerogel spreparation

A silica aerogel was prepared using a two-step acid-base catalyzed sol-gel process followed by supercritical drying. Tetraethoxysilance (TEOS), ethanol (EtOH), water and HCl were mixed under constant stirring conditions for 40 min at room temperature, which was followed by the addition of remaining water and ammonium hydroxide (NH_4OH) under vigorous stirring. The following molar ratio was used: TEOS: EtOH : H_2O : HCl : NH_4OH=1 : 10 : 4 : 6×10^{-3} : 1.8×10^{-2}. Pure water was used to prepare the desired concentrations of HCl and NH_4OH catalysts (1.2 mol/L and 1.4 mol/L). The as-prepared sol was cast into plastic cylinder molds with inner diameter of 11mm and allowed to gel. After 7 days of aging, silica wet gel was supercritically dried using EtOH as drying solvent in a stainless autoclave.

2.2 Character methods

The texture properties of the obtained silica aerogel were studied by adsorption of nitrogen at 77K with automatic instrument (NOVA 4200e, Quantachrome) over a wide relative pressure range from about 1.84×10^{-2} to 0.98. Prior to the measurement, the sample was degassed at 423K for 5h under vacuum to ensure that the sample was clean and free of moisture. The total pore volume was obtained by converting the amount of nitrogen adsorbed at a relative pressure of 0.98 to the volume of liquid adsorbed. The density of nitrogen employed for adsorption at 77K was 0.808g/cm^3. Pore size distribution was derived from the desorption isotherm according to BJH method.

The bulk density of samples was determined by their dimensions and mass measured after heated treatment at 150 ℃ for at least 4h.

3. Results and discussions

Fig. 1 (a) depicts the nitrogen adsorption/desorption isotherm of the investigated silica aerogel, and Fig. 1(b) shows the pore size distribution of it. It is obvious that all the pores in the material are less than 100 nm. Moreover, the test result shows that the average pore size is only 15.79 nm. However, it can be concluded that the information on the pore structures obtained by this method is not reliable if we compare the measured pore volume and the calculated value.

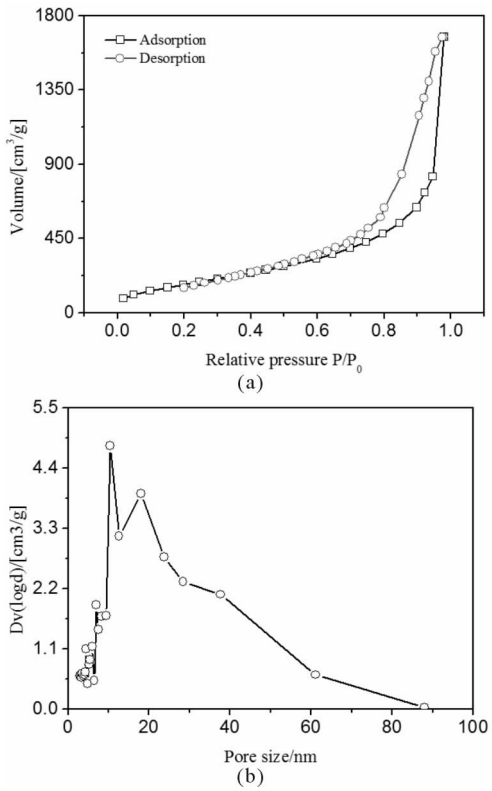

Fig. 1 (a) nitrogen adsorption/desorption isotherm of the investigated silica aerogel and (b) pore size distribution of it

The pore volume determined by nitrogen sorption is 2.59 cm^3/g, while the pore volume calculated according to equation (1) is 6.21 g/cm^3. Therefore, the volume of pores which are not detected by nitrogen sorption is 3.62 cm^3/g. This means that the volume of pores larger than 100 nm is 3.62 cm^3/g.

$$v=\frac{1}{\rho}-\frac{1}{\rho_s} \quad (1)$$

Where

v=pore volume,

ρ=bulk density of the sample. For the investigated silica aerogel, ρ=0.15g/cm^3,

ρ_s = skeletal density of the material under investigation. For silica aerogel, ρ_s = 2.2 g/cm^3.

In order to quantitatively describe the influence of

large pores on the gaseous thermal conductivity and tolerable internal gas pressure of VIPs, Kaganer model [16] established on Knudsen Number is used. In this model, the relationship between the gaseous thermal conductivity and the pore size of materials is described as

$$\lambda_g = \frac{\lambda_{g,0}}{1+2\beta K_n} \quad (2)$$

Where

$\lambda_{g,0}$ = thermal conductivity of the free gas at atmospheric pressure,

β=a constant including the interaction between gas molecules and the pore walls. For air, β=1.5,

K_n=Knudsen Number,

K_n is expressed as follows.

$$K_n = \frac{l_g}{D} \quad (3)$$

Where

l_g=mean free path of gas molecules,

D=pore size of porous materials.

The mean free path of gas molecules is a function of the temperature and gas pressure according to

$$l_g = \frac{K_B T}{\sqrt{2}\pi d_g^2 P_g} \quad (4)$$

Where

K_B=Boltzmann constant,

T=thermodynamic temperature,

d_g=average size of gas molecules,

P_g=pressure of the gas filled in pores.

It should be mentioned that formula (2) is derived for the gas transport in a gap between parallel walls, so the porosity of porous material must be considered when it is applied to this material. In this case, the formula should be expressed as

$$\lambda_g = \frac{\phi\lambda_{g,0}}{1+2\beta K_n} \quad (5)$$

Where

ϕ=the porosity of the porous material.

In case of a porous material with two different pore size D_1, D_2, and two contributions to the total porosity ε_1, ε_2, that act with respect to the heat transfer as parallel paths, the total gaseous thermal conductivity can be written as a superposition of two terms [17]

$$\lambda_g = \frac{\varepsilon_1\phi\lambda_{g,0}}{1+2\beta K_{n_1}} + \frac{\varepsilon_2\phi\lambda_{g,0}}{1+2\beta K_{n_2}} \quad (6)$$

For the investigated silica aerogel sample, ε_1 and ε_2 are 41.71% and 58.29% respectively. For simplicity, the measured averaged pore size (15.79nm) is used as D_1, and the assumed size of large pores is used as D_2, the calculated gaseous thermal conductivities at various internal gas pressures are shown in Fig. 2. It can be seen that the gaseous thermal conductivity at all gas pressures significantly decreases with decreasing size of large pores. That is to say, the tolerable internal gas pressures can be increased with decreasing size of large pores. Fig. 3 shows the tolerable internal gas pressures required to suppress the gaseous thermal conductivity to 0.003 W/(m·K), 0.002 W/(m·K), 0.001 W/(m·K) and 0.0005 W/(m·K) as a function of the size of large pores. It is more intuitive to see that reducing size of large pores has a positive influence on the tolerable internal gas pressure. Moreover, there is a liner relationship between the tolerable internal gas pressure and the size of large pores in log-log coordinate as shown in Fig. 4.

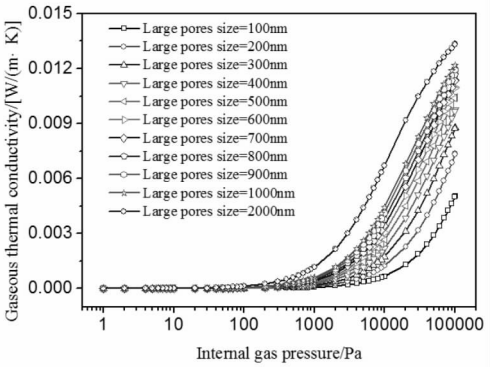

Fig. 2 Calculated gaseous thermal conductivity of VIPs, whose core material is silica aerogels with different large pores, as a function of internal gas pressure

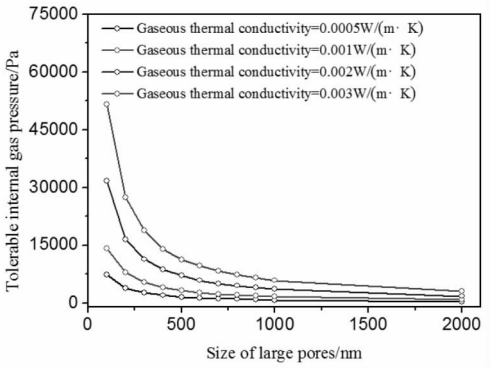

Fig. 3 Relationship between the tolerable gas pressure of VIPs and the size of large pores in silica aerogels

The percentage of large pores in the total pore volume of silica aerogels also has a significant influence on the thermal insulation performance of VIPs. Fig. 5 shows the calculated gaseous thermal conductivities of VIPs at different internal gas pressures. In these calculations, the sizes of large pores in silica aerogels are assumed as 100nm, 500nm and 2000nm respectively, and the percentages of them vary from 58% to 0. It is obvious that the gaseous thermal conductivity decreases with decreasing percentage of large pores. The variation of tolerable internal gas pressure, at which the gaseous thermal conductivity can be reduced to 0.003 W/(m·K), 0.002 W/(m·K), 0.001 W/(m·K) and 0.0005 W/(m·K), is described in Fig. 6. It is noted that the required gaseous thermal conductivity can be reached even at ambient pressure when the percentage of large pores is sufficient low. For example, the calculated gaseous thermal conductivity shown in Fig. 5(a) is below 0.02 W/(m·K) at ambient pressure when there is no large pores in the investigated silica aerogel, so the requirement to reduce gaseous thermal conductivity to 0.002 W/(m·K) and 0.003 W/(m·K) can be fulfilled at ambient pressure as shown in Fig. 6(a). From Fig. 6, we also can see that the internal gas pressure needed increases when the percentage of large pores decreases.

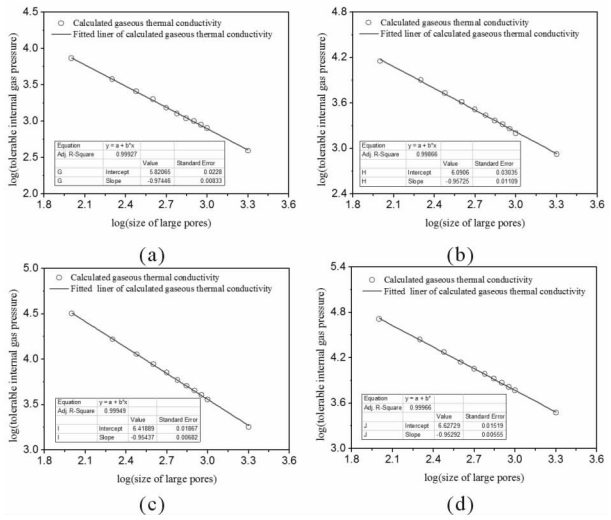

Fig. 4 Relationship between the tolerable gas pressure of VIPs and the size of large pores in silica aerogels in log-log coordinate

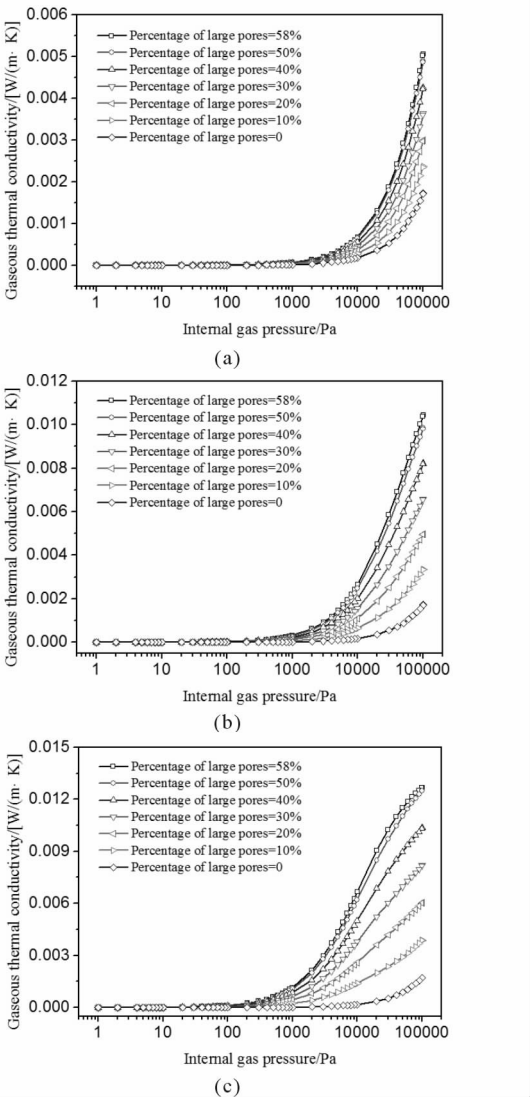

Fig. 5 Calculated gaseous thermal conductivity of VIPs, whose core material is silica aerogels with different percentage of large pores, as a function of internal gas pressure. The size of large pores are assumed as 100nm (a), 500nm (b) and 2000nm (c)

4. Conclusions and outlook

Nitrogen sorption measurement indicates that the volume of large pores occupies more than 50% in the total pore volume of the investigated silica aerogels. Calculations using Kaganer model shows that with decreasing size or percentage of large pores in silica aerogel, the gaseous thermal conductivity of VIPs decreases while the tolerable internal gas pressure increases. Moreover, there is a linear relationship between the tolerable internal gas pressure and the size of large pores in log-log coordinate.

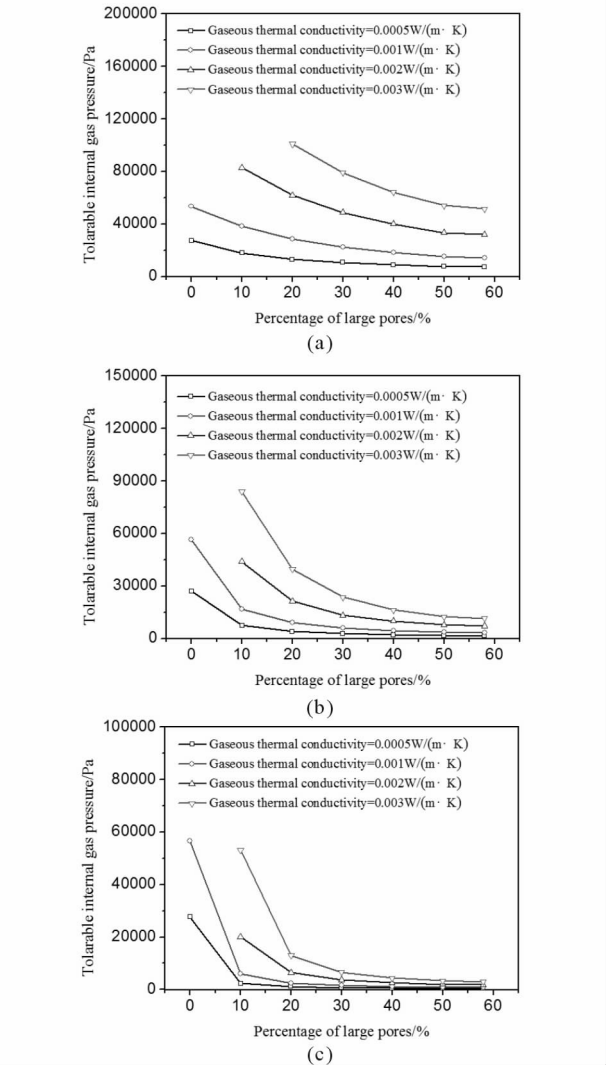

Fig. 6 Relationship between the tolerable gas pressure of VIPs and the percentage of large pores, whose size are assumed as 100nm (a), 500nm (b) and 2000nm (c)

With the improving of VIPs technology, this material will become a more trusted choice for thermal insulation in more and more projects.

References

[1] R. Reuter et al. non-fluorocarbon insulation, refrigeration and air-conditioning technology workshop, 1993.

[2] E. K. Simen et al. Applied Energy 116 (2014) 355 – 375.

[3] M. Bouquerel et al. Energy and Building 54 (2012) 320 – 336.

[4] M. Alam et al. Applied Energy 88 (2011) 3592 – 3602.

[5] R. Baetens et al. Energy and Building 42 (2010) 147 – 172.

[6] R. Baetens et al. Energy and Building 43 (2011) 761 – 769.

[7] Z. Li et al. Materials Letters 129 (2014) 12 – 15.

[8] A. B. Jarzebaski et al. Chemical Engineering Science 50 (1995) 357 – 360.

[9] P. R. Aravind et al. Microporous and Mesporous Materials 96 (2006) 14 – 20.

[10] Z. T. Mazraeh-shahi et al. Journal of Non-Crystalline Solids 376 (2013) 30 – 37.

[11] Y. Tokudome et al. Journal of Colloid and Inerface Science 338 (2009) 506 – 513.

[12] J. Mrowiec-Bialon et al. Langmuir 20 (2004) 10389 – 10393.

[13] G. Liu et al. Colloids and Surface A: Physicochemical ans Engineering Aspects 436 (2013) 763 – 774.

[14] Z. Shao et al. Materials Chemistry and Physics 142 (2013) 570 – 575.

[15] H. Tamon et al. Journal of Colliod and Interface Science 188 (1997) 162 – 167.

[16] M. G. Kaganer. Thermal Insulation in Cryogenic Engineering, 1969

[17] G. Reichenauer et al. Colliods and Surface A: Physicochemical ans Engineering Aspects 300 (2007) 204 – 210.

3D MET Characterization of Precipitated and Fumed Silicas: Focus on Statistical Size Distributions

Genevieve Foray[a*], Lucian Roiban, Emmanuelle Pons[a,b], Bernard Yrieix[a,b]

a. MATEIS, INSA Lyon, UCBL, CNRS, Université de Lyon, 7 av. Jean Capelle F-69621 Villeurbanne, France

b. EDF R&D, Materials and Mechanics of Components, EDF Lab les Renardières, F-77818 Moret-sur-Loing, France

Abstract

The optimization of VIP core for durable performance is still a challenging topic. A characterization bottleneck needs however to be passed: can we get true 3D imaging of the raw nanostructured material at the micro and mesoscopic scale. A specific protocol was successfully built, so as to allow electronic transmission tomography (AET) of raw nanostructured silica, with a pixel size of less than 0.2nm. Statistical size distribution analysis were then performed focused on: (i) secondary silica particle (ii) silica aggregates (iii) pore thickness. Fumed and precipitated silica, aged or not, are characterized by very specific and different aggregate architecture. Such silica morphologies explained differences in functional properties, and ageing and open opportunities to tune new microstructure.

Keywords nanostructured silica, characterization, 3D TEM, statistical analysis, pore, particle

1. Introduction

Design of efficient long term performance superinsulating materials (SIM) remains a challenging topic [1]. Most of the SIM are highly architecture composites, including more than 6 compounds, but their price efficiency ratio is driven by silica, which stand as the highest volume fraction component. Moreover knowledge of silica ageing has recently been pointed out as the weak scientific point in durability prediction [2].

To improve SIM design, and pass the durability bottleneck, a specific protocol was designed to image silica at the micro and mesoscale. The aim is to get qualitative information on silica morphologies and to gather statistical information on pore size distribution at the tiniest scale. 3D imaging without damaging nanostructured silica require both a specific sample preparation and an advanced imaging protocol [3-4]. Two parameters were evaluated with this protocol, (i) the silica nature, two native raw material are compared, (ii) the ageing consequences, two accelerated ageing material were analysed.

2. Experimental techniques and materials

2.1 Advanced electronic tomography

AET was performed employing a JEOL 2100F transmission electron microscope including a post-column GATAN Tridiem energy filter and a FEG. Silica samples were dry sprayed on a microscopy grid previously normalized with colloidal gold particles as fiducially markers. Each tilt series, in low dose bright filed mode, were recorded in an angular range starting from $-71°$ to $+71°$ with an increment of $2.5°$ in Saxton scheme[5] resulting in 81 images of 2048×2048 pixels with a pixel size about 0.2 nm. The area of interest was barely exposed and in any case less than 0.5 s/projection. Such protocol allows the three dimensional (3D) analyses of very beam sensitive samples, such as high specific surface silica or worse aged silica. The volume imaged are about $300\times300\times300$ nm^3 in size,; other scale are already well described by complementary equipment such as X-ray tomography [6].

* Corresponding author, E-mail: Genevieve.foray@insa-lyon.fr

The volumes computations were performed employing 15 iterations of algebraic reconstruction technique algorithm (ART) [7] implemented in TOMOJ/EFTETJ. The 3D visualization, surface rendering, pores size and silica particles quantification were performed combining different tools implemented in the software ImageJ, 3D Slicer and Chimera.

2.2 Other microstructure analysis tools

A regular transmission electron microscopy (TEM) Jeol 2010 with a field emission gun (FEG) was used for the first transmission electron observation and provided zenithal 2D images.

Helium picnometry is performed on a Micromeretics Accupyc 1330 apparatus; the measured value is the mean of three determinations twenty cycles each. BET measurements were done with an ASAP Belsorp Max, using nitrogen as absorptive so as to determine specific surface. BJH calculation gave a first insight of pore volume.

Mercury porosimetry was performed with a Micromeretics Autopore III, 110 measurement points are taken, while the sample is submitted to increasing/decreasing pressure path [0.001 - 413 - 0.01MPa]. The pore volumes measured are associated to either compression of the powder skeleton, or intrusion of mercury or extrusion of mercury.

Conductivity measurements are performed on a HLC K202 Hesto guarded hot plate on 300×300×40 mm^3 sample under a temperature gradient of 10℃.

2.3 Materials studied

Sample 1 and 2 differ mainly by their production processes, the first is a fumed silica while the second is a precipitated silica.

Sample 3 and 4 are both fumed silica, after 280 days ageing under 48℃ 65% RH for sample 3, and 50° 90%RH for sample 4.

3. Results

3.1 Silica type compared

For both silica aggregates showing different thickness are depicted by regular TEM, but morphology is beyond acquisition mode.

2D zenith TEM (Fig. 1) only depicted fully communicating open pore with a parallel orientation w/r to TEM column, these are scarce and less than 30nm in size for precipitated silica. These viewed in fumed silica are smaller.

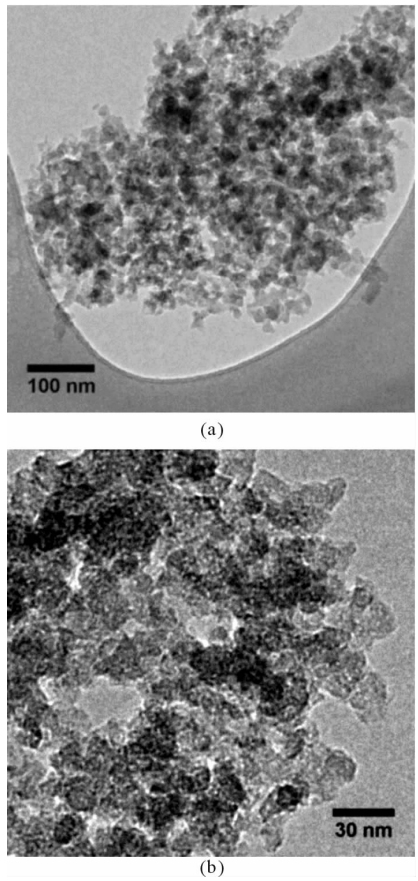

Fig. 1 S 2_p, aggregates and pores viewed by TEM

Precipitated silica studied here had slightly lower skeleton density, and specific surface compared to fumed silica. Mercury did not succeed in measuring all the porosity but the analysed content was more than twice less for precipitated silica (6 $cm^3 \cdot g^{-1}$) compared to (14.9 $cm^3 \cdot g^{-1}$) precipitated silica. Volumes measured while lowering the pressure were equal for both (Tab. 1).

Tab. 1 Microstructure features for non-aged silica

Sample	He. Picno	N_2 Pysisorption		Hg Porosimetry	
	ρ_s / $kg \cdot m^{-3}$	Spe. Surf. / $m^2 \cdot g^{-1}$	Pore size / nm	Pore vol. / $cm^3 \cdot g^{-1}$	Rev. vol / $cm^3 \cdot g^{-1}$
1_f	2000	192	14±3	14.9	0.9
2_p	1930	165	13±3	6.0	1.2

In Fig. 2 (a) the darker gray pixel represents the silica particles and the lighter grey characterizes the pores distribution within a fumed silica sample.

3D TEM revealed first with orthogonal slice within the reconstructed volume that aggregates are hollow aggregation of particles (Fig. 2(a)) composed of a skin with a given thickness (30nm) and a texture. , Beyond this skin an intra-aggregate pore is delimited a few tens of namoter in size. The particle delimited pores observed within the skin are less than 10nm in size (Fig. 2(a)), the inter-aggregates pores are less than 50nm.

The 3D volume (Fig. 2(b)) gave access to how aggregates are organized in the space: a grape fruit arrangement of aggregates for fumed silica, whereas a sphere arrangement occurred for precipitated silica.

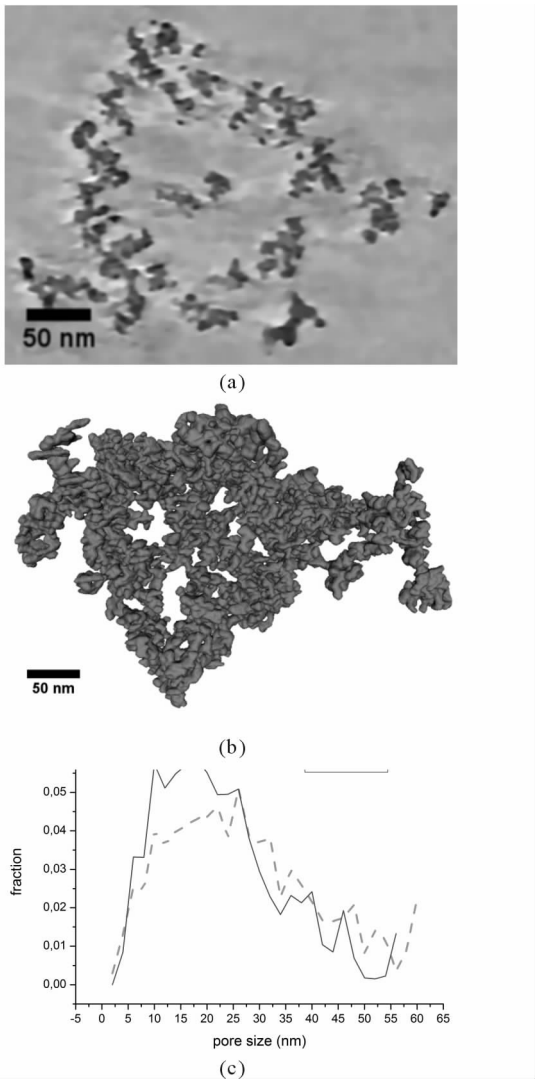

Fig. 2 (a) Cross sections parallel to the XY plans extracted from the volume computed for S1_f.; (b) reconstructed volume, silica particle viewed only in green for S1_f.; (c) Porous network characterization issued from the reconstructed volume. Continuous line stand for S1_f, green dot line stand for S2_p

Tab. 2 3D quantifications provided by AET, silica particles length (L) and width (w), the average pores size formed between the silica particles (small) and between the aggregates (big), the porosity within the 300x300x300 nm³ volume within a sample, the pore network tortuosity.

Sample	Particle Size/nm		Poressizes		ε /(%)	Tortu-osity
	w	*L*	Small/nm	Big/nm		
1_f	10	20	5~10	35~45	63	1.59
2_p	15	33	10	50~60	66	1.55

Previously F. Despetit [8] published reconstructed aerogel, showing that basic synthesis produced neck less morphologies, whereas colloidal synthesis gave spheroid arrangements. But the volume imaged were too small (less than 100nm size and 4 particles layer) to get quantitative information and rather focused on particle analysis.

Quantitative analysis of pore (Fig. 2(b)) and particle confirmed that the bimodal porosity and particle distribution are both smaller for the precipitated silica studied here (Tab. 2).

Considering a cubic volume, with a 200nm edge size, the overall porosity measured was equal for both samples, such as the pore network tortuosities.

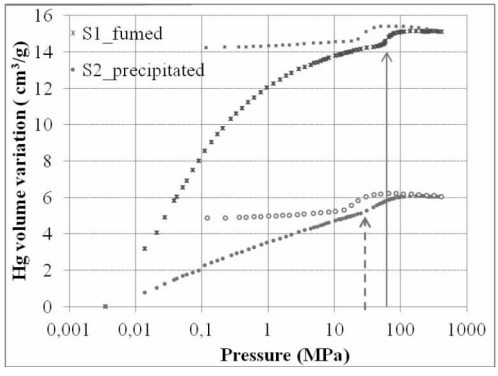

Fig. 3 Mercury porosimetry cumulated volume variation under pressure

AET results are consistent with mercury data, (i) the smaller pore size for fumed silica are intruded at higher pressure compared to precipitated silica (ii) the grape fruit morphology produce less compact arrangement than the spheroidal one, thus mercury volume measured by compression and buckling of the silica skeleton was more than twice less (Fig. 3).

3.2 Ageing scenario compared

The first results have confirmed that ageing produced an increased specific surface values and did modify the particle morphology. As the non-aged silica is not available for analysis, the comparison was focused on how relative humidity impaired ageing. The image and quantitative analysis will be depicted in detail in the conference.

4. Conclusions and perspectives

A protocol was successfully designed to get 3D AET observation of nanostructured silica used in superinsulation, very sensitive to beam damage.

Qualitative information were gathered at the scale of particles and aggregates, moreover, the volume studied were fair enough to compute statistical size distribution.

Combining 3D AET observations, with X - ray Tomography and regular pore size characterization tools, one can get a full pore size distribution for a SIM material.

Synthesis route and ageing scenario may be associated to morphology change at the particle andaggregate size. Such information provided by 3D AET analysis could help to develop new raw silica and price efficient SIM materials.

References

[1] M. Alam, H. Singh, MC imbachiya, Applied Energy, 2011.

[2] S. Brunner, K. Ghasi Wakil, Vaccum, 2014, 100, 4.

[3] G. M. Pajonk, A. Wenkastevara rao, N. Parvathy, E. Alaoui, J. of Mat. Sci, 1996, 31, 5683.

[4] I. Florea, L. Roiban, C. Iliman et al, Adv. Eng. Mat. 2011, 13, 123.

[5] W. Saxton, W. Baumeister, M. Hahn, Ultramicroscopy, 1984, 13, 57 - 70.

[6] E. Maire, J. Adrien, C. Petit, CR physique, 2014, 15, 674.

[7] C. Messaoudi, T. Boudier, C. O. S. Sorzano, S. Marco, BMC Bioinformatics, 2007, 8, 288.

[8] F. Despetit N. Bengourma, B. Lartigue, JNCS, 2012, 358, 1180.

Low Thermal Conductivity of High-Silica Glass Fiber Felt by Nano-modification

Wang Zhenpeng[a*], Zhang Qi[a], Guo Renxian[a], Shang Lei[b], Zu Qun[a], Liu Songliang[c]
ChenYang[a], Zhang Yan[a], Xu Yan[a], Zhao Xiaoru[a]

a. Sinoma Science & Technology Co. Ltd, Nanjing, Jiangsu, 211112, P. R. China
b. AVIC Shenyang Aircraft Design & Research Institute, 110035, P. R. China
c. Naval Representative Office in Shenyang, 110031, P. R. China

Abstract

A large number of small pores were formed in raw high-silica fiber after acid treatment process, these holes exist to improve fiber porosity and reduce thermal conductivity. Nano-modified high-silica glass fiber felts possess excellent water resistant in comparison to the traditional high-silica glass fiber felts, resulting in properties of lower thermal conductivity and better thermal insulation property. It can replace traditional thermal insulation materials such as rock wool felts, silicate felts that which be widely applied as functional structure interlayer, filling layer and composite layer for thermal preservation and insulation, for example parts and equipments for molten metal, high-temperature filters, fireproof and protective materials. In this research, the influence of component, fiber diameter, acid treatment, silicon value, sintering and forming process was also investigated. The effect of processing parameters on the quality of the resultant were discussed.

Keywords high-silica, glass fiber, low thermal conductivity, nano-modification, water resistant

1. Introduction

With the progress of science and technology and the development of aerospace technology, the demand for high temperature insulation material is also rising. The traditional high temperature insulated material such as asbestos, mineral wool cannot meet the requirements because of their high thermal conductivity [1]. High silica glass fiber is a kind of high-temperature-resistant inorganic fibers which have the high softening point and can be used on the condition of 900℃ for a long time. Meanwhile there are some other benefits that high silica fiber can be used for thermal insulation materials such as good thermal insulation performance, small thermal expansion coefficient, light quality, etc [2]. To compare with quartz fiber and high-temperature-resistance silicate aluminum fiber, one of most important benefits of high silica fiber is that the fiber contains a lot of closed and semi-closed pore after dealing with acid treatment and sintering [3]. On one hand these pores increase the porosity of high silica fiber felt, on the other hand, the pore maintains the felt's hydroscopicity [4]. High silica fiber felt with hydrophobic treatment can be used to improve its performance, in order to decrease felt's hydroscopicity and improve its high-temperature-resistant heat insulation. It is well known that most of water repellents are organic materials which cannot resist high temperatures and emit lots of harmful gases when it is heated.

In this paper, a new method was introduced to solve the problem of the felt's lower hydroscopicity and to develop the benefits of felt's higher porosity, in order to increase its heat insulating property.

2. The main factor affecting thermal conductivity

There are lot of pores in the fibers of the felt after dealing with acid treatment. The capillary effect of the

* Corresponding author, E-mail: wzp811230@126.com

pores made the felt absorb moisture. The thermal conductivity (λ) of water is 0.580W/(m·K) much higher than the thermal conductivity of air which is 0.026W/(m·K)[5]. Hence, the moisture that was absorbed by the felt may increase the thermal conductivity of felt and decrease the felt's heat insulating property. Felt property variation from before drying to after drying condition is shown in Tab. 1.

Tab. 1 Density and thermal conductivity of the felt drying in the air

Sample	Before drying		After drying	
	Density / kg·m^{-1}	λ / W/m·K	Density / kg·m^{-1}	λ / W/m·K
felt	153	0.035 1	142	0.033 0

The felt's water percentage was 7.75%, thermal conductivity increased to 0.002 W/m·K by ratio of 6.1%. This indicates that the existed water that could increase the heat conductivity and decrease the heat-insulated performance.

3. Nano-modification

3.1 Technological process of nano-modified high silica fiber felt

Nano-modification is the processes where by nanopartricles are used to cover a felt's surface in order to provide the felt with the nano-modified property[6]. In this test, nano-silicon dioxide was used as modified ingredients. First, the hydrophobic nano-silicon dioxide was dissolved in the water, and then the solution was added to the slurry in proportion. The nano-silicon dioxide should was accumulated on the felt surface during the process of sheeting, so that, this process can provided the felt with the nano-modified property.

The main process is showed on Fig. 1.

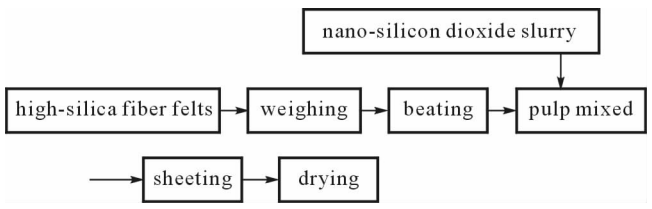

Fig. 1 Technological process of Nano-modified high silica fiber felt

3.2 Hydrophobicity test of nano-modified high silica fiber felt

High silica fiber felt is almost water resistant after the nano-modification. Fig. 2 shows the test process that dripping some water on the surface of high-silica glass fiber felt in order to verify the hydrophobicity of the felt. From the test, it can be seen that the nano-modification efficiently improved the hydrophobicity of the felt because the infiltrating angle of the water drop was greater than 90 degrees.

Fig. 2 Test of hydrophobicity

3.3 The heat-insulated performance of nano-modified felt

There are more pores in high silica fiber felt than other heat insulated felt because high silica fiber felt contained a lot of pores which were produced by the acid treatments. Meanwhile, the pores should increase the felt's heat-insulated property for the macro level pore is small enough to move thus it prevent the thermal transmission. By the nano-modified process, while the capillary effect was almost eliminated, the heat insulated advantages can be greatly put into practice. Heat conductivity coefficient of felt after nano-modification is shown in table 2, thermal conductivity decreased by 15% compared to original felt.

Tab. 2 Thermal conductivity of felt after nano-modification

Sample	density / kg/m	λ(25℃) / W/m·K
High silica fiber felt	140	0.029 6

3.4 High-temperature-resistant performance of nano-modified felt

TG-test is a method to measure the changed weight of the felt during the heating, so as to reflect chemical stabilization. The less weight changed, the better chemical stabilization of the samples and vice versa. It can be concluded Fig. 3 shows the TG-test chart of high silica felt, we can conclude that weight loss ratio almost unchanged between 714℃ and 900℃ which remained 88.

7%. It illustrated that the high silica felt was provided with the high-temperature-resistance property.

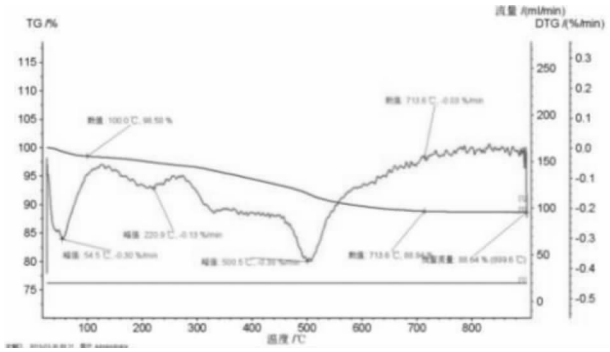

Fig. 3 The TG testing result of nano-modified felt

In order to test the variation of the thermal conductivity of high silica felt after nano-modification, the felt was placed in a high temperature furnace while the temperature increased to 800℃ at the rate of 10℃/min, and kept for 1000 seconds. The felt was placed under the normal room temperature for 48 hours in order to test the hydroscopicity and thermal conductivity. The detailed data is showed on Tab. 3.

Tab. 3 Variation performance of nano-modified felts

parameter	Before treatment	After treatment
hydroscopicity	2.97%	0.61%
λ/(W/(m·K))	0.029 64	0.029 09

Tab. 3 shows the variation of hydroscopicity and thermal conductivity that decreased after the nano-modification. The test illustrated that after going through with high temperature condition, the excellent properties of the felt still remained.

4. Conclusions

The high silica felt is provided with higher heat-insulted property after the nano-modified process. It can be used as high-temperature material repeatedly. It can meet various shaped equipments because of its soft property. There are great engineering values such as its convenient process, short production process and easy to industrialization.

References

[1] Xingming Zhou, et al. Chinese Journal of Materials Research. 02(2006).

[2] Yaoming Zhang, et al. Glass fiber and mineral wool encyclopedia. 03(2001) 866 - 871.

[3] Qun Zu, et al. Glass Fiber. 03(2004).

[4] Xiaoyan Liu, et al. Low Temperature Architecture Technology, 09(2009).

[5] Shiming Yang, et al. Heat Transfer, (1998) 22 - 23.

[6] Hui Su, et al. Plating & Finishing, 2005.

Effect of the Additive Amount of Nano Carbon Black on Thermal Insulating Performance of Vacuum Insulation Panel

Li Chengdong[a], Huang Fengkang[b*], Xia Yuming[b], Xia Dongxing[b]

a. Super Insulation Composites Laboratory, College of Materials Science and Technology, Nanjing University of Aeronautics and Astronautics, Nanjing, 210016, P. R. China
b. YinXing Electric Co., Ltd, Chuzhou 239000, P. R. China

Abstract

Vacuum insulation panels (VIPs) with both high efficiency in thermal insulation and long lifetime were desired in their engineering design and application. Core material is the kernel part of VIPs and greatly influences the thermal insulating performance of VIPs. In this paper, 1%, 3%, 5% and 10% of NCB was evenly blended with fumed silica, chopped polyester fibers, and titanium dioxide powder to form the hybrid core materials (HCM) for VIPs. The influence of the additive amount of NCB on the microstructure, BET specific surface area and thermal conductivity of the as-prepared VIPs was investigated. In order to achieve the optimal thermal insulating performance with low thermal conductivity and long service life, the additive amount of NCB should be 3%.

Keywords hybrid core material, vacuum insulation panel, carbon black, thermal conductivity, ageing mechanism

1. Introduction

In the recent decades, the thermal insulation market is booming due to the explosion of energy costs in the building sector, domestic appliances, aeronautics and astronautics[1, 2]. In order to reduce the energy consumption therein, the design and development of highly energy-efficient materials have received a lot of attention. Vacuum insulation panels (VIPs) offer extremely low thermal conductivity of less than 8 mW/(m·K) which is between 5 to 10 times lower than the traditional thermal insulation materials like mineral wool and polystyrene products [3]. Also, a lot of living space can be saved through installing the VIPs in the places where acquired.

A VIP consists of a porous core material encapsulated in a nearly impermeable envelope material. The envelope materials consist of several layers of thin metallic foil or metallized polymer film with a low emission coefficient for long-wave radiation. The core materials are packed with fine powders and/or fibers which are evacuated to pressures of 0.1 ~ 3 mbar. Mixtures of fumed silica powders (FSP), organic fibers and infrared opacifier are proved to be a good filling materials for VIPs[4]. Three modes contribute to the thermal conductivity of the VIPs, namely the solid conduction, gaseous conduction and radiation. Alam et al. quantified the opacifying properties of expanded perlite and measured the radiative conductivity of the hybrid core materials (HCMs) with different constituents. Yamada et al. proposed a method for determining the radiative characteristics of a single fiber and evaluated the radiative transfer in media of fibers with a large size parameter. Cheheb et al. [7] studied the radiative and conductive properties of semi-transparent materials using the theoretical and experimental method. Although a mass of work have been contributed to analyze the mechanism within the radiative thermal conductivity, few literature concerns

* Corresponding author, Tel:86 - 550 - 3075556, Fax:86 - 550 - 3075556, E-mail:peter.huang@yxelectric.com

the effect of the amount of opacifiers on the thermal conductivity of the VIP.

In this paper, different addition of nano carbon black powders (NCB) were blended with a certain content of FSP, chopped polyester fibers (CPF) and TiO_2 powders. The effect of the additive amount of NCB on the thermal conductivity and aging effect of VIPs was investigated. The objective of this paper was to develop high-efficiency and low-cost VIPs with long service life.

2. Experimental

Filling materials, including FSP, CPF, TiO_2 powders and NCB, and envelope materials used in this study were provided by YinXing Electric Co., Ltd. (Chuzhou, P. R. China). The five kinds of HCMs with length of 350 mm and width of 190 mm were fabricated by dry method. The recipe of the HCMs was listed in the Table 1. Firstly, a given mass of FS powders, PF and TiO_2 powders were mixed in a chamber (within a closed mixer) and then stirred by a rotational impeller for 10 min. Then, a certain amount of NCB powders were added into the chamber and rapidly agitated by the rotational impeller for 15 min, forming uniformly dispersed hybrid materials. Afterwards, the hybrid materials were bagged in a non-woven bag and then dried at 140℃ for 50 min. Thereafter, the dried HCMs were bagged in the envelope material. VIPs with the corresponding HCM were produced after vacuum process. Finally, the VIPs were flatten by a rolling stick and slightly compressed by a pressing machine, forming smooth VIPs with fixed dimensions.

The surface morphologies of the HCMs were performed on the field emission scanning electron microscopy (FE - SEM, Hitachi S - 4800). Nitrogen adsorption - desorption isotherms were measured using a specific surface area SSA - 4300 instrument (BUILDER, Beijing, China). Thermal conductivity of the VIPs were evaluated by heat flow meter (Netzsch HFM 436). In order to investigate the ageing effect of the as-prepared VIPs, the VIPs were placed in a closed chamber with temperature of 80℃ and relative humidity of 80% for 28 days. Thermal conductivity of the VIPs was recorded every 7 days.

3. Results and discussion

3.1 Microstructure

Fig. 1 shows the SEM micrographs of HCMs. As shown in Fig. 1(a), the CPF were randomly oriented in the HCMs while the FSP, TiO_2, and NCB constituted a continuum, forming the matrix for the HCMs. As shown in Fig. 1(b), the matrix of the HCMs, i. e. the filling powders, were fragile. Many cracks in the HCMs were found in the matrix. Meanwhile, some powders were packed together, forming a cluster which was independent from the neighboring powders and clusters. The long CPF helped to integrate the powders, lapping the skeleton for the HCMs. Hence, the load-carrying ability of the HCMs was reinforced.

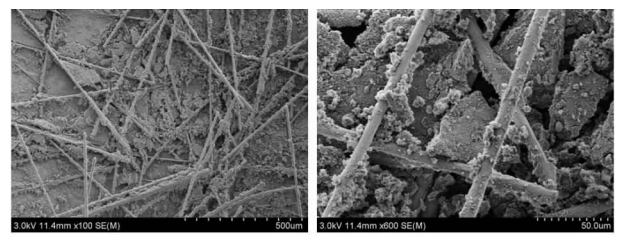

Fig. 1 SEM micrographs of HCMs: (a) ×100; (b) ×600 (enlarged images of red zone in (a))

3.2 BET specific surface area

For BET adsorption with finite layer molecule, it has following form[8]:

$$q = \frac{q_m c\varphi[1-(n+1)\varphi^n + n\varphi^{n+1}]}{(1-\varphi)[1+(c-1)\varphi - c\varphi^{n+1}]} \quad (1)$$

where q_m is the first layer adsorption amount with all the inner surface of the adsorbent is covered by the adsorbate molecule, mg/g, n is the maximum number of layers of adsorbed molecules, c is the BET constant and can be calculated by:

$$c = \exp\left(\frac{E_1 - E_2}{R_0 T}\right) \quad (2)$$

where E_1 (J/mol) is the heat of adsorption of the gas in the first adsorbed later, E_2 (J/mol) is the heat of liquefaction of the gas, R_0 (8.314 15 J/(mol·K)) is the gas constant and T(K) is temperature.

The specific surface area reflected the interactions between the material and the surrounding gases and liquids. In this paper, the surface adsorption of the filling materials occurred via two mechanisms: physisorption, and chemisorption. NCB provided two

special functions: (a) absorbing and reflecting ultraviolet rays; (b) absorbing gases within VIP enclosure. Fig. 2 shows the nitrogen adsorption and desorption isotherms of HCMs. The sorption isotherms of HCMs were evaluated in the relative pressure (P/P_0) ranged from 0 to 1. The adsorption isotherms matched pretty well with the desorption isotherms. The volume of nitrogen adsorption progressively increased with the rise in the relative pressure until the P/P_0 was 0.8. After that, the volume of nitrogen adsorption dramatically increase to a maximum of 456.951 cm^3/g when the P/P_0 was 0.98908.

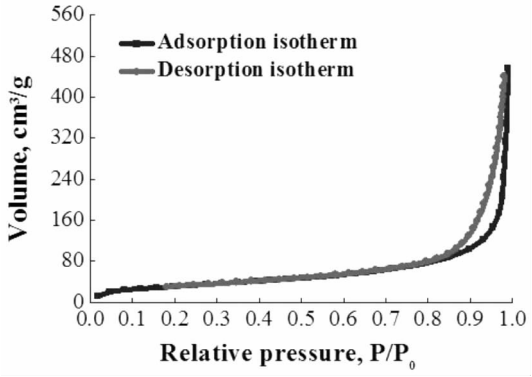

Fig. 2 Nitrogen adsorption and desorption isotherms of HCMs

Tab. 1 shows the microstructural geometric parameters of the HCMs from the N_2 sorption method. The total pore volume V was estimated on the basis of the amount adsorbed at $P/P_0 \approx 0.99$. As shown in Table 1, all of the specific surface areas ranged from 120 m^2/g to 210 m^2/g. Also, the specific surface areas increased with the addition of the NCB and reached a maximum of 204.736 m^2/g when the addition of NCB was 10%. This was mainly because of the nanostructure of the NCB. The BET mean pore radius r of the HCMs ranged between 7 nm and 12 nm and reached a minimum value of 7.11 nm when the NCB addition was 3%. Thus, the packing pattern of the filling materials with 3% addition of NCB was optimal because the HCM not only had small pores but also relatively large BET surface area.

3.3 Thermal conductivity of VIPs

Tab. 2 shows the density of the HCMs and the corresponding VIPs. Both the density of the HCMs and VIPs increased with the additive amount of the NCB. When the addition of NCB was equal and less than the 3%, the VIPs possessed a low density of between 170 kg/m^3 and 190 kg/m^3. By contrast, the density of the VIPs increased significantly above 210 kg/m^3 when the additive amount of NCB was equal and above 5%. The high density of the VIPs might limit the development of the VIPs in building sectors.

Tab. 1 Microstructural geometric parameters of the HCMs from the N_2 sorption method

Sample	Constituent	BET suface area S /(m^2/g)	Pore volume V /(cm^3/g)	BET mean pore radius r/nm
1	91%FS+8%PF+1%TiO_2	120.592	0.710558	11.78
2	90%FS+8%PF+1%TiO_2+1%NCB	126.871	0.825837	13.02
3	88%FS+8%PF+1%TiO_2+3%NCB	136.681	0.486109	7.11
4	86%FS+8%PF+1%TiO_2+5%NCB	137.688	0.654736	9.51
5	81%FS+8%PF+1%TiO_2+10%NCB	204.736	0.814524	7.96

Tab. 2 Density of the HCMs and the corresponding VIPs

Sample	Density/(kg/m^3)		
	Core material		VIP
	Before vacuum process	After vacuum process	
1	91.38	140.68	171.15
2	97.34	152.18	184.48
3	100.11	155.57	188.46
4	102.48	181.71	217.86
5	104.82	202.72	244.01

Fig. 3 shows the thermal conductivity of the HCM and VIP. The profile of the additive amount of NCB versus both thermal conductivity of VIP and HCM was like a concave parabola. Both the thermal conductivity of the VIP and HCM reached a minimum of 4.556 mW/(m·K) and 22.860 mW/(m·K) respectively when the additive amount of NCB was 3%. This was because the addition of the NCB might pose two very different roles on the total thermal conductivity of the VIPs. On the one hand, a certain amount of NCB might suppress the radiation thermal conductivity and thus decreased the total thermal conductivity. But with the growth of the additive amount of NCB, on the other hand, NCB had few contribution on further decreasing the radiation thermal conductivity. Thus, excessive NCB made the HCMs denser and increased the solid thermal

conductivity of the VIPs. Hence, in terms of decrease the thermal conductivity, the optimum additive amount of the NCB was 3%.

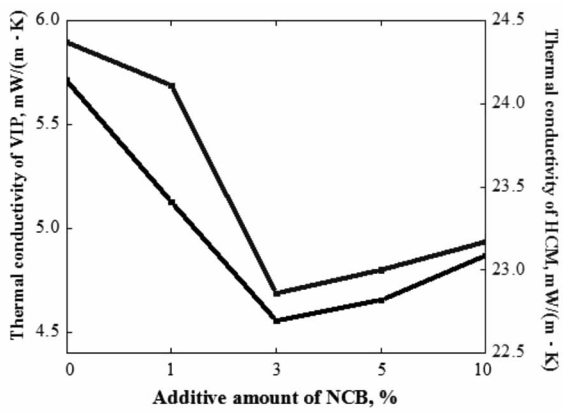

Fig. 3 Thermal conductivity of the HCM and VIP

3.4 Ageing of VIPs

The ageing effects influencing the thermal conductivity and service life of VIPs are (1) the rise of the internal pressure; and (2) moisture accumulation in the core material[9]. The moisture content in normal indoor conditions of 23 ℃ and 50% R. H. is about 4 % (mass percent). Also, the water vapor transmission rate (WVTR) is 10^3 up to 10^6 times the values of oxygen transmission rates (OTR) or nitrogen transmission rate (NTR) in equivalent units [9]. In this paper, a high temperature of 80 ℃ and high relative humidity of 80% not only accelerated the ageing of the envelop materials but also increased the penetration rate of the gases and moisture through the envelope material. The penetrated gases and moisture might accumulate in the core material, leading to an increase of thermal conductivity of VIPs.

The ageing of VIPs closely bounded up with the composition and microstructure of the HCMs. Fig. 4 shows the ageing curve of VIPs with different additive amount of NCB. The profile of the five curves of ageing time versus thermal conductivity was quite different. The thermal conductivity of the VIP without addition of NCB increased roughly linearly with the ageing time. As for the other four kinds of VIPs, all of the thermal conductivities of the VIPs increased dramatically at the first 7 days and then slightly increased with the following 21 days of ageing time. Also, the growth of the thermal conductivity of VIPs with NCB addition of 3%, 5% and 10% was not so much as that of 0% and 1%. This was because the nanoscale structure of the NCB absorbed massive moisture and gases within the VIP enclosure during the ageing of the VIPs. The negative effects of the water moisture and the gases on the thermal insulating performance of the VIPs were thus suppressed to a minimum.

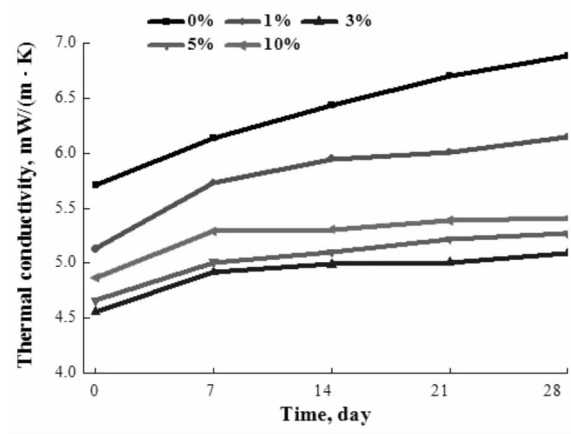

Fig. 4 Ageing curve of VIPs with different additive amount of NCB

Compared with other VIPs, the VIPs with additive amount of 3% NCB had not only the lowest initial thermal conductivity but also the most excellent ability in maintaining the thermal conductivity. Thus, additive amount of NCB of equal and less than 3% helped to increase the thermal insulating performance of the VIPs while an excess of additive amount of NCB of greater than 5% might weaken the thermal insulating performance of the resulting VIPs. The optimum additive amount of NCB was 3%.

4. Conclusions

The addition of NCB moidified the microstructure and density of the HCMs. In order to decrease the thermal conductivity and extend the service life of the VIPs, the optimum additive amount of NCB was 3%.

Acknowledgments

This work was supported by Funding for Outstanding Doctoral Dissertation in NUAA (BCXJ13-10), Funding of Jiangsu Innovation Program for Graduate Education (the Fundamental Research Funds for the Central Universities, CXLX13_149) and a Project Funded by the Priority Academic Program Development of Jiangsu Higher Education Institutions.

References

[1] Li CD et al. Mater Design 50 (2013) 1030 – 1037.
[2] Li CD et al. Dry Technol 31 (2013) 1084 – 1090.
[3] Li CD et al. J Mater Process Tech 214 (2014) 539 – 543.
[4] Heinemann U. Int J Thermophys 29 (2008) 735 – 749.
[5] Alam M et al. Energ Buildings 69 (2014) 442 – 450.
[6] Yamada J et al. Int J Heat Mass Tran 43 (2000) 981 – 991.
[7] Cheheb Z et al. Journal of Quantitative Spectroscopy and Radiative Transfer 4 (2008) 620 – 635.
[8] Zhang H et al. Int J Heat Mass Tran (2014) 947 – 959.
[9] Simmler H et al. Energ Buildings 37 (2005), 1122 – 1131.

The Effect of Novel Drying Technology on the Production and Thermal Conductivity of Fume Silica Vacuum Insulation Panel

Huang Fengkang[a,b*], Xia Yuming[a], Zhu Jianguo[b], Xie Lixu[b], Wu Leyu[a], Wang Tangyu[a]

a. YinXing Electric Co., Ltd, Chuzhou 239000, P. R. China

b. College of Materials Science & Engineering, Sichuan University, Chengdu, 610065, P. R. China

Abstract

Fume silica as core materials of vacuum insulation panel (VIP－FS) has been successfully prepared by using core pre-loading, drying, and vacuum packing. The drying is one of the most important steps which affect performance of core material and production costs of panel. Hot flue dryer (HFD) was used as traditional drying method to remove humidity, however it has been restricted because of high energy consumption. Microwave drying (MD) technology seems like good alternative because of many advantages like lower processing time, uniformity and energy saving. The method of combing with HFD and MD was adopted to accelerate drying. MD at 140℃ in 15min and then HFD at 140℃ in 15min have the same dehydration with HFD at 140℃ in 60min and the tests show it can remove about 1.24% water. Further experiments indicated that MD＋HFD exhibits optimum performance of 0.0049W/(m・K). The cost and efficiency has also been investigated, which MD＋HFD can save 0.28 dollar/m^2 and improve nearly doubled producing efficiency. The new-style drying method, MD＋HFD, offered a new way for mass production of VIP－FS.

Keywords fumed silica, vacuum insulation panel, microwave, thermal conductivity, drying, cost

1. Introduction

Vacuum insulation panel (VIP) has gained widely attention because of its low thermal conductivity, thermo-stability and non-pollution [1]. Generally, fume silica is porous and has large specific surface area with adsorbing permeability gas which make it become the main core materials of VIP [2]. VIP－FS was prepared by many steps: materials mixing, molding, loading in non-woven bag, drying, vacuum and sealing, etc. Drying plays an important role in performance and cost. The thermal conductivity of VIP－FS is measured and showed a significant increase of heat transfer through powder boards of fumed silica with an increasing water content [3]. Many researchers have tried lots of approaches to prepare lower water content in core materials. The traditional drying method, hot flue dryer (HFD), has been applied into many fields. However, its inefficient, long time drying and energy-wasting have limited further application.

A major aim for researching and production is to develop a high-efficient, inexpensive drying method. Under this condition, the microwave drying (MD) has been proposed. Microwave is a novel drying technology, generated by alternating current. The microwave drying would offer a number of advantages over conventional heating: rapid heating, heating from the interior of the core materials , energy transfer instead of heat transfer, higher level of safety and so on [4]. Due to its many advantages, microwave drying were used in various areas to dry kinds of materials. Among them, porous silica is generally very suitable for microwave drying. However, the enclosed type of MD go against moisture loss such that it will influences drying effect.

To solve these problems, efforts have been made to

* Corresponding author, Tel:86－550－3075556, Fax:86－550－3075556, E－mail:peter.huang@yxelectric.com

develop a new-type drying method of combing microwave drying with hot flue drying. In this paper, the production efficiency, cost and thermal performance was investigated by using comparative ways for three drying styles: HFD, MD, MD+HFD and we'll discuss why we chose MD+HFD heating way.

2. Experiment

The samples were produced by using an advanced powder technology. It has smooth surface and regular corner (Fig. 1(a)). To prevent the core materials from being broken in the subsequent processing, it is necessary to load it into non-woven bags (Fig. 1(b)). It should be pointed out that its drying temperature was limited (<150℃), because there are polyester fiber in the core materials and the non-woven is unable to bear high temperature. Here, three drying methods were used to heat fume silica core material. The first way is traditional drying method, HFD, at 140℃ in 60mins, the second is MD at 140℃ in 30mins and the last is MD at 140℃ in 15 mins after HFD at 140℃ in 15min. Then, three dried core materials were bagged in barrier film, including PA, PET, AL and PE. Finally, they were vacuum compressed to 0.1Pa to form VIP-FS. The rate of water of core materials were measured by moisture meter (YuDa FD-G1) and thermal performance of VIP-FS which was determined by heat flow meter thermal conductivity instrumentation (Netzsch HFM 436).

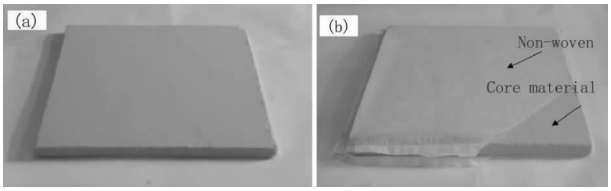

Fig. 1 Picture of fume silica core material

(a) core material; (b) core material loaded into non-woven

3. Results and discussions

3.1 Performance analysis

It was found that MD + HFD had better dehydration rate than the other from table 1 and its VIP-FS exhibited optimum performance. The dehydration influence and thermal performance of MD was the worst among them. The core material was put into firing instrument, heat up to preset temperature (140℃), and then its heating curves of upper, middle and bottom surface was measured and recorded by temperature collector (mini LOGGER GL220) to explain above discoveries.

Tab. 1 Parameters of three samples

Core materials	Size	Drying method	Dehydrating Rate (%)	K-value mW/(m·K)
Fume silica+ polyester fiber+ opacifier	350× 190× 10mm	HFD	1.20	5.0
		MD	1.01	5.3
		MD+HFD	1.24	4.9

The heating curves of core material in HFD was shown in Fig. 2(a). The heating rate is upper > bottom ≫ middle. It needs about 2000s to increase the temperature from middle of core materials to 140℃, which is of great influence on drying effect and consume a lot of energy. It could be proved from HFD heating principle, which hot-blast air was created from electric and make it disperse on uniformly in oven with convective mixing technology. This is a time-consuming way to transfer heat slowly from surface to inner of core material. The heating time should be prolonged to satisfy dehydration needs.

The MD attracted our attention for its rapid heating and Fig. 2(b) show its heating curves. The speed of middle temperature rising is also slower than sides, while only 900s could rise up to 140℃ and it is much faster than HFD. However, dehydration rate tests show its effect was worst and only removed 1.01% water. It may be caused by its confined space, which will prevent water vapor from volatilizing and damaging drying effect.

A high-efficient preparation method is critical to the long-term future of VIP. The method proposed was that the interior temperature of core material was rapidly increased with MD and then put it into Hot flue to accelerate elimination of water vapor which will remove moisture of core materials and reduce drying time. According to the discussion, MD could increase the temperature to 140℃ for 900s. The core materials was placed in microwave for 900s and then put into hot flue immediately for drying 900s. The results were shown in table 1 and found this method can evaporate maximum

water. When VIP - FS was prepared with this core material, it has an excellent thermal performance of 0.0049mW/(m • K).

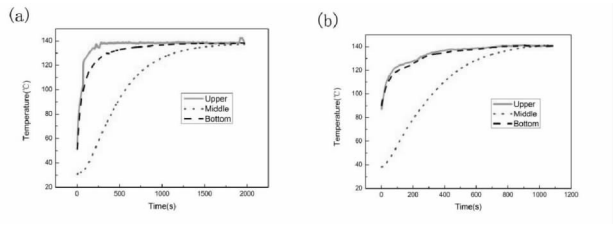

Fig. 2 Picture of heating curves of core materials in HFD(a) and MD(b)

3.2 Cost analysis

Generally, VIP - FS has excellent heat insulation effect and thermal insulation performance. However, high price has limited its development and application in many areas [5]. So, the price has drawn more and more attention of manufacturers and applications.

From the conclusion, the optimal VIP - FS could be produced by MD + HFD method. Meanwhile, the cost of three drying method as shown in Tab. 2 was also investigated. The energy consumption make it also the most innovative drying method. A more plausible way would be proposed by comparing the effect of drying method on fabricating cost. Per square metre drying cost of core materials was calculated (commercial electric utilization was calculated by 0.16 dollar/(kW • h). The cost of MD+HFD was cut by 0.28 dollar/m^2 compared with HFD or MD. The savings due to this new drying method would be about $ 280,000 annually for VIP manufacturers, when its sales is 1 million square metres. Moreover, the production efficiency would be doubled as its drying time shorten to 30min from 60min.

Tab. 2 The cost analysis of three samples

Drying method	Power kW • h	Effective area m^2	Drying time min	Energy - consuming kW • h	Drying cost Dollar/m^2
HFD	90	10	60	90	1.45
MD	144	8	30	72	1.45
MD+HFD	—	8	(15+15)	58.5	1.17

4. Conclusions and outlook

The VIP - FS has been produced by new-style drying method, which combined MD with HFD. The novel drying technology shows an excellent heating properties that can enhance insulation performance, provide savings in energy consumptions and improve production efficiency. A low cost producing way to manufacture VIP - FS on a larger scale has been provided by this technology. It is worth mentioning that production processes and equipment maintenance were more strictly than before.

Further optimization is towards continuous production line and ongoing aim with more energy saving method.

5. References

[1] Y. Yusufoglu, Application of Vacuum Insulation Panels (VIPs) on Refrigerators, Proceedings of the 11th International Vacuum Insulation Symposium (IVIS 2013), Empa, Switzerland, 19 - 20 September, 2009.

[2] R. Baetens et al. J. Energy and Buildings 42(2010)147 - 72.

[3] A. Beck et al, Influence of Water Content on the Thermal Conductivity of Vacuum Panels with Fumed Silica, Proceedings of the 8th International Vacuum Insulation Symposium (IVIS 2007), Würzburg, Germany, 18 - 19 September, 2007.

[4] J. A. Menendze et al. Fuel Processing Technology 91 (2010)1 - 8.

[5] M. Alam et al. Applied Energy 88(2011) 3592 - 602.

Effect of Sunscreen Additive on the Thermal Insulation Performance of Vacuum Insulation Panel

Huang Fengkang[a,b*], Mao Weixing[a], Zhu Jianguo[b], Xie Lixu[b], Wu Leyu[a], Wang Tangyu[a]

a. YinXing Electric Co., Ltd, Chuzhou, 239000, P. R. China

b. College of Materials Science & Engineering, Sichuan University, Chengdu, 610065, P. R. China

Abstract

Heat transfer through vacuum insulation panels (VIPs) is usually contributed to by solid heat conduction of core material, gas heat conduction, heat radiation and so on. Under vacuum state, heat radiation is the main factor on affecting the thermal conductivity performance of products. In this paper, the core materials doped with different kinds of sunscreen agents were prepared by wet method and the thermal conductivity was also studied. It was found that sunscreen particles on the surface of glass fiber by scanning electron microscopy can effectively absorb infrared light. The influence of different amount of TiO_2 additive on the thermal insulation performance of VIPs was further evaluated. Consequently, it turned out that the thermal conductivity of VIP reached the lowest value of 0.00168 W/(m·K) when the amount of TiO_2 additive was 5% and the internal pressure was 0.1Pa. Moreover, the addition of nanoparticles can increase the specific surface area of core material, which can also prolong the service life of the VIPs.

Keywords sunscreen, heat radiation, vacuum insulation panel, thermal insulation performance, service life

1. Introduction

As one of the main raw materials of vacuum insulation panel, glass fiber core material, has played an important role for their heat conduction performance. Recently, two approaches, wet method and dry method were usually adopted to prepare glass fiber core material, and the former was widely employed in China [1]. Conventional glass fiber has been used for core material for its unique advantages such as light quality, low coefficient of thermal conductivity and so on. However, some disadvantages such as low stability caused by deformation at high temperature, serious deformation of products after air leakage and so on have placed restriction on their actual utilization to some extent.

The introduction of nano-sunscreen with thermal barrier effect can not only decrease heat conductivity coefficient, but also reduce the rebound resilience of core materials. Besides, large specific surface area of nanoparticles provided their excellent adsorption. Furthermore, the air pressure inside the vacuum insulation panel can retain a long period of time for the reduced pore of composite core materials caused by the introduction of nanoparticles, thus increasing the service life. In this area, Depps new materials co., LTD of Suzhou developed the vacuum insulated panel with initial coefficient of thermal conductivity in 0.004～0.008 W/(m·K), flat surface, weak rebound resilience, good use effect for architecture applications through mixing glass fiber and various insulating particles [2]. In this study, a series of composite core materials were prepared using wet method by the addition of different amount of sunscreen (TiO_2), and their heat conductivity coefficient and service life were also investigated.

2. Experimental description

SiC, Si_3N_4 and TiO_2 are selected as sunscreens in the early experiments which show that TiO_2 has the

* Corresponding author, Tel: 86 - 550 - 3075556, Fax: 86 - 550 - 3075556, E - mail: peter. huang@yxelectric. com

most distinct effects on the thermal conductivity. Therefore, this paper takes TiO_2 as the object of study to investigate its impacts on the thermal performance and service life of the VIP. The experiment is conducted in the acidic environment. Fiberglass and different proportions of nano-scale TiO_2 particles that have shading functions are fully blended, stirred and dried to produce the glass fiber/titanium dioxide nanocomposite. The detailed experimental process is as follows:

First, an appropriate amount of concentrated sulfuric acid was added to a 0.67m^3 water slurry pool to make a solution with a pH value of 3.0. Then, 600g Alkali-free glass wool was added to the solution and soaked for 30 minutes. Next, TiO_2 with mass fractions of 0%, 1%, 5% and 10% are added respectively. After 30 minutes of mechanical stirring, the molded materials were dried at the temperature of 230℃ to get composites with different proportions of nano-particles. After cutting, drying, evacuation and packaging, the VIP was produced finally. The product thermal conductivity was detected by the Netzsch HFM 436, and the BET and SEM of the nano particles and composite core materials were detected by the Gemini V2380 automatic specific surface area and porosity analyzer and the Hitachi S-4800 respectively.

Three VIP samples were made with a size of 290mm×410mm×12mm, and then put in the oven with a temperature of 80℃ and a humidity of 80 RH%. The samples were taken out to test their thermal conductivities every week, and the thermal conductivity values are recorded for 28 days. Next, a chart was made using the time as the abscissa and the thermal conductivity value as the vertical coordinate. The slope of the line was the evaluation criteria of the service life. The larger the slope, the shorter the service life tends to be.

3. Results and discussion

Fig. 1 shows the SEM of the composite core materials produced by adding TiO_2 of different proportions. The figure shows that the diameters of the glass fiber range from 3 to 5μm, the distribution being relatively even. By amplifying the figure, it can be found that a small amount of particulate matters deposited on the fiber surface. The matters prove to be TiO_2 by EDS (Fig. 2), demonstrating that some TiO_2 successfully deposit on the fiber surface to complete the composition of the glass fiber and the nano particles.

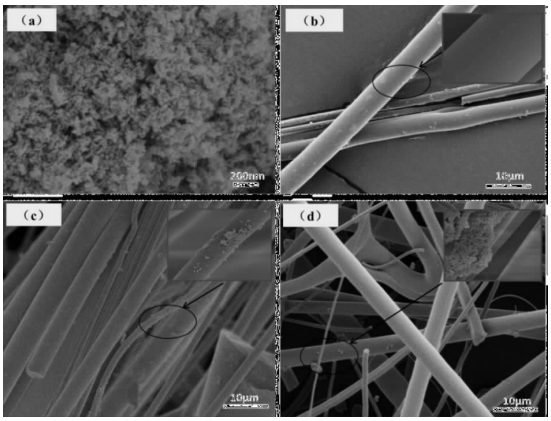

Fig. 1 SEM and EDS images of TiO_2 (a) and GF/TiO_2 (b~d: ω_{TiO_2} =1%,5%,10%)

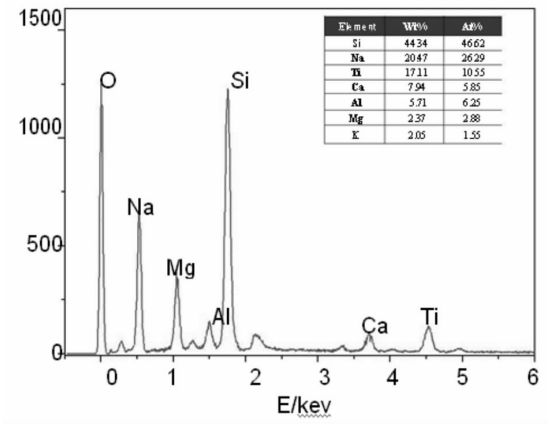

Fig. 2 EDS spectra of GF/TiO_2 (ω_{TiO_2} =10%)

Fig. 3 is a comparison of the thermal conductivities of the VIP produced at 0.1Pa with the composite core materials generated with additive TiO_2. The result shows that along with the increasing content of TiO_2, the VIP thermal conductivity value K tends to fall down first and then rise. The thermal conductivity value appears the lowest point when the additive amount is 5%. Regarding the reasons, as shown in the Fig. 1 (a)~(d), with the increase of the additive amount of TiO_2, the content of TiO_2 increases significantly on the glass fiber surface of the composite, and the agglomeration becomes more apparent. The agglomeration of the particles reduces the contacts between the fiberglass and the nano particles, making the TiO_2 unable to effectively scatter in the fiberglass

interspaces. Also, when the TiO_2 content increases to a certain extent, the conductivity of the internal solids of the core materials also increases, thereby affecting the thermal conductivity of the VIP.

Fig. 4 is the accelerated aging test curve of the composite materials containing different proportions of TiO_2. According to the analysis of the curve, with the increase of the additive amount of TiO_2, the slope of the aging curve decreases. The K value of the VIP product at the fourth week with 10% additive amount is 0.71mW/(m·K) lower than that with no TiO_2, which means that after the composite core materials are made into the VIP product, adding TiO_2 can prevent the materials from aging.

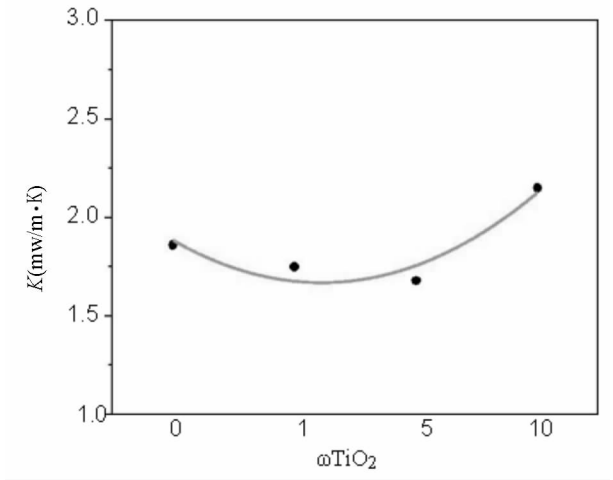

Fig. 3 K - value of samples with different samples

As it is well known, nano-scale TiO_2 is widely applied to various fields due to its large specific surface area and strong adsorption capacity [3-5]. Good adsorption capacity provides a guarantee for maintaining the stable pressure in the vacuum environment inside the VIP, which is the key factor to prolong the service life of the VIP board. In addition, there is also a small amount of nano particles in the glass fiber interspaces, which to some extent reduces the porosities of the material and increases the service life of the material in a vacuum environment. Tab. 1 compares the core material's specific surface area and pore size when with and without TiO_2. Based on the data analyses, with the increase of the TiO_2 content, the core material's specific surface area increases gradually and the pore diameter decreases. It exactly testifies the authenticity of the above argument.

Tab. 1 Surface areas of samples

Samples	TiO_2	GF	GF/TiO_2 (1%TiO_2)	GF/TiO_2 (5%TiO_2)	GF/TiO_2 (10%TiO_2)
Surface areas/(m^2/g)	86.40	1.12	1.55	2.55	3.68

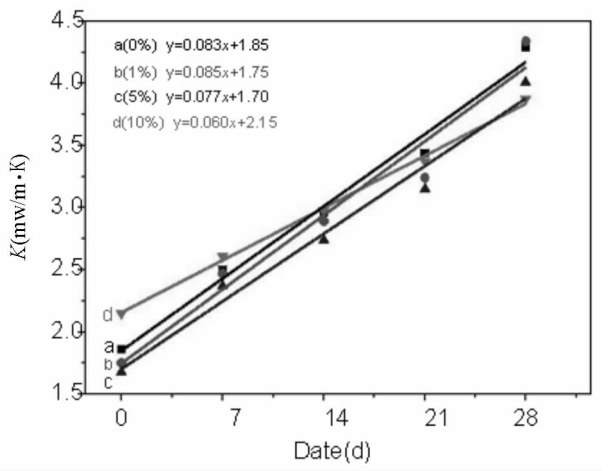

Fig. 4 Aging results of GF/TiO_2 after four weeks

4. Conclusion and outlook

This paper, taking TiO_2 as sunscreens, studies the effects of different additive amounts on thermal conductivity and service life of the VIP. The results show that the thermal conductivity reaches the lowest point at 0.00168 W/(m·K) when the additive amount of TiO_2 is 5%; the service life increases with the increase of TiO_2 contents. Good insulation performance and long service life provides a guideline for developing new nano-composite core materials. But the stability of the materials needs further researches. Therefore, the materials cannot be used for mass production at present. Further research is needed to find a more suitable mix of nano particles and glass fibers.

References

[1] Applied Mechanics and Materials. C. D. Li, et al. (2012) 174-177.

[2] 11th International Vacuum Insulation Symposium. Z. F. Chen, et al. (2013) 83-84.

[3] ACS Appl. Mater. Interfaces. Kati Raju et al. (2014) 8124-8133.

[4] J. New Mat. Electrochem. Systems 3. J. Luo et al. (2000) 249-252.

[5] RSC Adv. Y. C. Yang. et al. (2014) 31941-31947.

Ultrafine Fiberglass Core Material for Vacuum Insulation Panels Produced by Centrifugal-spinneret-blow Process

Chen Zhou, Chen Zhaofeng*, Xu Tengzhou

College of Material Science and Technology, Nanjing University of Aeronautics and Astronautics, Nanjing, 210016, P. R. China

Abstract

Vacuum insulation panel (VIP) is a high performance thermal insulator consisting of evacuated core material with getters encapsulated by a high barrier envelope material. Fiberglass core material is widely used for its light weight and high temperature durability. In this paper, Ultrafine fiberglass core material is prepared by centrifugal-spinneret-blow (CSB) process. The diameter and microstructure of fiberglass core material have been investigated by scanning electron microscopy (SEM) and vertical optical microscope (VOM). The thermal conductivity of fiberglass core material and VIPs was determined by heat flow meter thermal conductivity instrumentation. The results indicated that the diameter of fiberglass core material prepared by CSB process can reach the ultrafine grade ($d=1\sim4\mu$m). The thermal conductivity of core material was 0.0298W/(m·K) when the diameter was 3μm and the density was 62kg/m^3. The thermal conductivity of ultrafine fiberglass core material decreased with the reduction of fiber diameter when the density of glass fiber sample is constant. The lifetime of VIP of ultrafine fiberglass core material improved with the reduction of fiber diameter. In this paper, it is also concluded that the aging curves of VIPs of ultrafine fiberglass with different fiber diameter under different environment.

Keywords vacuum insulation panel, core material, ultrafine fiberglass, centrifugal-spinneret-blow process

* Corresponding author, Tel: 86-25-52112909, Fax: 86-25-52112626, E-mail: zhaofeng_chen@163.com

Mechanical Structures for Vacuum Insulation Panel (VIP) Cores

Alan Feinerman[a,b*], Tomas Juocepis[a], Ravi Patel[a], Tatjana Dankovic[b], Prateek Gupta[a]

a. Thermal Conservation Technologies, 8853 Kenneth Terrace, Skokie, Illinois, 60076, USA

b. Department of Electrical and Computer Engineering, University of Illinois at Chicago, Chicago, Illinois, USA

Abstract

A mechanical structure for a vacuum insulation panel (VIP) core would have superior thermal performance to a fumed silica or fiberglass core as long as it could maintain a higher ratio of mechanical stress to thermal conductivity. The thermal conduction component of the heat transfer across a VIP is reduced with a mechanical structure like periodic supports by the factor, $\left(\frac{k_{fs}\sigma_{sup}}{k_{sup}atm}\right)$. It has been demonstrated that supports fabricated from 25μm thick 304 stainless steel could support up to a 965 MPa load (σ_{sup}). Assuming thermal conductivities of 16 and 0.0025 W/(m·K) for stainless steel (k_{SS}) and fumed silica (k_{fs}) respectively. A fumed silica core would have up to a 50% higher thermal conduction than a mechanical structure. The ratio of the mass of a fumed silica core to a mechanical structure is $\left(\frac{\rho_{fs}\sigma_{SS}}{\rho_{SS}atm}\right)$, and can be 180 times higher for fumed silica assuming a density of 0.15 (ρ_{fs}) and 8.0 (ρ_{SS}) gm/cm^3 respectively. The reduction in thermal conduction and mass increase if a titanium alloy with a lower thermal conductivity and density is used instead of stainless steel. Glass columns would be another potential replacement since they could support a compressive stress of 50MPa and have a thermal conductivity of 1.1 W/(m·K). This research work did not evaluate commercially available filaments as tensile support structures.

Keywords vacuum insulation panels, mechanical core

1. Introduction

Vacuum insulation panels (VIPs) offer the opportunity to greatly increase the thermal insulation that can be achieved when space is constrained. Current VIPs utilize a fumed silica or fiber glass core which has a very low effective thermal conductivity as long as the pressure inside the VIP is maintained below 1.3 Pa. Replacing the current cores with a mechanical structure offers the opportunity to improve the thermal performance and reduce the weight of the VIPs.

2. Mechanical load

In order to support an atmospheric load a mechanical structure with a periodicity of λ has to withstand a stress σ_{sup} across a support given by equation (1).

$$\sigma_{sup}A_{sup} = atm\lambda^2 \quad (1)$$

where

A_{sup} = load bearing area of support,

atm = atmospheric pressure, 0.101 MPa.

The thermal conduction component of the heat flow in each period is given by equation (2).

$$k_{sup}A_{sup}\ \nabla T \quad (2)$$

where

k_{sup} = thermal conductivity of support,

∇T = temperature gradient across VIP.

The thermal conduction component of heat flow across a comparable VIP area with a fumed silica core is given by equation (3).

$$k_{fs}\lambda^2\ \nabla T \quad (3)$$

* Corresponding author, Tel: (312) 498-7584; fax: (312) 413-0447; E-mail: AFeinerman@tensileVIP.com

where

k_{fs} = thermal conductivity of fumed silica.

The ratio of these terms is given by equation 4 once the load bearing area of the support is eliminated.

$$\left(\frac{k_{fs}\sigma_{sup}}{k_{sup}atm}\right) \quad (4)$$

This ratio is 1.5 when 965 MPa is supported by stainless steel.

3. Periodicity choice and VIP mass

The number of supports/area is inversely proportional to the square of the period, so the larger the period the faster the mechanical support can be assembled. The VIP envelope contributes significantly to its cost, and when using stainless steel foil [1], the cheapest material/area is 0.051mm thick. Thinner stainless steel foil is commercially available but at a higher cost/kg which can eliminate any savings. An array of columns carrying a 50 MPa load with a 25.4 mm period would require the stainless steel foil supporting a tensile stress of at least ~320 MPa as given by equation 5.

$$\sigma_{env}\pi d_{sup}t_{env} = atm\lambda^2 \quad (5)$$

where

σ_{env} = is the stress in envelope,

d_{sup} = is the diameter of a cylindrical support,

t_{env} = is the envelope thickness.

The lowest ultimate tensile strength that austenitic stainless steel can support is ~515MPa [2] so the period could potentially be increased. Changing the shape of the load bearing area of the mechanical support from a circle to an annulus would lower the stress on the envelope.

The mass for one period of a VIP of a mechanical structure and fumed silica is given by equations 6 and 7 respectively.

$$\rho_{sup}A_{sup}t_{VIP} + 2\rho_{env}t_{env}\lambda^2 \quad (6)$$

$$(\rho_{fs}t_{VIP} + 2\rho_{env}t_{env})\lambda^2 \quad (7)$$

where

ρ_{sup} = mass density of support,

t_{VIP} = VIP thickness,

ρ_{env} = mass density of envelopet,

t_{env} = envelope thickness.

A 25.4 mm thick fumed silica VIP with a density of 0.15 gm/cm^3 inside a 0.13mm thick LDPE envelope with a density of 0.92 gm/cm^3 would weight 4.8 times as much as the same thickness VIP with stainless steel supports carrying 965 MPa in a 0.051mm thick stainless steel envelope.

4. Mechanical testing

In order to evaluate the mechanical strength of an array of 3×3 supports with a 25.4 mm period required loading them with ~60kg. Instead of using weights as shown in Fig. 1, or a volunteer to supply this load, a compact system was constructed and is shown in Fig. 2. The load is generated with a pancake air cylinder pushing on a load cell (Omega LC305-300). The load cell supports a plate that slides vertically on four linear bearings. The top plate can be replaced with one that has a large hole in the center to install ~50 kg weight to calibrate the load cell. This arrangement would let us safely measure forces up to ~2000 N (200 kg load) with our particular load cell.

Fig. 1 Columns can be loaded by adding progressively more mass. A towering stack of weights is a hazard

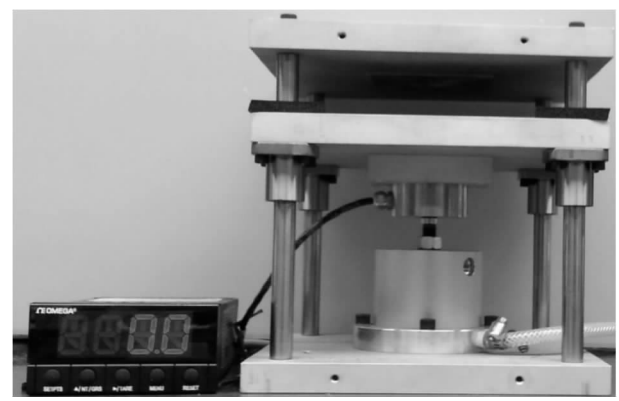

Fig. 2 Columns can be loaded by increasing the air pressure supplying the pancake cylinder in a compact tester

5. Mechanical results

The mechanical testing results are summarized in Tab. 1. It is assumed that grade 9 titanium (3% Al, 2.5% V) can carry the same load as the stainless steel foil. Annealed titanium was evaluated and it supported comparable stress as annealed stainless steel, 300 MPa. The full hard stainless supported 965 MPa. Data on filaments reported to have high tensile strength and low thermal conductivity (Nextel, 3M) are not reported since they broke at the point where they were clamped.

Tab. 1

	Glass	SS	Ti3 −2.5
σ_{sup}/Pa	50×10^6	965×10^6	965×10^6
k_{sup}/(W/(m·K))	1.1	16	7.8
ρ_{sup}/(kg/m^3)	2230	8000	4510
σ_{sup}/k_{sup}	4.5×10^7	6.0×10^7	1.2×10^8
σ_{sup}/k_{sup}	2.2×10^4	1.2×10^5	2.1×10^5

6. Conclusions and outlook

The mechanical properties of glass, stainless steel, and titanium foil structures have been evaluated. Arrays of these structures can lower the weight and increase the thermal performance of VIPs.

Acknowledgements

This study was sponsored by Thermal Conservation Technologies with support from NSF Phase II SBIR #1230294 and Clean Energy Trust "2011 Business Concept Award." Dr. Alan Feinerman is the majority owner of Thermal Conservation Technologies.

References

[1] A. Feinerman, ... Vacuum Insulation Panels (VIPs) Encased in Stainless Steel Envelopes, IVIS2013.

[2] A.C. Reardon, 2011, Metallurgy for the Non-Metallurgist, Second Edition, ASM International, p. 421.

Investigation of Non-evaporable Barium Matrix Composite Getter for VIPs

Di Xiaobo[a*], Chen Zheng'an[b], Lin Xiaobin[b], Chen Zhaofeng[a]

a. College of Material Science and Technology, Nanjing University of Aeronautics and Astronautics, Nanjing, 210016, P. R. China
b. Fujian Super Tech Advanced Material Co., Ltd., Xiamen, 361021, P. R. China

Abstract

To ensure superior thermal insulation performance and long service life, Vacuum Insulation Panels (VIPs) must have as low internal gas pressure as possible, especially for glass fiber core matetials thermal conductivity of which is sensitive to pressure increase. It is essential to add getter into VIPs with glass fiber core materials. The room temperature non-evaporable barium matrix composite getter is investigated in this paper, including chemical composition, preparation process and structure design, sorption capacity of which for nitrogen, oxygen and hydrogen are measured by constant volume method using a dedicated apparatus and for water vapor by weight method. Sorption process and soprtion mechanism are also discussed. Thermal conductivity change with time are tracking measured by thermal conductivity meter for VIPs with and without composite getter.

Keywords vacuum insulation panels, thermal conductivity, getter, sorption capacity, service life

1. Introduction

Vaccum insulation panels (VIPs) with glass fiber core materials have already been used widely in the fields of the refrigerator, automatic vending machine and water heater, because of distinguished low thermal conductivity < 2.5 mW/(m · K), even to 1.0 mW/(m · K) and low production cost [1,2]. It is estimated that in 2014 the production capacity of VIPs exceeded 5 million square meters in China. Twenty-five percent of energy can be saved without reducing the effective capacity of refrigerator when VIPs substitutes partial polyurethane rigid foams as insulation layer [3]. However, the thermal conductivity is sensitive to pressure increase owing to large pore size of glass fiber core materials and short service life in industrial application [4]. Thus, the getter or desiccant is essential to sorb residual gases released from glass fiber core materials and permeated by gas barrier film and heat seal layer [4,5]. By adding getter or desiccant into core materials, the low internal pressure of VIPs would be maintained, the thermal insulation performance would be improved and the service life would be prolonged [6].

Conventional getter materials must be activated or evaporated by heating to more than 450℃, while gas barrier film with plastics cannot be heated at temperature higher than 150℃. Therefore, the conventional getter materials can not be applied to VIPs, and the getter that does not require high temperature thermal activation is essential. It is indicated that Ba-Li (Barium-Lithium) alloy can sorb active gases such as oxygen (O_2), nitrogen (N_2), carbon dioxide (CO_2), carbon monoxide (CO), water vapor (H_2O) and hydrogen (H_2) at room temperature without requiring thermal activation [7]. The major permeation gases through the barrier film are H_2, H_2O, N_2, O_2 and CO_2, and the main residual gases, released from the glass fiber core materials and inner surface of barrier film, are H_2O and H_2 [8]. In addition, Lithium belongs to alkali metals and Barium belongs to alkaline earth metals, alloy of which reacts with water to form alkali

* Corresponding author, Tel: 86-592-6199967, E-mail: xiaobob_2008@163.com

and give off hydrogen. The chemical reaction of Ba-Li alloy with hydrogen, in essence, is that hydrogen dissolves into alloy to form solid solution that is an unstable compound. The hydrogen can be released from solid solution at a certain temperature and pressure. The thermal conductivity of hydrogen is seven times as high as that of air, which is extremely harmful to thermal insulation property of VIPs. Therefore, the Ba-Li alloy cannot be used alone as getter material for VIPs.

The room temperature non-evaporable barium matrix composite getter consisting of Ba-Li alloy, calcium oxide (CaO) and copper oxide (CuO) is investigated in this paper, including chemical composition, preparation process and structure design. The Ba-Li alloy sorbs O_2, N_2, CO_2 and CO and CaO sorbs H_2O and CuO sorbs H_2. The Sorption capacity for N_2, O_2, H_2 and H_2O are measured and sorption process and mechanism are also discussed. The effect of composite getter on VIPs service life is also studied.

2. Experimental Sections

2.1 Composite getter preparation

2.1.1 The preparation of Ba-Li alloy

According to Ba-Li alloy binary phase diagram, as shown in Fig. 1, one intermediate phase with composition corresponding to $BaLi_4$ is formed by peritectic reaction which melts incongruently at 156℃. A eutectic reaction at 10.5 at. % Ba occurs at 143℃. In this paper, the intermetallics $BaLi_4$ was prepared by vacuum median frequency smelting and the alloy was crushed and ground into powder with grain size less than 45 mesh under argon atmsphere.

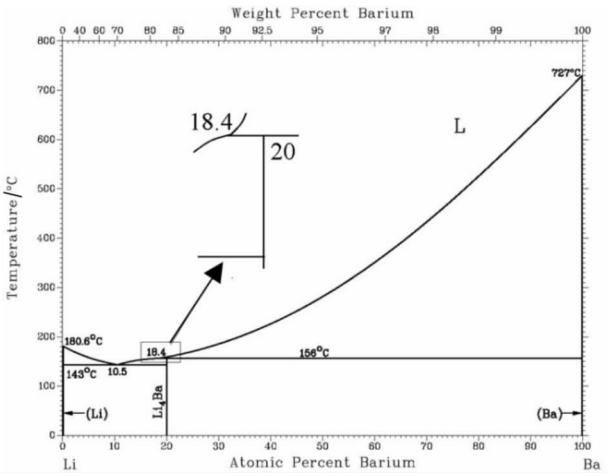

Fig. 1 The Ba-Li alloy binary phase diagram

2.1.2 The composite getter structure design

In order to avoid chemical reaction of Ba-Li alloy with water vapor, the principle of structure design is "first desiccation, then sorption gas", as shown in Fig. 2 [7]. The composite getter consists of CaO for sorption water vapor, CuO for sorption hydrogen and $BaLi_4$ alloy for sorption dry gases.

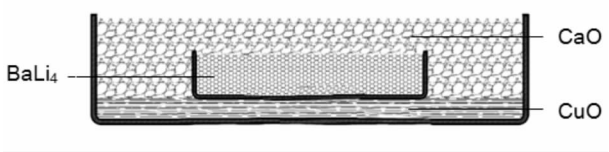

Fig. 2 The sketch drawing of composite getter

2.2 Preparation of VIP test specimens

Two kinds of VIPs were manufactured with a four-layer structure high gas barrier laminate which contains three layers of aluminum-coated polyethylene terephthalate (MPET) and one layer of low-density polyethylene (LDPE) and glass fiber as core material, half of which the composite getter were added into core materials for performance comparison. All VIPs were stored in air with constant temperature and humidity (25℃/50% RH) and measured regularly throughout an overall period of 2 years.

2.3 Testing apparatus

The thermal conductivity was measured by thermal conductivity meter (EKO HC-072-200). The surface morphology and specific area of CaO and CuO powder were analyzed by SEM and BET. The chemical composition and crystal structure were studied by XRD. The water absorption of CaO was measured by weight method. The sorption capacity of composite getter for N_2, O_2, H_2 were measured by constant volume method using a dedicated apparatus whose schematic diagram is shown in Fig. 3, leakage rate $<1.5\times10^{-4}$ Pa·L/s and base pressure $<1.0\times10^{-4}$ Pa.

The testing procedure is as follows:

(1) The sample chamber and vacuum globe valve were detached and put into glove box under argon atmsphere.

(2) The getter sample was put into sample chamber then the vacuum globe valve was closed in glove box.

(3) The sample chamber and vacuum globe valve

were taken out from glove box then connected with test apparatus.

(4) Turned on the fore vacuum pump (double step rotary vane vacuum pump), when pressure $<$ 50 Pa, turned on turbomolecular pump (TMP), when pressure $<1.0\times10^{-4}$ Pa, shut off goggle valve and TMP, then filled high purity argon into vacuum chamber until 1 atm.

(5) Turned on vacuum globe valve and goggle valve, when pressure $<$ 50 Pa, turned on TMP, when pressure $<1.0\times10^{-4}$ Pa, goggle valve and vacuum system were shut off, then filled test gas into vacuum chamber.

(6) The pressure decrease with time was obtained.

Therefore, the test sample is not exposed to air in sample installation process.

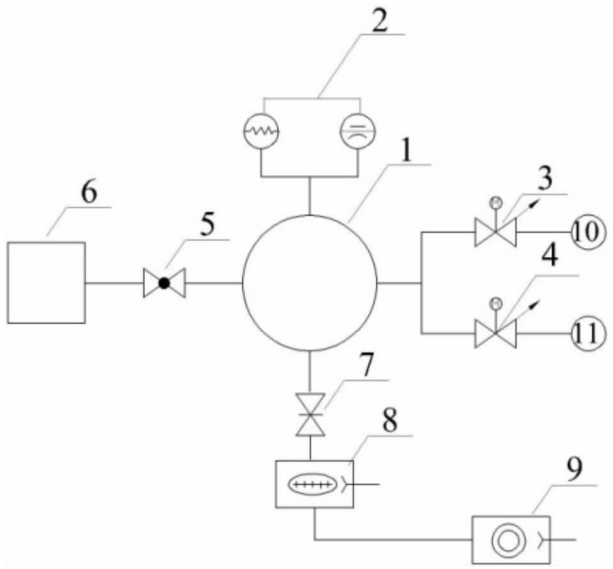

Fig. 3 The schematic diagram of sorption capacity test apparatus

1—Vacuum chamber; 2—Vacuum gauge;
3,4—Gas dosing value; 5—Vacuum globe valve;
6—Sample chamber; 7—Goggle valve;
8—Turbomolecular pump; 9— Fore vacuum pump

3. Results and discussions

3.1 Physical and chemical properties of getter materials

3.1.1 $BaLi_4$ alloy

The powder of $BaLi_4$ alloy, shown in Fig. 4, reacts with water to give off hydrogen and lots of heat in humid air, and then spontaneous combustion and explosion, which is difficult to properties test. Only XRD was used for chemical composition and crystal structure analysis in this paper. To prevent chemical reaction during exposure in the diffractometer, the powder sample was mixed with Vaseline and then produced a paste which was stable during exposures of less than one half hour [9].

Fig. 4 The $BaLi_4$ alloy powder

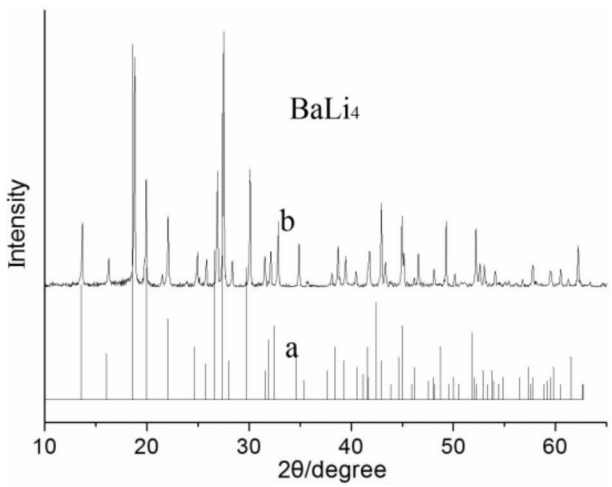

Fig. 5 The XRD test result of $BaLi_4$ alloy

a—standard diffraction pattern;
b—diffraction pattern of $BaLi_4$ sample

The $BaLi_4$ alloy, test result shown in Fig. 5, belongs to hexagonal cell with low impurity content and no segregation phase, which indicates that the alloy sample is not contaminated during smelting, grinding and testing, and the alloy with high purity is obtained.

3.1.2 Active calcium oxide

To sorb thoroughly a little water vapor in VIPs, the high active CaO is investigated in this paper. The surface morphology of unactivated CaO and activated CaO powder are shown in Fig. 6, which shows that the unactivated large particles become activated nano-sized

particles agglomerate. The BET surface area increases from 1.5 m^2/g to 16.5 m^2/g, approximately one order of magnitude.

The XRD test results shown in Fig. 7 indicate that the crystal structure of CaO is not changed in the activation treatment, both of which are NaCl crystal type. Compared with unactivated pattern C, the diffraction peak of activated pattern B become wider, indicating that the crystal defects increase and the specific surface area become larger. Therefore, activation process only changes the physical state of CaO and increases the activity.

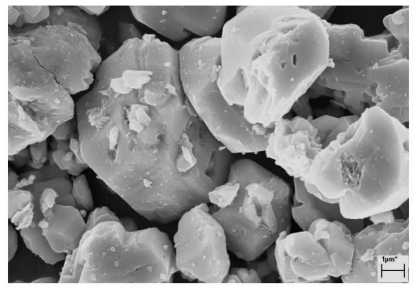

(a)

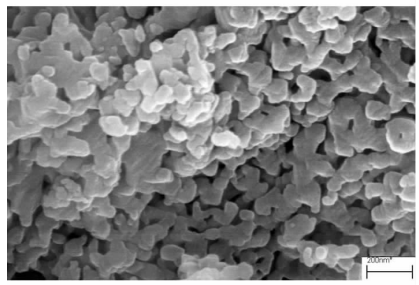

(b)

Fig. 6 The SEM images of CaO powder

(a) Theunactivated CaO powder;

(b) The activated CaO powder

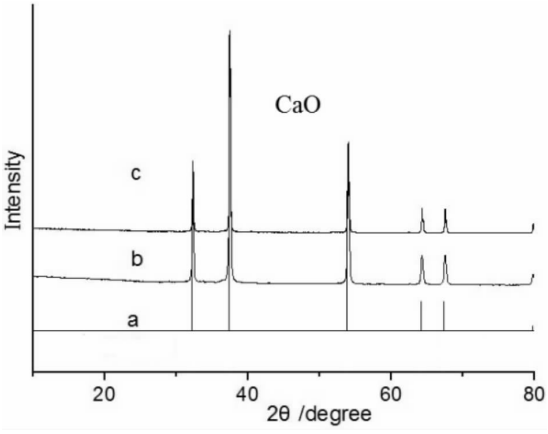

Fig. 7 The XRD test results of activated CaO and unactivated CaO

a—standard diffraction pattern;

b—diffraction pattern of activated CaO;

c—diffraction pattern of unactivated CaO

3.1.3 Active copper oxide

Similarly, to sorb trace amounts of hydrogen, the high active CuO is also investigated in this paper. Fig. 8 and Fig. 9 show separately the surface morphology and XRD test results of unactivated and activated CuO powder. The unactivated large particles of CuO powder become activated nano-sized particles agglomerate and the BET surface area increases from 0.7 m^2/g to 7.8 m^2/g. The diffraction peak of activated pattern C become wider, which indicates crystal defects, specific surface area and activity increase.

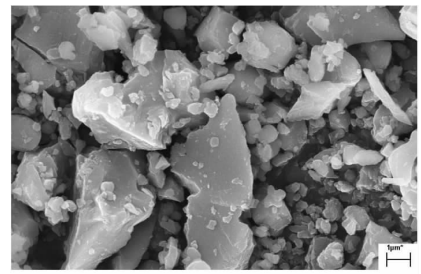

(a)

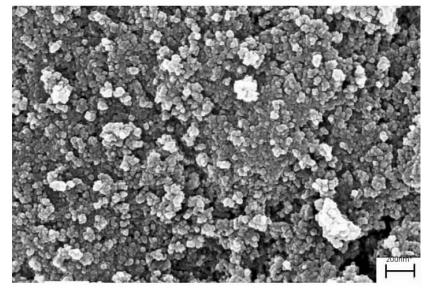

(b)

Fig. 8 The SEM images of CuO powder

(a) Theunactivated CuO powder;

(b) The activated CuO powder

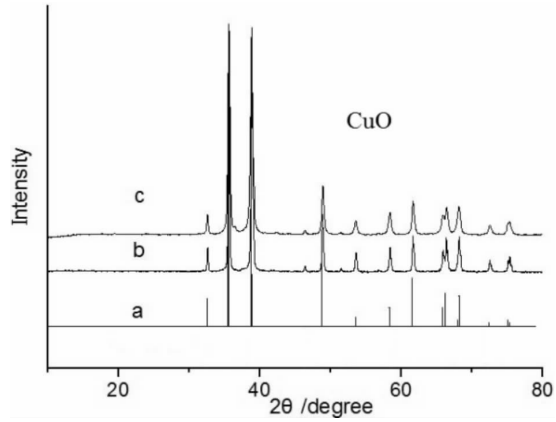

Fig. 9 The XRD test results of activated CuO and unactivated CuO

a—standard diffraction pattern;

b—diffraction pattern of unactivated CuO;

c—diffraction pattern of activated CuO

3.2 The sorption capacity of composite getter

The Sorption curves of composite getter for N_2, O_2 and H_2 are shown in Fig. 10～12. Taking sorption N_2 for example, the adsorption process is explained. From Fig. 10, the curve can be divided into three stages:

(1) The getter has great adsorption rate for N_2 in the initial 300 minutes. $BaLi_4$ powder is compacted into porous materials with great specific surface area, which can physically adsorb a large amount of N_2, at the same time, along with the beginning of the chemical reaction.

(2) From 300 minutes to 4000 minutes, the adsorption reaches an equilibrium state. The physical adsorption gas diffuses continuously into getter by bulk diffusion and then occurs chemical absorption. Compared with 1st stage, the adsorption rate becomes slow. The slope of fitting line ($0.01515 Pa \cdot s^{-1}$) indicates pressure decrease rate with time, which multiplies by the volume of vacuum chamber (6.73L) and then obtains the average sorption velocity, equaling to 1.70×10^{-3} $Pa \cdot L \cdot s^{-1}$.

(3)4000 minutes later, the adsorption rate decreases sharply. The reason is that gas molecules collided with the getter surface in unit time reducing with gas pressure decrease. In addition, the getter is consumed partly. Similarly, the average sorption velocity is obtained, equaling to 1.03×10^{-4} $Pa \cdot L \cdot s^{-1}$.

The sorption capacity of getter equals to the product of pressure difference (88Pa) and the volume of vacuum chamber (6.73L), equaling to 592.2 $Pa \cdot L$.

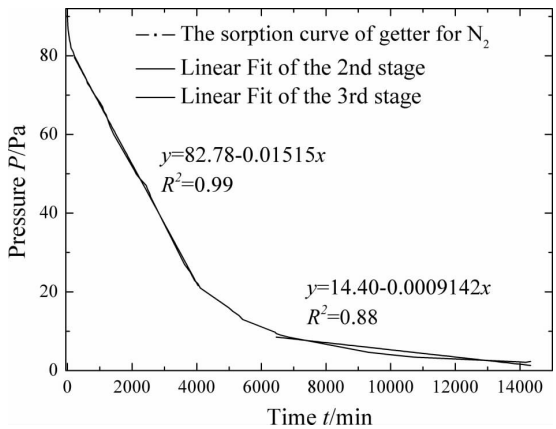

Fig. 10 The sorption capacity of getter for N_2

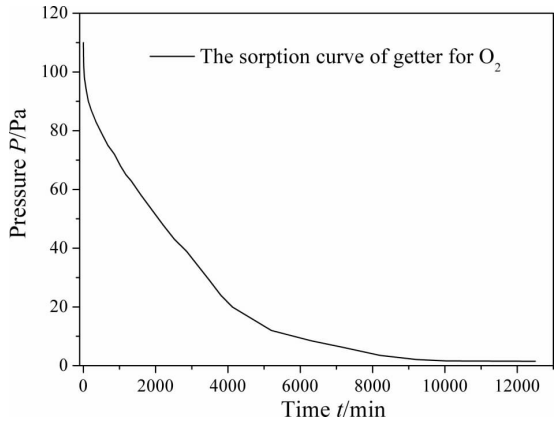

Fig. 11 The sorption capacity of getter for O_2

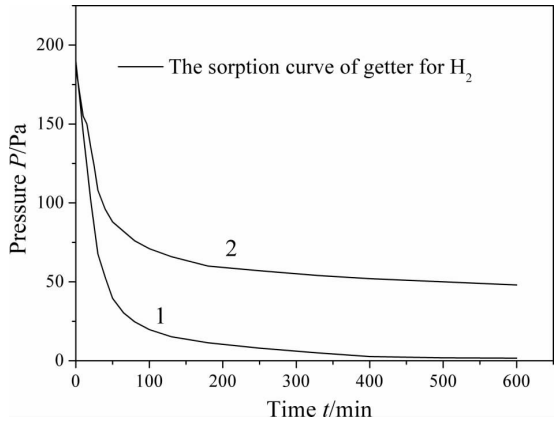

Fig. 12 The sorption capacity of getter for H_2

The water absorption of CaO was tested by weight method at a constant temperature and relative humidity (25℃/23% RH). Figure 13 shows the water absorption change of CaO with time. The nano-sized high active CaO that absorbs water vapor by hydration reaction has great water adsorption rate in the initial stage, which is essential to absorb thoroughly a little water vapor within VIPs.

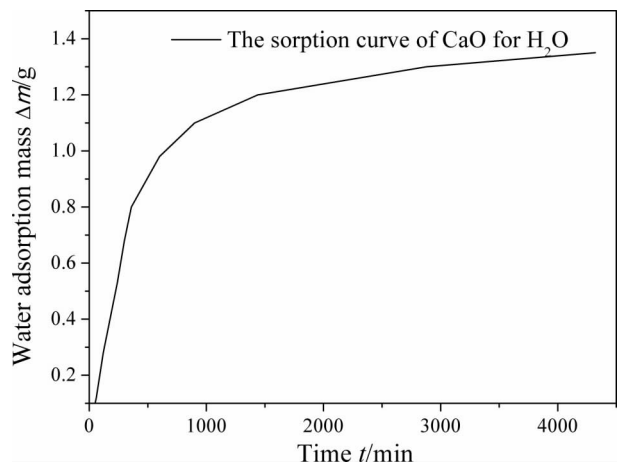

Fig. 13 The sorption capacity of CaO for H_2O

3.3 The effect of composite getter on VIPs service life

The tracking test results of thermal conductivity change with time for VIPs with and without composite getter are shown in Fig. 14. The thermal conductivity of VIP without composite getter increases by 3.2 mW/(m·K) after 2 years, but for VIP with composite getter, it only increases by 0.4 mW/(m·K). For VIP with getter, the anticipate service life exceeds 30 years, the thermal conductivity about 11.3 mW/(m·K) based on linear extrapolation.

Therefore, the composite getter can effectively absorb the residual gases and maintain low pressure in VIPs, the thermal insulation performance of which would be improved and service life would be prolonged.

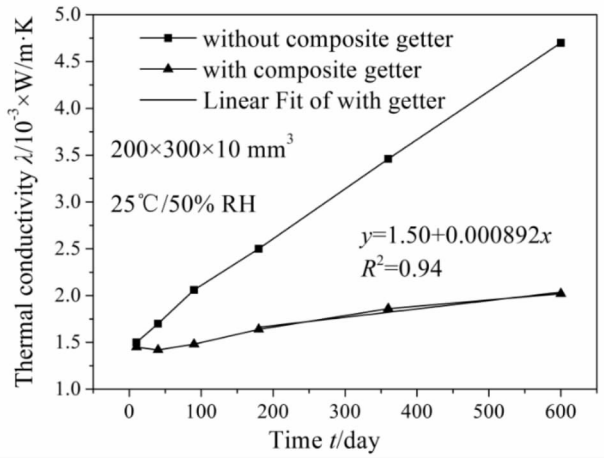

Fig. 14 Test results of thermal conductivity change with time for VIPs with and without composite getter

4. Conclusions and outlook

Despite excellent sorption property, the composite getter is not widely used in VIPs due to $BaLi_4$ alloy high chemical activity with the danger of spontaneous combustion and explosion. The alloy modification and new alloy will be investigated in the further work.

Acknowledgements

The authors appreciate the support of Research & Development Center, Fujian Super Tech Advanced Material Co., Ltd, and College of Material Science and Technology, Nanjing University of Aeronautics and Astronautics.

References

[1] K. Araki, D. Kamoto, S. I. Matsuoka, Optimization about multilayer laminated film and getter device materials of vacuum insulation panel for using at high temperature, Journal of Materials Processing Technology 209 (2009) 271 – 282.

[2] X. B. Di, Y. G. Gao, C. G. Bao, S. Q. Ma, Thermal insulation property and service life of vacuum insulation panels with glass fiber chopped strand as core materials, Energy and Buildings 73 (2014) 176 – 183.

[3] C. G. Yang, Y. J. Li, X. Gao, L. Xu, A review of vacuum degradation research and the experimental outgassing research of the core material – PU foam on vacuum, Physics Procedia 32 (2012) 239 – 244.

[4] X. B. Di, Y. G. Gao, C. G. Bao, Y. N. Hu, Z. G. Xie, Optimization of glass fiber based core materials for vacuum insulation panels with laminated aluminum foils asenvelopes, Vacuum 97 (2013) 55 – 59.

[5] H. Schwab, U. Heinemann, A. Beck, H. P. Ebert, J. Fricke, Dependence of thermal conductivity on water content in vacuum insulation panels with fumed silica kernels, Journal of Thermal Envelope and Building Science 28 (2005) 319 – 326.

[6] X. B. Di, Y. M. Gao, C. G. Bao, On getters for vacuum insulation panels, in: The 10th International Vacuum Insulation Symposium, 2011, pp. 205 – 207.

[7] P. Manini, F. B. Arluno, Device for Maintaining a Vacuum in a Thermally Insulating Jacket and Method of Making Such Device, US Patent No. 5544490 (1996).

[8] H. Jung, C. H. Jang, I. S. Yeo, H. T. H. Song, Investigation of gas permeation through Al-metallized film for vacuum insulation panels, International Journal of Heatand Mass Transfer 52 (2013) 4436 – 4462.

[9] V. Douglas, J. Keller, F. A. Kanda, A. J. King. Barium-Lithium equilibrium system. Journal of Physics Chemical 62 (1958) 732 – 733.

Thermal Radiation Reduction Materials in the Application of the Glass Fiber Core Material for Vacuum Insulation Panel (VIP)

Yang Shengli*

Fujian Super Tech Advanced Material Co., Ltd., Xiamen, P. R. China

Abstract

This paper introduces the application background, the purpose and function of thermal radiation reduction materials in glass fiber core material for vacuum insulation panel (VIP). The thermal insulation mechanism of thermal radiation reduction materials to improve glass fiber core material for vacuum insulation panel (VIP) were analyzed. The kinds, shape, dispersion form, distribution effect of thermal radiation reduction material were compared. Also, a study of thermal radiation reduction materials in glass fiber core material for vacuum insulation panel in addition amount and the differences on thermal insulation effect was performed. Differences in thermal insulation effect can be measured through testing the thermal conductivity; the larger thermal conductivity, the poorer thermal insulation effect, whereas, the better thermal insulation effect. This paper also expounds the application prospect and the good benefit of thermal radiation reduction materials in the field of high efficient thermal insulation, but also points out the existing problems and the improvement of thermal radiation reduction materials.

Keywords thermal radiation, thermal radiation reduction materials, vacuum insulation panel (VIP), glass fiber, glass fiber core material, thermal insulation

* Corresponding author, Tel: 86 - 592 - 6199917, E - mail: ysL@supertech - vip. com, ysL_0592@126. com

The Technology and Application of the Free Activation Combinations-getters in VIP

Ai Xueming, Zhong Xiang*

Nanjing Thanko Vacuum Electronics Co. Ltd., Nanjing, 210016, P.R. China

Abstract

This paper describes the technology of combinations-getters used as key materials in VIPs. Gas molecules can spread through the barrier membrane of VIP, and amounts of gases are contained in the core material, so the pressure inside VIP increases with time. In the field of room temperature and the pressure is between 10^{-2} Pa to 10^{2} Pa, getters are necessary for VIPs. The combinations-getters introduced in this paper can absorb active gases such as H_2O, O_2, N_2, CO, CO_2 in large quantities, particularly H_2. What is more important is the combinations-getters can be used without activating and exposed in dry air temporarily; they will be widely used in VIP's or other fields.

Keywords free activation, getter, getters, vacuum insulation, VIP, STP

1. Introduction

Vacuum insulation panel (VIP) is a new and efficient thermal insulation material, which is based on the principle of vacuum insulation and researched in recent years. In order to achieve the ideal adiabatic effect of thermal insulation and purpose of energy saving, maximizing vacuum degree within the plate and filling in core layer insulation material were used to isolate the heat conduction [1]. Compared to the traditional thermal insulation materials such as polyurethane foam or fiberglass, the thermal conductivity of VIP is 1/10 of theirs, or even lower. Ozone Depleting Substance (ODS) was never used in the process of VIP's production and application, and the thickness of VIP is only 1/7 of the ordinary insulation, so VIP has dual advantages of environmental protection and energy saving.

The present market situation is that getters only used in VIPs when they are required to have a longer service life and lower thermal conductivity, most of the VIP manufacturers produce their products with desiccants, but they only absorb humidity. Especially in the field of construction, the VIP products also called as STP even without any getters material. Usually, the life-span requirement for home appliance is 5～10 years, and the service life of construction requires at least more than 30 years. If getters material was not used or used incorrectly, the service life will be no guarantee. Only in pursuit of short-term benefits will damage the VIP's industry reputation and long-term healthy development.

This paper's structure is as follows: part 2 introduces several kinds of commonly used VIPs, and the experimental data shows that the heat preservation performance of VIP has improved largely after using the getters; part 3 summarizes the advantages and disadvantages of international getters, puts forward a new type of free activation composite getters; part 4 gives the aging experiment data of VIPs with the getters, it shows that the coefficient of thermal conductivity is lower and performance is superior to the desiccant VIPs; part 5 summarizes the full text and puts forward the improvement direction.

* Corresponding author, Tel: 86 - 18362989968, E - mail: axm@thanko.com

2. The analysis of VIP's common manufacturing form

A common form of VIP manufacturing: ①thermal insulation core material +barrier envelope + getter; ②thermal insulation core material +barrier envelope+ desiccant; ③thermal insulation core material +barrier envelope. The following is a simple analysis of these VIP materials.

2.1 The core material of VIP

Now the core material of VIP is mainly divided into three categories: ①Chopped glass fiber (Size: 6～11 microns, length: 8～12 mm); ②Glass wool (Size: 0.5～4 microns, length: 1～8 mm); ③Silica powder. In normal conditions, the initial value of coefficient of thermal conductivity of these three core material is different.

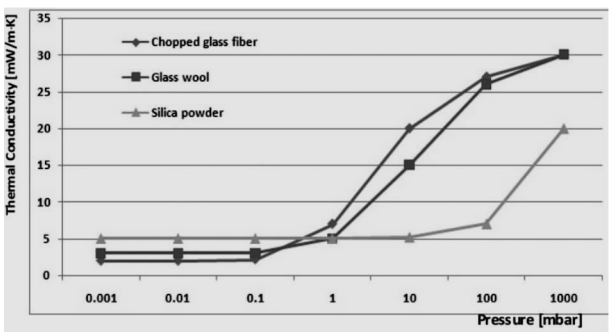

Fig. 1 The comparison chart of coefficient of thermal conductivity of three kinds of core material

The initial value of the thermal conductivity can be found in Fig. 1: the value of chopped glass fiber is 1.5～2.5 mW/(m·K); the value of glass wool is 2.5～3.5 mW/(m·K); the value of silica powder is 4.0～6.0 mW/(m·K). At low pressure, chopped silk has a minimum thermal conductivity, glass wool second, silica is highest. But as the vacuum pressure increases, the rise change rule of the coefficient of thermal conductivity become, silica powder changes most slow and chopped silk changes the fastest.

2.2 The barrier membrane of VIP

At present, the barrier membrane of VIP mainly has two categories: ① Aluminum foil membrane; ②Aluminum plating film.

Using aluminum foil membrane is based on the fact that aluminum foil membrane has a good barrier properties and the price is relatively cheap, and the use of aluminum plating film is based on the reduced heat transfer of VIP marginal effect.

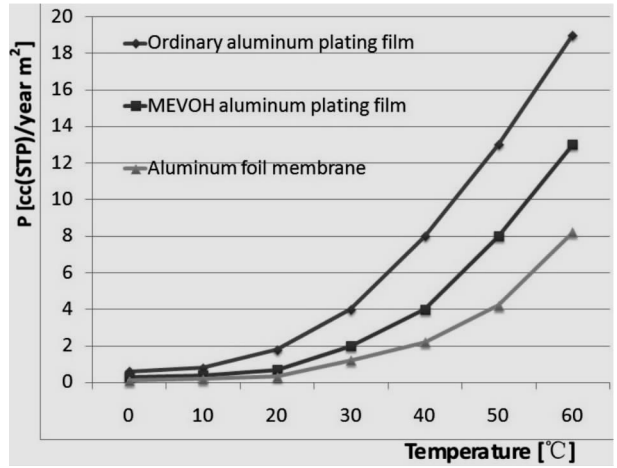

Fig. 2 The Comparison chart of permeability rate between Aluminum foil membrane and Aluminum plating film [2]

As seen in Fig. 2, aluminum foil membrane is superior to aluminum plating film for the air blocking. And as temperature rises, the air through rate of blocking film also rises greatly. The actual manufacturing process of VIP usually includes the frilled edge handling of barrier bag, the aluminum layer of membrane will damage in different degrees at the hem and sharp corners, resulting in the air transmittance of membrane material increases further.

2.3 The getters for VIP

Look from the present market, the main used getter material is "getters", "desiccant + molecular sieve" and "desiccant".

Getters is able to adsorb all reactive gases (H_2 and N_2, O_2, CO, CO_2, H_2O) and some organic gases in the air; desiccant is able to absorb water vapor; the selective adsorption of certain gases and water vapor can be done by molecular sieve.

We analyzed the above three kinds of typical materials of VIP by means of the influence factors such as their respective behavior characteristics and prices:

A. Core material: Chopped silk has the minimum thermal conductivity, glass wool takes the second place, and the highest data belongs to silica. Silica is most expensive, glass wool is second, and chopped silk has the minimum cost.

B. Barrier membrane: Aluminum foil membranes perform better than the aluminum plating films, and the costing of aluminum foil membrane is lower than the aluminum plating film.

C. Getter material: In terms of sorption properties, getters have a more excellent performance, but they are also expensive than desiccants and molecular sieves.

Of course, the requirement is different in different applications or occasions. So the choice of targeted material combination needs to meet the application requirement.

Undoubtedly, to create the product with better heat insulation performance, longer life assurance and the lower price is the development trend of VIP industry.

For these reasons and more, the initial thermal conductivity of VIP is mainly decided by the core material, shown as Fig. 1. The change of the vacuum degree within the VIP is mainly decided by the barrier membrane, as shown in Fig. 2. We assume that the degassing treatment of the core material and curing processing of the barrier membrane are both sufficient, and air content of the material itself is negligible. The key factor that results in the change of vacuum degree within the VIP is air penetration through the barrier membrane, and the air penetration is inevitable. VIP still absorbs residual gas after sealed, and it also will absorb the infiltration and the released gases from the core material. In order to maintain the vacuum degree inside VIP, the getters material is essential.

Once the inner pressure reaches to 10Pa, coefficient of thermal conductivity of VIP will rise rapidly. However, the pressure from 10^{-2} Pa or less to 10^{2} Pa belongs to the work scope of getters.

A new kind of free activation combinations-getters for VIPs is introduced in this paper. This product not only can absorb the water molecule, but also can absorb the active gases such as O_2, N_2, CO, CO_2 in large quantities, particularly H_2. What is more important is that the combinations-getters can be used without active and exposed in dry air temporarily, and it is suitable for large scale production.

3. The free activation combinations-getters TK107

On the present market, the mainly used getter material has three categories: ① desiccant; ②desiccant +molecular sieve; ③getters.

Most desiccants are alkaline-earth metal oxides, such as calcium oxide, barium oxide and magnesium oxide, etc., which is the main water absorbing material. But due to factors like cost, safety considerations, calcium oxide was mainly adopted as SAP. Chemical absorption of CO_2 lets calcium oxide change to stable $CaCO_3$. Calcium oxide can also adsorb some reactive gases physically, but it is unstable. Because the physical adsorption process is reversible, the gases will release again along with the change of temperature. In addition to temperature, the inhalation rate of calcium oxide is related to the specific surface area and loose intensity.

Reaction equation and the adsorption quantity are as follows:

$CaO+CO_2=CaCO_3$ (405 mbar · L/g)

$CaO+H_2O=Ca(OH)_2$

Water regain of calcium oxide is generally about 32% of its weight. Processing of Calcium oxide not only needs the purity of more than 95% of the calcium oxide ingredients, but also needs the high specific surface area. Then, the calcium oxide powder after the specific process will have a strong capacity of water absorption and absorption rate. The product model for TK205 desiccant of Nanjing Thanko Vacuum Electronics Co. ltd. and the product model for SMART desiccant from Italy SAES company were tested under 80℃, 80% humidity and 24 hours, respectively. Measured bibulous rate of both has reached 45% of the weight of the product itself.

In addition to H_2O and CO_2, the adsorption quantity of other reactive gases is very less, which limits the use of the desiccant in the VIP.

Molecular sieve has the function of selective absorption; different molecular sieve structure can absorb different gas molecules. Generally, the osmotic gas through the barrier membrane is multifarious, only a few species of osmotic gases can be adsorbed with a few kinds of molecular sieve used as the getters

material. If loading all the molecular sieve material to absorb all gas in the getters, this certainly will increase the manufacturing difficulty and cost of the getters. Moreover, the absorption of gas through molecular sieve is physical mostly, and the process is reversible. When the temperature rises, the adsorption gas overflows. This is unfavorable in the use of some particular situations like buildings and water heater industry, etc. Now this getters combination is unusual, only a handful of manufacturers do a little development and application.

The best getters material at current industry is the free activation composite getters. Due to the limitation of using conditions, the getters used in VIPs cannot contain any high temperature activation getters material. Here, therefore, the new kind of getters are called free activation combinations-getters. The ability of absorbing all the reactive gas in the air is required.

Barium lithium alloy $BaLi_4$ is one of the major components of composite getters. Firstly, an introduction of the two metallic elements: barium and lithium will be made. Barium is one of the most widely used getters material. Its chemical activity is very big, and it is the most active alkaline earth metal in the second group of the periodic table, only after lithium, cesium, potassium, sodium and Rb in the first group. Because of radioactivity, radium in the second group and francium in the first group are not considered. Barium is a body centered cubic crystal type. Another metal, lithium elements can react with a large number of inorganic and organic reagents, especially there will be an intense reaction with water. It is the only alkali metal that can generate stable hydride but enough to melt without decomposition. Lithium can combine with oxygen, nitrogen, sulfur and others, is the only alkali metal which can react with nitrogen at room temperature to generate lithium nitride (Li_3N). It is also a body centered cubic crystal type.

Barium and lithium can form a binary alloy $BaLi_4$. The alloy has the structure of hexagonal close packed lattice; its characteristic is a little hard and brittle. It is easy to mill, so it is very beneficial for large-scale industrial production. The reactive gas is easy to diffuse to internal crystal structure of the alloy; eventually, barium and lithium react with each other to generate a more solid compound. The reaction equation and inspiratory capacity are as follows:

$3Ba+N_2=Ba_3N_2$ (55 mbar L/g)

$Ba+H_2=BaH_2$ (165 mbar L/g)

$2Ba+O_2=2BaO$ (83 mbar L/g)

$3Ba+2CO=BaC_2+2BaO$ (110 mbar L/g)

$5Ba+2CO_2=BaC_2+4BaO$ (66 mbar L/g)

$2Ba+H_2O=BaH_2+BaO$ (83 mbar L/g)

$4Li+O_2=2LiO$ (817 mbar L/g)

$6Li+N_2=2Li_3N$ (545 mbar L/g)

$4Li+CO_2=2Li_2O+C$ (817 mbar L/g)

Besides reacting with inorganic active gas, lithium can also react with part of the organic gas to play a good role on absorption.

While barium lithium alloy has a strong suction performance, however, its first reaction is to generate H_2 with water vapor. And generating hydrogen gas has a great influence on thermal conductivity in the VIP.

$Ba+2H_2O=Ba(OH)_2+H_2\uparrow$

$2Li+2H_2O=2LiOH+H_2\uparrow$

Tab. 1 Coefficient of thermal conductivity of gases

Gases	Temperature/℃	Coefficient of thermal conductivity/(mW/(m·K))
air	0	24
air	100	31
hydrogen	0	170
nitrogen	0	24
oxygen	0	24
carbon dioxide	0	15
water vapor	100	25

It can be seen from the Tab. 1; the coefficient of thermal conductivity of hydrogen is 7 times of the amount of nitrogen. Such tests have been performed by putting lithium barium alloy into the bottom of the metal carrier, covered it with calcium oxide in the above, and then packed them into VIP to do the high temperature and high humidity aging test. After testing, it was found that thermal conductivity of the VIPs rises quickly, even worse than these VIPs' which not involve any getters material. Therefore, the first important problem needed to resolve is barium lithium alloy is preferred to generate hydrogen by reacting with

water. At present, two main kinds of technologies are known:

(1)Barium lithium alloy+ Precious metal oxides+ Desiccant. Such a technology is proposed by an Italian company SAES in the patent literature ZL 95193987.4 of China [3]:

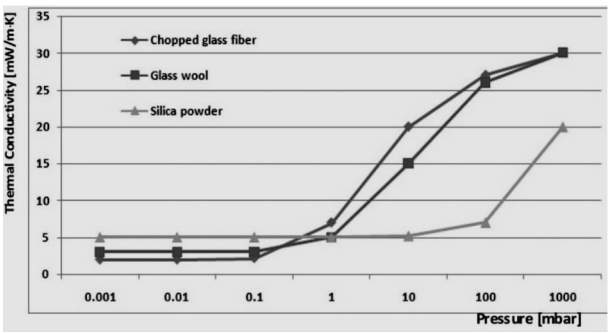

Fig. 3 Product schematic diagram of SAES Company

In these getters, barium lithium alloy is the main getter material, precious metal oxides such as cobalt oxide, palladium oxide, copper oxide is the catalyst. Constant hydrogen combines with oxygen to form water, and then the water molecules will be absorbed by calcium oxide. In addition to being able to absorb water molecules, calcium oxide also can cut off the gas in a short time. Getter is vacuum packed before use, but it must be put into VIP in a very short time (generally within 15 minutes) to keep a vacuum station. Otherwise, excessive exposure to the atmospheric environment will lead to the loss of gas absorption efficiency and even the getters will be disabled.

(2)Barium lithium alloy+ Non evapotranspiration getters alloy+ Desiccant. This technology is proposed by Nanjing THANKO Vacuum Electronics Co. Ltd. in the patent literature ZL 201220671837.5 of China [4]:

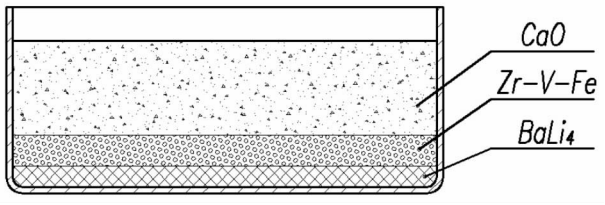

Fig. 4 Product schematic diagram of Nanjing Thanko Vacuum Electronics co. ltd

In this getters, barium lithium alloy is the main getter material, non evapotranspiration getters such as zirconium vanadium iron and aluminum zirconium alloy is the hydrogen absorbing material. The type of non evapotranspiration getters material has a strong ability of hydrogen adsorption; the hydrogen absorption capacity of each mg of zirconium vanadium iron alloy is about 13Pa · L.

In the zirconium vanadium iron alloy getters, the content of zirconium, vanadium and iron is 70%, 24.6% and 5.4%, respectively. It can be the active in 10 minutes when the pressure is lower than 10^{-1} Pa and the temperature is 400℃, and maintain a strong ability of absorbing hydrogen in a wide temperature range. The inhaling steps of non evapotranspiration getters device into three parts: First, the reactive gas molecules get to the surface of a getters and decompose; Second, reactive gas and getters produce chemical adsorption on the surface; Third, the reactive gas molecules diffuse into the depth of the getters under a certain temperature. When the getters worked for a period of time or exposed to atmosphere, a passivation layer composed of oxides and carbide would form on the surface of the getters particles. While heating can make the gas molecular of the surface diffuse into the body, then the fresh surface can be exposed to restore the getters' inspiratory capacity. This process is called active [5].

The balance pressure of hydrogen absorption for zirconium vanadium iron alloy getters is very low, so a large amount of hydrogen gas can be absorbed. But its application difficulty lies in the activation temperature is at 400℃, such a high temperature is not allowed in the process of the use of VIP. Therefore, manufacturers need to activate it beforehand, and then it can be used directly without activation.

The getters contains about 1 gram of zirconium vanadium iron alloy. In the process of manufacturing the getters, non evapotranspiration getters alloy is activated before loading. In hydrogen absorption tests, the actual absorption of hydrogen is more than 10000Pa · L. The direct adsorption of hydrogen technology is adopted to solve the problem that the barium lithium react with water to generate hydrogen. Meanwhile, non evapotranspiration getters material not only has strong adsorption ability for hydrogen, but also has the absorption ability for other reactive gas, and can assist

the barium lithium alloy for gas adsorption. The upper covered calcium oxide can be used as a material to absorb water molecules, and have the effect of obstruction for a short time.

4. Examples of application

The same getters (barium lithium alloy + zirconium vanadium iron alloy+ calcium oxide), same barrier membrane (aluminum foil membrane) and two different kinds of core material (chopped silk and glass wool) were used to manufacture two categories of VIPs to do the accelerated aging test. Experimental comparison is as follows:

Experimental conditions: Temperature 70℃; Humidity 80%

Test conditions: Temperature (23 + 2)℃; Humidity (50+10)%

Equipment conditions: Hot side (35 + 0.5)℃; Cold side (5+0.5)℃

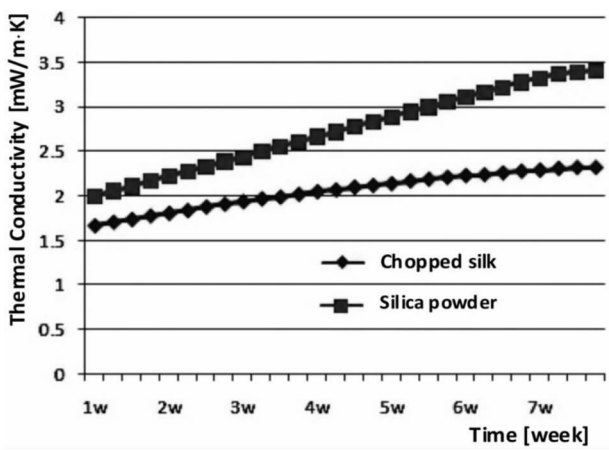

Fig. 5 Changes of thermal conductivity of the two kinds of VIPs with different core material in the accelerated aging tests

The Fig. 5 shows that the thermal conductivity of glass wool VIP is about 3.3mW/(m • K) and the data of chopped silk VIP is about 2.3mW/(m • K) 7 weeks later in the accelerated aging test. This indicates the chopped silk is more suitable to be the core material of VIP.

Three kinds of VIPs were produced to do the accelerated aging test. These VIPs involved the same core material (chopped silk) and same barrier membrane (aluminum foil membrane). But one kind of VIP contained the free activation combinations-getters (barium lithium alloy+zirconium vanadium iron alloy+ calcium oxide), another on contained the desiccant (calcium oxide), and the last kind didn't include any getters material. Experimental comparison is as follows:

Experimental conditions: Temperature 70℃; Humidity 80%

Test conditions: Temperature (23 + 2)℃; Humidity (50+ 10) %

Equipment conditions: Hot side (35 + 0.5)℃; Cold side (5+0.5)℃

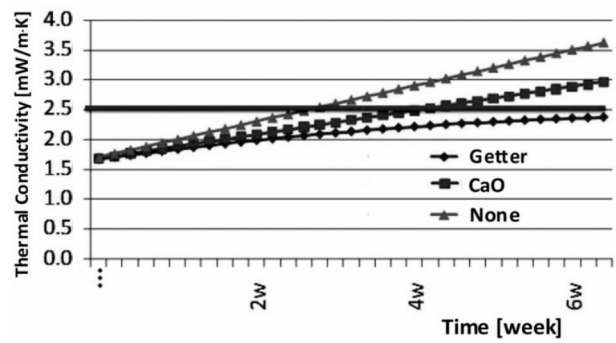

Fig. 6 Changes of thermal conductivity of the three kinds of VIPs with different getters material in the accelerated aging tests

The Fig. 6 shows that the thermal conductivity of the VIP containing getters, Cao and no getters material was about 2.3mW/(m • K), 2.9mW/(m • K) and 3.6mW/(m • K), respectively. The data of VIP involved the free activation combined getters is lowest.

With the passage of time, the gap value of the thermal conductivity of the three VIPS in Fig. 6 will further expand. This indicates that the advantage of using getters is very obvious for VIPs.

5. Conclusions

It is easy to find thatgetters material is the most important guarantee for VIP to maintain its low inner pressure and long service life after analyzed the characteristics of all component materials. In numerous getters materials, free activation combinations-getters have the most superior performance. Except the water vapor and reactive gases can be absorbed, the combinations-getters can also absorb some parts of organic gases. Therefore, the correct use of free activation combinations-getters is the most reliable guarantee for VIP's low thermal conductivity and long

service life. It is the future development trend and the goal of continuous efforts for insiders to make the VIP products more adiabatic, cheap and to extend its application field to substitute traditional heat preservation materials.

The current cost of manufacturing free activation combinations-getters is relatively high. Therefore, to improve the efficiency of the product's mass production to reduce the cost is the direction and goal of the field that should strive to.

References

[1] Yonggang Wen, et al. Vacuum insulation panels (VIP) technology and its development[J]. Cryogenic engineering, 2009, (6): 35 - 39.

[2] Yoash Carmi, Vacuum Insulation Panel Laminates-Progress in Evaluation Techniques, Lecture.

[3] Manini P., Belloni F. The device and its manufacturing method to maintain the vacuum in the insulating jacket, China, Patent for invention, ZL 95193987.4, 1995 - 07 - 03.

[4] Xiang Zhong. Acompound getters for Vacuum insulation panel, China, Utility model, ZL 201220671837.5, 2012 - 12 - 07.

[5] Haiyi Dong. Research of performance for St707 non evaporable getters [J]. Vacuum, 2000, (2): 26 - 28.

Low Cost Vacuum Insulation Panel (VIP) Using Farm Materials as Core

Pang Yi*

Marvel Technologies, LLC, Rockville, MD 20850, USA

Abstract

Farm materials are usually inexpensive to obtain. More importantly they are friendlier to the environment. Materials obtained from farm crops are biodegradable. Some farm materials may also have the characteristics which are desirable for vacuum insulation panel (VIP) core application. Clay contains a variety of hydrated silicates, alumina, alkali metal oxides and alkaline earth metal oxide. The particles of clay are often in fine colloidal size. Rice husk ash (RHA) contains over than 70% of silica in amorphous fine particle form. Straw contains mainly cellulose fiber and has fine structure. An innovative new application of clay or RHA particles and straw combination as core material for VIP has the potential to achieve very high thermal insulation and significant cost reduction over other types of VIPs. In this paper, straw mixed with various amount of clay and /or RHA particles as VIP core materials is studied, and experimental will be conducted in the following days. In the previous experiments, the thermal conductivity of the VIP with mainly straw core was measured at 3.8 mW/(m·K), comparable to that of a typical fiber glass VIP. We are expecting a better result than that of the straw VIP and with significant longer life.

Keywords VIP, farm materials, core materials

* Corresponding author, Tel:+1301-937-6183, Fax:+1301-937-5731, E-mail: ypang@marveltech.com

Thermal Conductivity of VIP Silica Core at Different Levels of Vacuum and External Pressure

Kjartan Gudmundsson*, Peyman Karami

Department of Civil and Architectural Engineering, KTH - Royal Institute of technology, Stockholm, Sweden

Abstract

The thermal conductivity of low-density nanoporous silica used as VIP core material is known to vary with the levels of gaseous pressure and external loads. This study shows how a new self-designed device, with two cylindrical cavities, that is connected to a TPS instrument can be used to carry out thermal tests on powders at different levels of vacuum and external mechanical pressure. The materials used in this study are a commercially available silica aerogel and two newly developed precipitated silica "powders". The materials are evacuated from atmospheric pressure down to 0.1 mbar while applying different levels of external pressure up to 4 bars. The use of the TPS technique is validated by comparing measurement values with available data for commercial silica as well as through independent stationary measurements with a hot plate apparatus and with the THB method. The different materials illustrate clear but different trends for the thermal conductivity as a function of the level of vacuum and external pressure. The analysis of experimental results suggests that the utilization of the transient method is less suitable for low-density silica aerogels, probably due to the presence of radiation heat transfer.

Keywords vacuum insulation panels, core material, thermal conductivity, transient and stationary methods, TPS and THB

1. Introduction

A VIP consists of an impermeable envelope enclosing a porous core from which the air has been evacuated. A typical VIP panel, as known today, is made out of a multilayer envelope of aluminium and polyester film and a core of fumed silica. There are however many possibilities of combining alternative core materials and envelopes in different typologies as described in previous work [1]. The mechanisms of thermal transfer across the VIP core materials include gaseous and solid conductions as well as radiation, with negligible gaseous convection due to extremely small pore sizes and low pressure. Radiative heat exchange between the interior surfaces is reduced by the use of opacifiers. Conduction through the collision of gas molecules can be diminished by using core material with pore size less than the mean free path of the gas molecules. Nanoporous materials make excellent candidates for core material. Aerogel, fumed silica and precipitated silica offer some of lowest thermal conductivity ranges owing to low density, large surface area and small pores in Nanoscale range [2,3]. Silica aerogel material has therefore been suggested as VIP core material.

Aerogel for example, has a large surface area (~1600 m^2/g) and pores in the range between 5 and 100 nm [4]. These pores occupy about 80 to 99.8% of their total bulk volume. A bulk density as low as 0.003 g/cm^3 has been reported, while for typical application aerogel with values of about 0.07~0.15 g/cm^3 is used. A low thermal conductivity of 17~21 mW/(m·K) at ambient pressure has been established [3,4]. Fumed silica on the other hand has porosity greater than 90% and a bulk density in the range of 0.06~0.22 g/cm^3. The material also has a specific surface area in the range of 100~400 m^2/g which varies with the particle size and a maximum pore size value of about 300 nm has been reported by Gun'ko [5]. A thermal conductivity of

* Corresponding author, Tel.:46-7906590, E-mail: kjartan.gudmundsson@byv.kth.se

about 20 mW/(m • K) at atmospheric pressure has been proven [6,7].

A good insulation material is the one where the sum of the contributions from radiation and solid conduction is at a minimum. This in addition to the gas (air) conduction 26 mW/(m • K) for conventional insulation gives a total thermal conduction down to a minimum around 0.030 W/(m • K). For nanoporous material such as aerogel or fumed silica the gas conduction may be reduced to 15 mW/(m • K) or below, even at atmospheric pressure owing to their nanoscale pores. Despite their obvious technical advantages, their utilization in building industry is limited due to their high market price [3 - 6]. The current manufacturing processes of silica aerogel thermal insulating materials is laborious and uneconomical [5, 8]. New and economical methods for producing aerogels with properties comparable to these of fumed silica are therefore being pursued.

2. Compression and thermal measurements

The influence of particle packing on total thermal transport properties of granular samples, including silica, has been shown in several studies [9 - 11]. Silica materials do often show exceptional thermal performance, but the thermal properties depend on both particle packing and compression. In general, granular materials of similar size show a variation in fundamental mechanical properties in terms of their plasticity and elasticity, fracture strength and brittleness. Particle shapes and material actual density will obviously change with increased compression loads which will then influence the thermal performance of low-density insulation. The influence of the mechanical properties of granular materials on particle packing or compression is an important aspect in the field of powder technology. The problem has been discussed theoretically and experimentally in several studies [12 - 15]. Recently, Neugebauer et al. [16] applied a technique for compacting a bed of granular silica aerogel, achieving a reduction of thermal conductivity from 24 mW/(m • K) to 13 mW/(m • K) with compaction. The authors concluded that there is an optimum level of compaction that minimizes the thermal conductivity; at higher levels of compaction, the contact area between the granules increases and the granules density, increasing conduction through the solid. One of the aims of our study is to examine the potential effect of factors such as bulk density, particle shapes and area of contact surfaces on the thermal properties of the materials.

Thermal conductivity measurements can be carried out with steady-state or transient methods. Suitable methods for the measurement of heat transfer through silica core materials include long-term measurements with a Guarded Hot-Plate (GHP) or a Heat Flow Meter (HFM) apparatus (see, e.g. [17]). Recently, the GHP method is commonly used for measuring the thermal conductivity of commercial products [17 - 18]. Several methods have also been developed for transient measurements of thermal conductivity as well as thermal as thermal diffusivity of low conductive materials, such as the Transient Hot Bridge (THB) method, the Transient Line Source (TLS) method as well as the Transient Plane Source (TPS) method. The TPS method has previously been demonstrated in a study by Gustafsson [20] and actions for improving the technique can be found [21 - 25]. The TPS method is relatively fast, simple and the test can be conducted on samples of any shape and with relatively small sizes. The method is based on Fourier's second law of conduction that puts some restrictions on its use [26]. The technique is, for instance, not theoretically applicable to materials where the term of radiative heat transfer constitutes a significant share of the total heat transfer, such as low-density thermal insulators. The radiative heat contribution is governed by the Radiative Transfer Equation (RTE) which takes into account the emission, the absorption and the scattering of the radiation by the participating medium [26]. Several studies on low-density silica have also shown that parameters such as the density of the testing sample and the physical properties of the probe, such as the length and the thermal inertia of the wire and the heating power or the thermal contact resistance, have a significant influence on accuracy of transient methods [26 - 31]. Longer measuring time and smaller thickness of testing samples are important factors influencing possible radiation inaccuracies. Measurements of total heat transfer through a coupled conduction - radiation mechanism in a

so-called "semi-transparent media" can be seen [28 - 29]. The conclusion was that transient methods may be applied when the extinction coefficient (defined as the sum of the absorption coefficient and the scattering coefficient) exceeds a certain minimum value. A methodology to adapt a transient method to measure the intrinsic diffusivity of a so-mentioned "semi-transparent media" was proposed [30]. Coquard et al. [26] includes theoretical and experimental investigations that show the method could be generalized to so-called "semi-transparent media" at certain conditions regarding the dimensions of the apparatus as well as the density of the sample itself. An important conclusion is that significantly higher values in temperature rise can be shown near the probe (wire) when the sample is too transparent to behave as an "optically thick" material. The analysis of experimental results of [27] confirmed that the utilization of the transient method is not sufficient in cases for low-density silica aerogels with large thermal inertia. Cohen [31], on the validity of the transient hot-wire method for low-density silica aerogel, showed a radiative heat transfer of about 17%.

3. Methods

The current work involves the assessment of the thermal transport properties of silica materials as a function of gaseous pressure and mechanical loads, the latter incorporating the impact of particle packing and compression. Our previous study [32] included a comprehensive theoretical discussion of methods that applied in this work. A hot plate apparatus used in the experiments (Fig. 1) consisting of two independent flat tanks of stainless steel. The warmer tank was connected to a temperature controlled liquid vessel (Lauda K4R) where the temperature is kept constant with an accuracy of ±0.2℃, while the colder tank was connected to a temperature control unit (Kebo-Grave) that kept the temperature constant with an accuracy of ±1℃. To minimize the surrounding effects, the samples were placed in a cylindrical void in the center of a low conductive hard polyurethane sheet with a size of 400×400×20 mm^3. Two Heat Flow Meters (PU 43) and six copper-constantan thermocouples are mounted in sheets of polymethylmetacrylate, one mounted above and the other below the sample, while the temperature was recorded every 15th seconds through the use of a Mitec data logger. Prior to the measurements, a standard reference material® (SRM 1450d) was used for calibrating the HFM sensors.

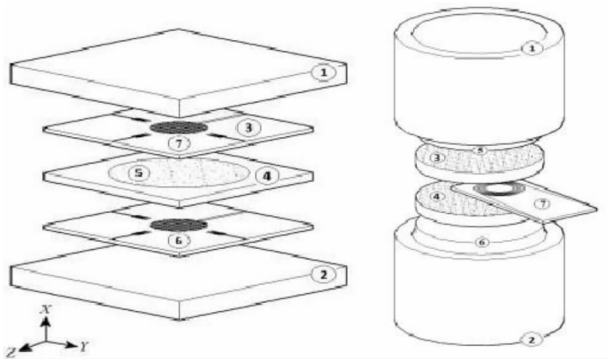

Fig. 1 The Hot plate apparatus (left) and the self-designed device applied with TPS method (right)

The THB method is based on the theory of transient temperature increase over a flat surface that also serves as a heat source (DIN EN 993 - 14, DIN EN 993 - 15). The measuring procedure of the TPS is similar to that of the THB method but a difference can be observed between the measurement sensors. The TPS probe (TPS 2500S - ISO/DIS 22007 - 2.2) consists of a 10 μm thick double metal spiral which is fitted between two layers of 25 μm thick Kapton. Heat generates in the coil due to supplying a constant current to the prob. This causes the temperature to rise and an increase in the resistance of the spiral while the heat is being absorbed by the test sample.

The voltage across the "meander spiral" is then registered. The rate of increase in temperature is due to the thermal transport properties of the samples surrounded the probe. The rate of change in the registered voltage corresponds to the resistance variation of the metal spiral when the electric power is held constant. The short time interval makes it possible to neglect the end effects of the finite size of metal strip and the temperature distribution around and in the coil is identical to that of an infinitely long plane heat source.

The TPS sensor was connected to a self-designed cylindrical device (Fig. 1) for holding the powder in place and is capable of performing thermal tests from atmospheric pressure down to 0.1 mbar vacuum conditions combined with different external loads up to 4 bars. The

device composes of two 15 mm thick Plexiglas cylindrical voids with 60 mm interior diameter, while two Plexiglas pistons with outer diameter of 59.1 mm were placed into the vessels to keep the powder in place. The gap between the cylinders and pistons was sealed with 2 mm thick sealing rubber rings. It must be noted that the "thermal penetration depth" or "thermal wave" generated in a thermal experiment must not reach the outside boundaries of the test sample pieces during a transient test. The self-designed device was connected to a VALUE 2 stages vacuum pump (VE215N) with a gas flow rate of 421/min that results in an ultimate total vacuum pressure of 15 micron, corresponding to 2 Pa. The pump was sealed to the upper cylindrical void with two 1/4" SAE hoses while an analogical vacuum gauge in line with the hoses and with a vacuum resolution of 10 mbar, was used for monitoring the gas pressure inside the samples.

Prior to the thermal conductivity test, the deformation of the specimen height as a function of an increasing load was monitored in a separate experiment, resulting in a curve showing the load-displacement of a defined quantity of the samples (volume and mass). This was done with a cylindrical void and piston designed for the TPS measurements. The powders were placed in a cylindrical vessel of Plexiglas, with a compression fixture consisting of two pistons. The lower piston was stationary and sealed to the vessel while the upper piston can be lowered in order to accomplish a load on the sample. Consequently, the displacement in the void and piston fixture can be used to calculate the load on a sample. After performing the load-displacement measurements for each sample the vessel and the pistons were removed from the compression machine and connected to the TPS sensor and the vacuum pump. The thermal transport properties were then measured as a function of gaseous pressure and external compression loads.

4. Results and discussions

4.1 Test at atmospheric pressure, without loads

The transient measurements were carried out with a sample temperature of 25℃ while the hot plate measurements had an average plate temperature of 25℃. The duration of the transient measurements were in the range of 45～60 s for the THB and the TPS had a measurement time of 160 s, while an initial time of up to 20 min is needed for the sample to achieve the desired test temperature. The steady-state measurements lasted for 12 h. The materials used in this comparative study are granular materials consisting of nanoporous grains (sample A), and two precipitated silica "powders" (samples B and C).

Sample A is a commercially available silica aerogel material (Cabot Aerogel P100) consisting of visually translucent spherical aggregates with a particle size of 0.01～4.0 mm and a pore diameter of about 20 nm. Samples B and C are new types of nanoporous silica powders consisting of opaque particles, developed as described in a previous study [33]. The powders of these two materials consist of spherical particles with sizes ranging between 1.0 and 100 μm (0.001 and 0.1 mm) and have a pore diameter of 5～12 nm. The material properties of samples are listed in Tab. 1.

Tab. 1 Material properties

Sample ID	SBET (m^2/g)	PS nm	V_{tot} (cm^3/g)	ρ_b (g/cm^3)	Porosity (%)
A	686	26	3.5	0.085	96.1
B	241	12	0.5	0.08	96.4
C	427	5	0.8	0.054	97.6

SBET – BET specific surface area, PS – Pore size centred on maxima peaks in DFT pore size distribution, Vtot – total volume of pores between 1nm and 100 nm, ρ_b – tapped density, porosity is calculated on the basis of a skeletal density of 2.2 g/cm^3.

The commercial material (sample A) has already been characterized [31]. Our previous study [33] also includes a description of a preparation method for newly developed nanoporous silica powders and their physical and porosity properties. The powder A has an actual density of 0.074 g/cm^3 and consists of comparatively bigger grains while samples B and C have higher actual densities of 0.077 and 0.09 g/cm^3, respectively. The samples were prepared by drying at 105℃ during 24 h. The samples were measured immediately after drying, so that there was very little hygroscopic moisture in the material at the time of measurement. When it comes to the TPS measurements, the temperature increase in the material near to the sensor is not more than 3～5℃, and the measuring time is no longer than 160 s it is reasonable to assume that impact of the sorption and

transfer of moisture has a negligible effect. The stationary measurements were carried out with plate temperatures and an indoor climate that provided a relative humidity of about 30% or less in order to reduce the effects of sorption and heat transfer by mass transport. The thermal transport properties of the samples were first studied at atmospheric pressure and without external loads (Tab. 2).

Tab. 2 the data measured at atmospheric pressure and without external loads

Samples	Measuring Procedure	Thermal Conductivity mW/(m·K)	Thermal Diffusivity mm^2/s	Precision	Accuracy
A(P-100)	Hot Plate	19.5	—	—	—
	THB	23.5	0.1183	1%	5%
	TPS	29.1	0.216	1%[a]	5%
	Hot Plate	36	—	—	—
B	THB	36.4	0.2509	1%	5%
	TPS	38.7	0.328	1%[a]	5%
	Hot Plate	34.2	—	—	—
C	THB	38.5	0.2071	1%	5%
	TPS	38.8	0.249	1%[a]	5%

[a] Typical values for TPS under reproducibility conditions.

In the case of aerogel materials, a thermal conductivity of 17 ~ 21 mW/(m·K) at ambient pressure has been established [3, 4]. The thermal conductivity measured for the commercially available sample A from previous work [31] is 19.7 mW/(m·K), at ambient pressure. By assuming an approximate lambda value of 19.7 mW/(m·K) for sample A with an actual density of 0.074 g/cm^3, our methods show the greatest difference for material A with the hot plate method being much closer to the data from [31], showing a difference of only 1% while the THB and TPS method differ by more than 16% and 32% respectively, from the data of the manufacturer and [31]. The noticeable fact is that in the case of precipitated silica structure, samples B and C show very similar results from the stationary and transient measurements. All the transient experiments in this study were conducted with an adequate probe in terms of wire thickness and length. The heating power was kept at same level for all measurements (0.005 W) while the measuring time was set to 160 s. A time lapse of 20 min between each reading was employed. The foregoing phenomena can be explained as follows. Material A has a comparatively low actual density of 0.074 g/cm^3 and consists of comparatively bigger grains (0.01~4.0 mm) while materials B and C are relatively more compact, with particle size of 1.0~100 μm (0.001~0.1 mm) and actual densities of 0.077 and 0.09 g/cm^3, respectively. The report of IEA/ECBS Annex 39 [34] illustrates a descending radiative contribution and an increase in solid conduction with increasing density. This suggests that the comparatively greater differences in the results for powder A are due to greater radiative contribution. It is therefore possible that a relatively larger contribution of the radiative heat transfer in the sample A may affect the accuracy of transient methods as described in previous section. The impact of radiation distribution on accuracy of transient method has been pointed. Previously [26 - 31]. The magnitude of the extinction coefficient of the materials has not been measured in this study, but the results indicate that material A is not an optically thick material.

4.2 Test at vacuum conditions with external loads

The purpose of performing tests on granular silica materials with different mechanical properties was to examine the trend of the thermal conductivity versus external compression as well as to see the effect of particle packing on density of the heat flux through the powder when particle volume varies due to mechanical load. The mass and initial volume of the samples was the same as for measurements at atmospheric pressure. The samples A, B and C had measured actual densities of 0.074, and 0.077 and 0.09 g/cm^3, respectively. The results of load-displacement curves, acquired from more than 250,000 measurements, were then converted to stress - strain curves by using the cross-sectional area of the specimens (28.8 cm^2) and the original heights of the specimens. The thermal conductivity of the test samples is shown as a function of gaseous pressure (bar) and mechanical external pressure (bar) in Figs. 2 - 4. The most notable result is the obvious trends between thermal conductivity and both different gaseous pressure through the samples and mechanical compressions.

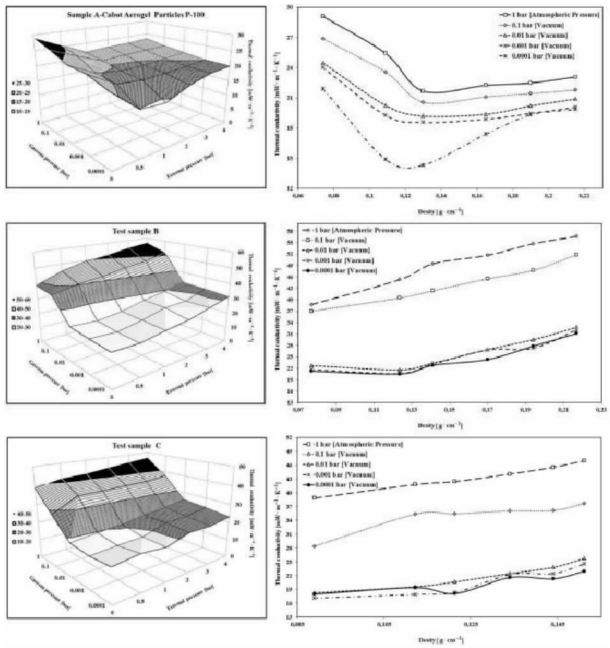

Fig. 2, 3, 4 The thermal conductivity of samples, A (Upper), B (Middle) and C (below) as a function of different levels of gaseous and compression. High resolution graphs are available in [32]

The measured thermal conductivity of sample A, at atmospheric pressure and without application of external compression loads, was 29.1 mW/(m • K) at actual density of 0.074 g/cm^3, and then decreases as the air is evacuated as well as when the sample is compressed up to 1 bar (Fig. 2). It can also be noted that it increases slightly again when the mechanical load is increased at each level up to 4 bars. The lowest thermal conductivity of 14 mW/(m • K) is obtained at an actual density of 0.13 g/cm^3, when the granules are compressed with 1 bar pressure at 0.1 mbar gaseous pressure (vacuum condition). On the contrary, the thermal conductivities of the precipitated silica structure powders B and C (Figs. 3 ~ 4) are low at atmospheric pressure and without external pressure application and then slightly increase with mechanical load. But it is obvious that the thermal conductivity decreases as the air is evacuated independent of the applied external pressure. The thermal conductivity of the sample B, at atmospheric pressure and without external loads, is 38.7 mW/(m • K) at an actual density of 0.077 g/cm^3 while the lowest thermal conductivity of 20.5 mW/(m • K) is obtained at an actual density of 0.124 g/cm^3, when the powder is compressed with 0.5 bar external pressure at 0.1 mbar vacuum pressures. In the case of the sample C, the thermal conductivity at atmospheric pressure and without applications of external compression, is 38.8 mW/(m • K) at an actual density of 0.09 g/cm^3, while the lowest thermal conductivity of 17 mW/(m • K) is obtained at the same density (without any external load) at 0.001 bar vacuum pressures. The foregoing phenomena are most likely due to the impact of particle packing and compression loads on total thermal transport properties of the testing samples as shown in previous works [35 - 37]. Recent work of Coquard et al. [38] shows variation in thermal conductivity values of nano-structured porous silica materials versus compression, while it has been found out that the contact resistances and contact areas between the sample grains have notable effect on the thermal conductive properties when the particles volume is diminished by mechanical compression load. Our work illustrates how the thermal transport properties of the granular powder samples vary with the mechanical compression load. This may be explained by the decrease in porosity with com-action but can also depend on the shape and size of particles and the effect on the grain-to-grain geometric and contact resistances. It's reasonable to assume that gradual compressing of the, relatively small spherical particles of the precipitated silica powders B and C, will reduce the gap between the particles. Mechanical compression may also lead to an increase of the mean number of contacts between particles and thus to an increased heat conduction in the solid matrix. Densification, or the collapse of the microstructure, would also lead to an increased conductivity. In the case of sample A, where the particles are comparatively bigger spherical aggregates, the application of mechanical compression loads reduces the gap between the particles but the results suggest that the contact area between the particles does not increase as much with the load as is the case for samples B and C. The density of the heat flux of the powder will therefore be governed by the space between the conducting particles that will enhance heat flow through conduction and convection. Evacuating the air from sample particles does therefore have a comparatively strong influence on the heat

transfer via convection and conduction in the gas. The different effects of compaction can be explained by the effect of pore size on gas conduction in the pores. The relationship between gas conduction and free air conduction can be calculated from the Knudsen number that describes the ratio between the mean free path of air molecules and the characteristic size of pores, as described in previous work [39]. This means that the contribution of gas conduction is low or negligible in the mesoporous range (2～50 nm) while mounting to a value of about 10 mW/(m·K) with a characteristic pore size in the macroporous range (150 nm). Therefore, the thermal conductivity of material A decreases with an increase in density, as depicted in Fig. 2, because of the effect of initial compaction on the macro pores while the mesopores of materials B and C do not show this behaviour. The decrease in the resulting thermal conductivity of sample A continues until the heat transfer through the material becomes almost entirely due to conduction in the solid skeleton that will increase with density. The very low pore volume of the particles of materials B and C, as shown in Tab. 2, give a reason to argue that the thermal conductivity increases as the intraparticle voids are reduced with compaction.

Our previous study Twumasi et al. [33] includes the SEM images of new developed samples in different tapped densities. The trends shown in Fig. 1 are similar to these of our study. It is obvious that material A, with a lower actual density (0.074 g·cm^{-3}) is a better thermal insulator than the newly produced precipitated silica structure powders B and C with relatively higher actual densities of 0.077 g·cm^{-3} and 0.09 g·cm^{-3} respectively. Fig. 8 shows that the lowest thermal conductivity is obtained when the sample A is loaded somewhere between 0.5 and 1 bar while the range of thermal conductivity slightly increases again with greater load. The notable fact is the very similar tends of the total thermal conductivity versus density (Figs. 1 and 8). The densities of samples B and C are higher than the limit, at which the heat transfer through pure conduction in solid becomes dominant in comparison with radiative heat transfer, and the measured thermal conductivity increases continuously with the density. It is therefore reasonable to assume that the relatively higher thermal conductivity of materials B and C is due to a high contribution of solid conduction. To summarize, the results illustrate the influence of material density on thermal conductivity. Furthermore, it has been explained how this effect can be related to the influence of the different mechanisms of heat transfer and how they depend on the porosity, the pore size, particle geometry, the opacity and possibly the contact area between particles.

5. Conclusions and outlook

A new self-designed device has been used together with a TPS instrument to conduct measurements of the thermal conductivity of granular VIP core materials at different levels of gaseous pressure and different external compression loads. The principal conclusions from all thermal experiments of this work are:

- With transient techniques, the required measurement time is relatively short (minutes) while the steady-state measurement requires comparatively long measuring times (hours – days). The probe and measuring equipment of transient technique are physically small, simple and easy to use. The size of the test samples required is relatively small and the measurement could be performed on samples of any shapes, whereas the stationary method with plate apparatus requires of large and standard dimensions of the testing samples which can make it difficult to test materials with high manufacturing cost. Both the thermal conductivity and the thermal diffusivity can be acquired simultaneously with the transient methods while two measurements are generally required when using stationary hot plate apparatus. At current, the cost of acquiring the equipment for the transient measurements is also much higher.
- The transient method is less suitable for measuring the thermal transport properties of low-density transparent porous media since the technique is based on Fourier's law of thermal diffusion. This technique is therefore less applicable to materials where the term of radiative heat transfer is not negligible. It can be observed in Tab. 2 of our study that the methods show the greatest difference for material A which includes relatively greater particle size and has

comparatively lower actual density (0.074 g/cm^3) while the sample is too transparent to behave as an optically thick material. In this case, the stationary hot plate method is much closer to the data from the manufacturer and previous work [30], showing a difference of only 1% while the THB and TPS method (transient methods) differ by more than 16% and 32%, respectively. The notable fact is the much closer results of the stationary and transient methods in the case of samples B and C that are compact materials with relatively lower particle size having higher actual densities (0.077 and 0.09 g/cm^3, respectively). Consequently, the transient method is less adapted to nanoporous silica materials when the density is lower than a limit where the radiative heat transfer becomes dominant compared to conduction in the solid matrix. The deviation in results, due to radiative distribution, was significant for the sample with an actual density of 0.074 g/cm^3 whereas in the case for more compact samples with actual densities of 0.077 and 0.09 g/cm^3, it was found to be negligible.

• Granular materials of similar size show a great variation in fundamental mechanical properties in terms of their plasticity and elasticity, fracture strength and brittleness. The thermal properties are also related to the particle packing and compaction. The results of this study show different trends for the thermal transport properties of three silica samples with varying gaseous pressure and external compression loads. The thermal conductivity measurements give the lowest thermal conductivity at an actual density of 0.130 g/cm^3 for silica aerogel sample A with relatively bigger spherical grains. On the other hand, the newly developed precipitated silica samples B and C have the lowest values at actual densities of 0.124 g/cm^3 and 0.09 g/cm^3, respectively. This effect must be related to the morphology of the material, the effects of which have been discussed. This is an important aspect in the development of vacuum insulation panels and further investigations of the matter will be a part of future work.

Acknowledgements

The authors wish to thank the FORMAS.

References

[1] J. M. Cremers. 7th Intl. VIP Sumposum(2005),189 - 196.
[2] L. GQ et al. Vol. 4, Eds. (2004)1 - 12.
[3] R. Baetens et al Engy&Bldgs 42 (2010) 147 - 72.
[4] N. Hüsing Angew. Chem. Int. Ed. 37(1998) 22 - 45.
[5] V. M. Gun'ko, Colloid&interf. Sci. 289 (2005) 427 - 45.
[6] M. Alam et al. Applied Energy 88(2011) 3592 - 602.
[7] D. Quenard et al. 2th Nanotechnology Symp(2005).
[8] RA. Venkateswara, MatChem&Ph77 (2002) 819 - 25.
[9] W. Evans, HeatMassTrans 51 (2008)1431 - 1438.
[10] Y. B. Yi, Acta Materialia 56 (2008) 2810 - 2818.
[11] C. Argento Heat Mass Tra. 39 (1996)1343 - 1350.
[12] K. Kawakita, Reprinted Elsevier 4 (1971) 61 - 68.
[13] K. Kawakita, Japanese App Phys 4(1965) 56 - 63.
[14] K. Kawakita, Che So. of Japan39(1966)1364 - 68.
[15] K. Kawakita, Powder Techogy 4 (1970/1971) 61.
[16] A. Neugebauer, Enrgy&Bldg 79 (2014) 47 - 57.
[17] C. Langlais, ASTM STP 789, 1983, pp. 563 - 581.
[18] M. Alam, Enrgy&Buildings 69 (2014) 442 - 450.
[19] K. Ghazi Wakili, Ergy&Bldg 43 (2011)1241 - 1246.
[20] SE Gustafsson, Zeit. FurNaturfors 22(1967) 1005.
[21] SE Gustafsson, Appl Phys 12 (1979) 1411 - 1421.
[22] SE Gustafsson, Patent, # 5044 (1991a)767.
[23] SE Gustafsson, ScientificIns. 62 (1991) 797 - 804.
[24] T. Log, Fire and Materials 19 (1995)43 - 49.
[25] Y. He, Thermochimica Acta 436 (2005) 122 - 129.
[26] R. Coquard, Heat&MassTran 49 (2006) 4511 - 24.
[27] R. Coquard, Thermal Scis 65 (2013) 242 - 253.
[28] H. P. Ebert, HighTemp-HighPre 30 (1998) 655 - 69.
[29] U. Gross, HeatMassransfer 47 (2004)3279 - 3290.
[30] M. Lazard, Heat Mass Tran 47 (2004) 477 - 487.
[31] E. Cohen, (Master thesis), MIT, 2011.
[32] P. Karami et al. Enrgy&Bldgs 85 (2014) 199 - 211.
[33] ET. Afriyie, Ergy&Bldgs 75 (2014) 210 - 215.
[34] IEA/ECBS Annex 39 (Subtask A), 2005.
[35] W. Evans, HeatMassTrans 51 (2008)1431 - 1438.
[36] Y. B. Yi, Acta Materialia 56 (2008) 2810 - 2818.
[37] C. Argento, HeatMassTrans 39(1996)1343 - 1350.
[38] R. Coquard Non-CrystSolids 363(2013) 103 - 115.
[39] R. Baetens, Ergy&Bldgs 42 (2010) 147 - 172.

Examination of Thermal Technical Properties of Organic Based fiber Insulation Core Materials under Low Pressure

Jiří Zach, Jitka Hroudová*, Vítězslav Novák

Brno University of Technology, Faculty of Civil Engineering, Institute of Technology of Building Materials and Components, Veveří 331/95, 602 00 Brno, Czech Republic

Abstract

A major part of vacuum insulations consists of core inorganic insulation materials based either on pyrogenic silica (aerogels) or on glass fiber materials. The paper describes the results of the research-oriented use of fibrous insulation materials based on organic (natural and synthetic fibers), which could be used as core insulation for vacuum insulation production. The paper focuses on the one hand on the selection of suitable fibers and the manufacture of insulating materials and on the other on studying their thermal insulation properties under low pressure.

Keywords vacuum insulation panels, fiberd core insulation materials, thermal conductivity, organic insulation materials, low pressure

1. Introduction

The society's requirements on the reduction of CO_2 emission and energy consumption bring the need for changes in the energy efficiency of buildings [1]. In many countries, energy consumed on heating and cooling of buildings exceeds 50 % of total energy consumption. For this reason civil engineering has been dealing for several years with near zero energy and passive buildings which meet the new, modern energy requirements. However, many existing and historical buildings do not meet these requirements. One of the solutions to this is the addition of building envelope insulation [2]. Currently, and in Europe especially, mineral wool and expanded polystyrene are mostly used for building insulation; their advantage is a low price and good thermal insulation properties with thermal conductivity λ_d ranging from 0.034～0.040 $W \cdot m^{-1} \cdot K^{-1}$. Nevertheless, in terms of thermal insulation properties, a much better choice seems to be the use of vacuum insulated panels which are, however, still at early stages of development. Despite the first patent having been granted as early as 1930, the first practical implementation of such insulation materials was performed at the end of the 20th century, in 1999 [3]. Based on the surveys performed, outcomes of extensive research by a number of European experts were found, especially from Sweden, Denmark, Switzerland, Germany, Slovenia, Greece but also from Canada, China, the Republic of Korea, etc., all of whom dealing mainly with the development, production and application of these materials. In many countries, practical implementations with subsequent research were performed with the purpose to determine heat and moisture transport in these materials [1－11]. Vacuum insulated materials (VIP) exhibit 5 to 10 times greater thermal resistance in comparison with conventional materials [1, 2, 6]. Thanks to this property, it is possible to significantly reduce the thickness of the wall insulation which is meaningful especially in case of protected historical buildings where thermal insulation properties can

* Corresponding author, Tel: 420－541－147－525, E-mail: hroudova.j@fce.vutbr.cz

thus be improved without excessive increase in wall thickness.

A disadvantage of these materials is their high price and their precise design for a specific structure. What is also necessary is the training needed for the workers who would manipulate with the materials and fit them onto the structure. The sensitivity to breaching the vacuum inside these materials is one of other possible disadvantages which can then have a negative impact on the final thermal insulation of the structure. It is also necessary to note that VIP are not vapour-permeable. Such materials act as a vapour barrier which could entrap moisture in the construction on the interior of the VIP. However, many studies have proven that the VIP did not increase the moisture content in the wall after retrofittings [2].

Common core materials of VIP are fumed and precipitated silica, open-cell polyurethane and several types of fiberglass. Some research suggests [12] that natural fibers (of both plant and animal origin) can be successfully used for the production of a core VIP insulator as well. An advantage of these fibers is the fact that they are vascular fibers which are often composed of clusters of very fine fibers (a few microns thick) which must be only be defiberd, their length adjusted and again joined into mats of optimal bulk density. An advantage of these insulators is the low energy cost of their production and the use of easily renewable sources of secondary raw materials provided the fibers used are agricultural crop leftovers, waste fabric, etc. Research performed on this type insulator at normal pressure suggests that in order to attain the best possible thermal insulation properties, it is necessary to use fibers with the lowest possible thickness [13]. For this reason, cotton fibers appear especially suitable as they have primary fiber thickness of around 10 microns depending on the species of cotton and time of growth [14]. When organic insulators are used in the production of VIP, they are vacuum sealed in a vapour proof film. For this reason, the properties of the insulator cannot degrade and the insulator does not become contaminated nor exposed to biotic attack. Natural fibers therefore need not be further adapted to be used in VIP which makes manufacturing simpler and reduces the price and energy consumption, contrary to conventional thermal insulation made from natural fibers. After vacuum sealing, thermal conductivity is significantly reduced. Compared with an insulator at normal pressure and humidity, thermal conductivity can be reduced ten times. Unfortunately, this is a very new area of application of these materials and there is only little knowledge available. The goal of the research being conducted at Brno University of Technology is to find alternative core materials based on natural fibers which are easy to recycle and do not put strain on the environment.

2. Specimens

In order to determine the possibilities of using insulators based on organic (textile and bast), specimens of thermal insulation mats were designed and made to be used in experiments. The following types of fibers were used:

(1)Pure flax fibers (flax fibers with low content of shives up to 5 %);

(2)Raw flax fibers (flax fibers with high content of shives up to 40 %);

(3) Cleaned cotton fibers from defiberd waste textile (high content of cotton over 96 %);

(4)Raw cotton fibers from defiberd waste textile - selected jeans textile (high content of cotton over 95 %);

(5)Recycled PES fibers from waste carpets.

Fig. 1 Photograph of raw fibers (top left - flax fibers; top right - cleaned cotton fibers; bottom left - PET fibers; bottom right - raw cotton fibers)

Five types of specimens were made from the fibers described above. They had high bulk density of 70～130

kg • m^{-3} according to the type of fibers. The aim was to achieve higher bulk density to ensure the insulators' minimum mechanical properties necessary for vacuum sealing [15]. At lower values of mechanical properties, the vacuum sealing would significantly affect the shape of the material and thus also its properties.

The specimens were made using bicomponent binding on a production line using the technology of making an air-lay mat. Thermo fixation was performed at+145℃. In order to bind the specimens, 15%～20% of synthetic bicomponent fibers were used.

Tab. 1 Overview of the composition of the specimens

Specimen no.	Flax 1	Flax 2	Cotton 1	Cotton 2	PES	BiCo
1	80					20
2		80				20
3			40		40	20
4					80	20
5				45	40	15

3. Test methods

In the initial phase, the properties of the fibers were determined — their structure was microscopically analysed and subsequently their thickness measured.

The insulation mats were cut into specimens sized 200mm × 200mm. Physical, mechanical and thermal insulation properties were determined for these specimens:

• determination of thickness in accordance with EN 823 [16],

• determination of density in accordance with EN 1602 [17],

• determination of thermal conductivity in accordance with EN 12667, ISO 8301 depending on volume weight [18], [19],

• determination of mechanical properties — Determination of compression behaviour according to EN 826 [20].

The key thermal insulation properties were determined using FOX 200 Vacuum at medium temperature+10℃ and temperature gradient 10 K at normal pressure and at reduced pressure down to vacuum ($p < 0.1$mBar).

4. Test results

Microscopic analysis of the fibers was performed and it was found that in none of the cases defibration down to primary fibers took place during basic processing. The thickness of the fiber clusters was determined. The values are in the following table:

Tab. 2 Overview of the thickness of raw fibers

Specimen no.	1	2	3	4	5
Type	Flax 1	Flax 2	Cotton 1	PES	Cotton 2
Thickness/μm	19.8	120.1	25.9	21.1	20.1

First, the specimens were measured for thickness, bulk density and compressive stress at 10 % strain. The measurement was performed for the maximum holding pressure enabled by the equipment for determining thermal conductivity. Holding pressure was 1.5 Pa. The results are in Tab. 3.

Tab. 3 Overview of physical and mechanical properties of the specimens

Specimen no.	1	2	3	4	5
Thickness /mm	22.49	19.52	20.08	23.09	38.32
Density /(kg • m^{-3})	98.3	123.8	119.7	101.5	128.6
Tension at 10%/kPa	2.9	12.8	4.2	2.9	3.7

The results indicate that the mechanical properties of the insulators are relatively low and thus the specimens will be partly deformed during the vacuum sealing itself.

Next, thermal conductivity was determined with the specimens at normal pressure and at reduced pressure near vacuum ($p < 0.1$mBar). The results are in the table below.

Tab. 4 Overview of thermal insulation properties at normal pressure and vacuum

Specimen no.	1	2	3	4	5
λ_{Normal} /(W • m^{-1} • K^{-1})	0.0352	0.0386	0.0354	0.0360	0.0373
λ_{Vacuum} /(W • m^{-1} • K^{-1})	0.0078	0.0094	0.0051	0.0058	0.0051

After the determination of thermal conductivity at extremely reduced pressure near vacuum, the tests continued by measuring thermal conductivity in dependence on pressure which was increased prior to each measurement up to 500 mBar. The results are in Fig. 2 below.

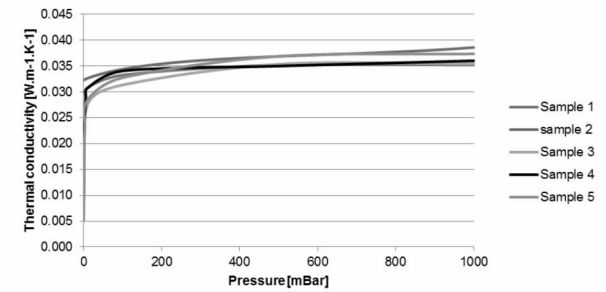

Fig. 2 Dependence of thermal conductivity of the specimens on pressure (1000 mBar is normal pressure)

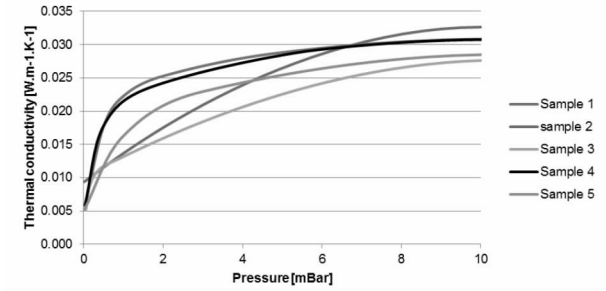

Fig. 3 Dependence thermal conductivity of the specimens on pressure (low pressure area)

5. Discussion

The measurements show that fibrous insulators based on organic waste fibers see a reduction of thermal conductivity at reduced pressure down to a value which is in most cases suitable for the production of VIP. The thermal conductivity of the materials was reduced by 76% ~ 86% down to 0.0051 $W \cdot m^{-1} \cdot K^{-1}$ (in specimens no. 3 and 5).

Core insulation specimens based on cotton appear to be the most promising as their thermal insulation properties degrade the slowest during increasing pressure and it can be assumed that with better fiber processing and higher bulk density, these materials could be a potential core insulator for the production of VIP.

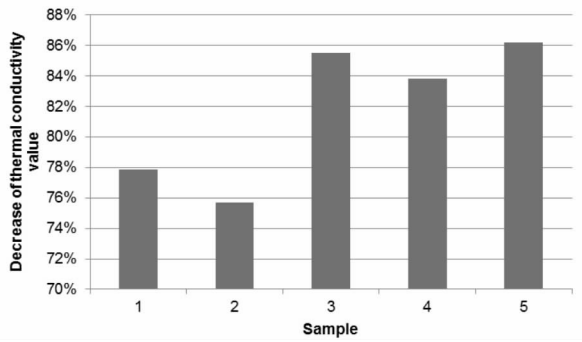

Fig. 4 Overview of percentage decrease of thermal conductivity

6. Conclusions and outlook

In this paper, the development of core insulation based on organic fibers was investigated. They were organic fibers from easily renewable raw material sources (flax fibers) and next fibers from recycled clothing and technical fabric (cotton and PES fibers). The initial experiments show the materials to be very promising, especially materials based on cotton appear interesting; it is, however, necessary to achieve greater fineness of the fibers and greater bulk density. However, the advantages are that the initial raw material is widely available (waste textile with a high portion of cotton is essentially available worldwide), that secondary raw materials are used and that the production is energy and cost efficient.

Acknowledgements

This paper was elaborated with the financial support of the project GA 13-21791S Study of heat and moisture transfer in the structure of insulating materials based on natural fibers and project No. LO1408 AdMaS UP — Advanced Materials, Structures and Technologies, supported by Ministry of Education, Youth and Sports under the National Sustainability Programme I.

References

[1] P. Johannson, S. Geving, C. E. Hagentoft, B. P. Jelle, E. Rognvik, A. S. Kalagasidis, B. Time, Interior insulation retrofit of a historical brick wall using vacuum insulation panels: Hygrothermal numerical simulations and laboratory investigations, Building and Environment 79 (2014) 31-45.

[2] P. Johannson, C. E. Hagentoft, A. S. Kalagasidis, Retrofitting of a listed brick and wood building using

vacuum insulation panels on the exterior of the facade: Measurements and simulations, Energy and Buildings 73 (2014) 92 – 104.

[3] S. Brunner, K. G. Wakili, T. Stahl, B. Binder, Vacuum insulation panels for building applications—Continuous challenges and developments, Energy and Buildings 85 (2014) 592 – 596.

[4] X. Di, Y. Gao, Ch. Bao, S. Ma, Thermal insulation property and service life of vacuum insulation panels with glass fiber chopped strand as core materials, Energy and Buildings 73 (2014) 176 – 183.

[5] I. Mandilaras, I. Atsonios, G. Zannis, M. Founti, Thermal performance of a building envelope incorporating ETICS with vacuum insulation panels and EPS, Energy and Buildings 85 (2014) 654 – 665.

[6] P. Mukhopadhyaya, D. MacLean, J. Korn, D. van Reenen, S. Molleti, Building application and thermal performance of vacuum insulation panels (VIPs) in Canadian subarctic climate, Energy and Buildings 85 (2014) 672 – 680.

[7] F. E. Boafo, Z. Chen, Ch. Li, B. Li, T. Xu, Structure of vacuum insulation panel in building system, Energy and Buildings 85 (2014) 644 – 653.

[8] S. Park, B. H. Choi, J. H. Lim, S. Y. Song, Evaluation of Mechanically and Adhesively Fixed External Insulation Systems Using Vacuum Insulation Panels for High-Rise Apartment Buildings, Energies 7 (2014) 5764 – 5786.

[9] E. C. Hammond, J. A. Evans, Application of Vacuum Insulation Panels in the cold chain e Analysis of viability, International Journal of Refrigeration 47 (2014) 58 – 65.

[10] H. Jung, I. Yeo, T. H. Song, Al-foil-bonded enveloping and double enveloping for application to vacuum insulation panels, Energy and Buildings 84 (2014) 595 – 606.

[11] V. Nemanic, M. Žumer, New organic fiber-based core material for vacuum thermal insulation, Energy and Buildings 90 (2015) 137 – 141.

[12] J. Véjelienė, Impact of technological factors on the structure and properties of thermal insulation materials from renewable resources, Doctor dissertation, Vilnius Gediminas Technical University, Lithuania (2012).

[13] J. Véjelienė, A. Gailius, S. Vejelis, et al., Evaluation of Structure Influence on Thermal Conductivity of Thermal Insulating Materials from Renewable Resources, Materials Science-Medziagotyra, National Conference on Materials Engineering, 17 (2011) 208 – 212.

[14] A. Kljun, H. M. E. Dessouky, T. A. S. Benians, F. Goubet, F. Meulewaeter, J. P. Knox, R. S. Blackburn, Analysis of the physical properties of developing cotton fibers, European Polymer Journal, 51(2014) 57 – 68.

[15] S. Brunner, K. G. Wakili, T. Stahl, B. Binder. Vacuum insulation panels for building applications—Continuous challenges and developments. Energy and Buildings, Volume 85 (2014),592 – 596.

[16] EN 823 Thermal insulating products for building applications. Determination of thickness.

[17] EN 1602 Thermal insulating products for building applications. Determination of the apparent density.

[18] EN 12667 Thermal performance of building materials and products. Determination of thermal resistance by means of guarded hot plate and heat flow meter methods. Products of high and medium thermal resistance.

[19] ISO 8301 Thermal insulation. Determination of steady-state thermal resistance and related properties. Heat flow meter apparatus, Amd1: 2010.

[20] EN 826 Thermal insulating products for building applications — Determination of compression behaviour.

Comparative Centre of Panel Thermal Performance Analysis on Various Glass Fiber Based Vacuum Insulation Panel Core Materials Consisting Different Fiber Diameter and Pore Size

Xu Tengzhou[a], Chen Zhaofeng[b*], Nie Lili[b], Zhu Kun[b], Zhou Jianming[a], Zhou Yanqing[a], Song Jun[a], Zhu Peichao[a], Wu Yuan[c]

a. Suzhou VIP New Material Co. Ltd, Hong Da Fang Yuan Group, Suzhou, 215400, P. R. China

b. Super Insulation Composite Laboratory (SICL), College of Material Science and Technology, Nanjing University of Aeronautics and Astronautics, Nanjing, 210016, P. R. China

c. Hefei Meiling Co. ,Ltd, Hefei, 230000, P. R. China

Abstract

In this paper, comparative centre of panel thermal conductivity (K_{cop}) analysis was performed on 3 distinctly different samples of Vacuum Insulation Panel (VIP) core materials made from glass fibers. The first sample consisted of fibers produced from centrifugal spinneret blow system (C－fiber sample), second sample was from chopped strand fibers (Chopped strand sample) and the final one was from a mixture of Centrifugal and flame attenuated fibers (Centrifugal-Flame mix fiber composite). Measured with Netzsch HFM 436 hot plate device, the K_{cop} of C-fiber core structure with fiber diameter (d) of 3～5μm, pore size (ϕ) 58μm was around 1.5～1.8mW/(m·K) in average at evacuated conditions. Similarly, K_{cop} of the Chopped strand sample (d=5～6μm/ϕ=70μm) was measured as 1～1.2mW/(m·K) in average, which is perhaps the lowest possible thermal conductivity measured from a VIP core sample till date. The Centrifugal－Flame mix fiber composite core material sample, which had the smallest pore size (ϕ=45μm), provided intermediate level thermal conductivity of 1.8～2.2mW/(m·K) between the 3 samples. Utilizing real-time measurements of K_{cop} and corresponding dynamic internal pressure, effective gaseous thermal conductivity (K_g) was deduced, from which the average pore size of the core structures was determined using suitable mathematical relationship. The results from this experiment suggest that effective thermal conductivity at evacuated state (K_s+K_r) remain unchanged for all these 3 samples at higher pressure, since the fiber orientation angle at x－z direction was close to 10 degrees in average. Further, such comparative analysis for different glass fiber type core materials is vital for preparing VIPs for projects that require specific constraints on factors related to thermal insulation, service life and cost.

Keywords glass fiber, VIP, pore size, centrifugal glass fiber, composite fiber; chopped strand fibers

1. Introduction

Increased ecological concerns and energy issues have prompted policy makers around the world to set stringent standards in order to improve energy performance of buildings and appliances. Since effective thermal insulation can reduce energy consumption rates and inevitably reduce CO_2 emissions dramatically, there is a need to develop materials with enhanced thermal insulation characteristics. The evacuated insulation technology of Vacuum Insulation Panels (VIP) enables approximately 5～8 times higher thermal resistance than conventional thermal insulation at similar thickness. Hence, equipped with super insulation characteristics and space saving attributes, VIPs are widely recognized as a promising solution for achieving enhanced energy efficiency requirements set by policy makers [1].

Basic structure of VIP consists of highly open

* Corresponding author, Tel:86－18952018969, E－mail: zhaofeng_chen@163.com

porous core structure with very low thermal conductivity, encapsulated within an envelope material under vacuum. The envelope material would have higher thermal conductivity than the core material, and moisture/air absorbers such as getters/desicants can be present within the core material. Types of core material differ depending on the type of insulative application. Normally, VIPs with core material from powder type silica, are normally used in building insulation, due to long service life ($\geqslant$ 25 years) [2]. With proper getter, fibrous core materials such as glass fibers, are traditionally used in refrigeration insulation due to its cheap cost and ultra low thermal conductivity at evacuated conditions compared to powder or foam type materials [3].

Although this technology is still quite new, several critical publications have been reported on silica core VIPs, depicting long term effective thermal insulation performance, service life and cost reduction possibilities [2, 4 - 6]. Published information regarding glass fiber core VIPs however, seem to be inadequate and outdated. Most of these papers provide suitable theoretical analysis through mathematical relationships that has the potential to optimize and improve performance of glass fiber VIPs [3, 7, 8]. Only a handful of publications related to glass fiber VIPs have delved into validating their practical performance data through these relationships [9, 10]. Then again, critical practical data on aspects such as effect of pore size on internal pressure, effect of fiber length and orientation angle at x - z direction on solid conductivity were unfortunately nonexistent in these papers.

The aim of this paper is not only to provide practical comparative analysis on effective thermal performance between VIPs made from different fibers, but also will validate such results using the said theoretical models. The data will also include information regarding structural pore size and fiber orientation angle. By utilizing the feedback from validated results, optimized fiber manufacturing enabled increased performance of the VIP core materials. This resulted in measurement of the lowest thermal conductivity for glass fibers at evacuated state till date.

2. Theoretical study on the performance of Glass Fiber VIPs

Effective thermal transport in VIP occurs via solid (K_s), gaseous (K_g) and radiative (K_r) conductivity. A theoretical study on separate heat transfer mechanism ensures possible improvement of thermal performance of VIP, by effectively identifying crucial optimization parameters.

2.1 Radiative thermal conductivity

The mechanism for gaseous and radiative conductivity is similar for all 3 major types of core materials, i. e. powder, fiber and foam. Radiative conductivity, K_r for an optically thick specimen with mean temperature T_m is determined by the following mathematical relationship [3]:

$$K_r = \frac{16n^2\sigma T_m^3}{3E_R(T_m)} \tag{1}$$

where n is the index of refraction, σ is the Stefan-Boltzmann constant. The Rosseland mean extinction coefficient (E_R) is calculated by:

$$E_R(T_m) = e(T_m)\rho \tag{2}$$

with $e(T_m)$ being the mass specific extinction and ρ being the density. This consequently presents K_r as inversely proportional to bulk density of the core material. Therefore core structures produced from glass fibers generally consist of negligible thermal radiative values due to high density. This aspect was thoroughly explained by Jongmin and Song [8] through a graph which portrayed glass fiber core samples of densities beyond 200 kg/m^3 having K_r of less than 0.7mW/(m·K). In contrast to silica core samples, which normally consist of densities less than 100 kg/m^3 and K_r between 1~1.5mW/(m·K), such values of K_r for glass fiber core materials could be deemed negligible.

2.2 Gaseous thermal conductivity

Since VIP core material structure consists of open porous cell, the pockets of air within the structure become one of the primary sources of thermal transfer. Therefore, evacuation of the core structure within the envelope ensures negligible thermal conductivity. However, vacuum is slowly lost after long period due to permeation of air through the heat sealing, deemed as one of the primary aspects of VIP aging. Internal pressure rises with permeation of air and hence pore size

of the core structure becomes crucial.

Silica cores structures consist of nanometer range pore sizes which is why heat transfer of gas molecules are effectively hindered by numerous collisions with the solid structure. The reason for this is primary due to the pore size being very close to mean free path of the molecules, therefore effectively blocking the movement of molecules.

However, traditionally the pore sizes of glass fiber core material have been often beyond 70～80μm. On top of that, since the orientation of the fibers (due to short fiber length) has been random, resulting in highly random pore sizes. Fig. 1 shows the effect of pore size has on gaseous conductivity of core materials.

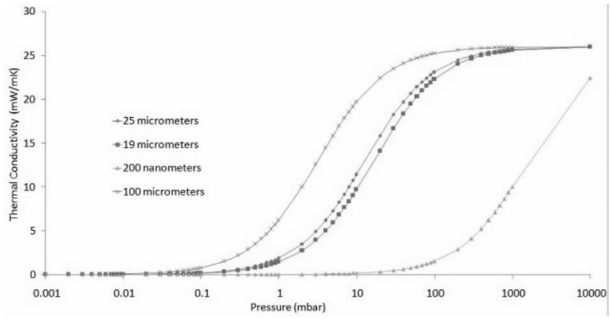

Fig. 1 Gas conductivity with internal pressure for different pore sizes

The graph demonstrates that micrometer pore size structures have excessive sensitivity towards internal pressure increase which leads to massive increase of gaseous conductivity after long term permeation. Hence glass fiber core VIPs normally have lower service life compared to silica core VIPs. However, to maximize the effective service life, optimization of envelope material, improved getter material and most importantly reduction of pore size can be undertaken to reduce the effect of long term gas permeation. The relation between gaseous conductivity (K_g) and pore size (ϕ) is given as:

$$K_g = \frac{K_{go}}{1 + \frac{0.032}{P\phi}} \quad (3)$$

where, K_{go} is the thermal conductivity of air at room temperature and P is the internal pressure. This relation is critical as it enables us to determine pore size as well as deduce service life of VIPs by observing the corresponding effect of gaseous conductivity at different pressure levels [11].

3. Arrangement of fiber in core material and pore size

Fig. 2 shows the arrangement of fiber in core material. The fiber in centrifugal core material arranges in CD/MD direction and in the pore. In chopped, fiber arranges only in CD/MD direction. In composite core material, flame fiber arranges in the pore , and centrifugal fiber in the CD/MD direction.

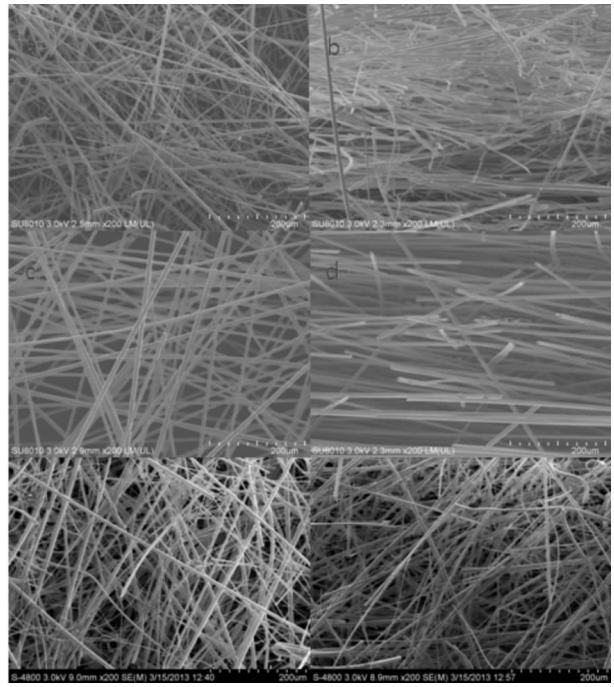

Fig. 2 arrangement of fiber in core material

a—Centrifugal fiber (front); b—Centrifugal fiber (section);
c—Chopped (front); d—Chopped (section);
e—composite fiber (front); f—composite fiber (section)

Tab. 1 Fiber physical state of different core material

Compositionof core	Thickness per layer	diameter /length	Pore size
centrifugal fiber	1.0mm	3.5μm/30mm	58μm
chopped	1.0mm	5.5μm/30mm	70μm
composite fiber	1.0mm	2.5μm/20mm	45μm

Tab. 1 shows the physical state of different core material with different pore size in VIP.

4. The K_{cop} and ALT

Tab. 2 shows the K_{cop} of VIP with different core material.

Tab. 2 K_{cop} of VIP with different core material(VIP size is 290mm ×290mm×12mm, measured by Netzsch HFM 436)

Composition of core material	Thickness per layer	Kcop(mW/(m·K))
centrifugal fiber	1.0mm	1.500
chopped	1.0mm	1.015
composite fiber	1.0mm	1.700

Fig. 3 shows different core material VIP ALT dates. K_{cop} of chopped VIP increased value is about 2 times than composite fiber VIP, 1.5 times than centrifugal fiber. The ALT test environment is 50℃ 80%RH.

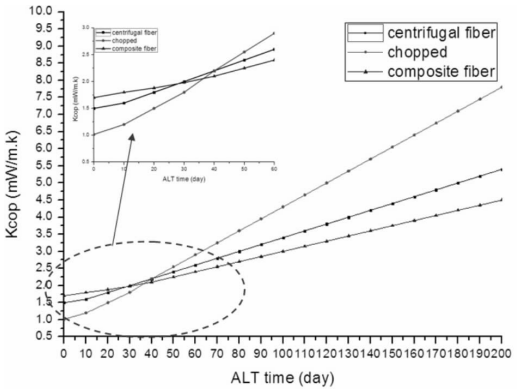

Fig. 3 ALT dates of different core material VIP

3. Conclusions

The K_{cop} of C-fiber core structure with fiber diameter (d) of 3～5μm, pore size (ϕ) 58μm was around 1.5～1.8mW/(m·K) in average at evacuated conditions. Similarly, K_{cop} of the Chopped strand sample (d = 5 — 6μm/ϕ = 70μm) was measured as 1～1.2mW/(m·K) in average, which is perhaps the lowest possible thermal conductivity measured from a VIP core sample till date. The Centrifugal－Flame mix fiber composite core material sample, which had the smallest pore size (ϕ = 45μm), provided intermediate level thermal conductivity of 1.8～2.2mW/(m·K) between the 3 samples. Utilizing real-time measurements of K_{cop} and corresponding dynamic internal pressure, effective gaseous thermal conductivity

K_{cop} of chopped VIP increased value is about 2 times than composite fiber VIP, 1.5 times than centrifugal fiber.

Acknowledgements

The authors would like to thank the financial support from Jiangsu Project BA2013097 and National Project 2015DFI53000.

References

[1] Alam, M., H. Singh, and M. Limbachiya, Vacuum insulation panels (VIPs) for building construction industry — a review of the contemporary developments and future directions. Applied energy, 2011. 88(11): p. 3592－3602.

[2] Simmler, H. and S. Brunner, Vacuum insulation panels for building application: Basic properties, aging mechanisms and service life. Energy and Buildings, 2005. 37(11): p. 1122－1131.

[3] Kwon, J. S., et al., Effective thermal conductivity of various filling materials for vacuum insulation panels. International Journal of Heat and Mass Transfer, 2009. 52(23): p. 5525－5532.

[4] Alam, M., et al., Experimental characterisation and evaluation of the thermo-physical properties of expanded perlite—Fumed silica composite for effective vacuum insulation panel (VIP) core. Energy and Buildings, 2014. 69: p. 442－450.

[5] Brunner, S., T. Stahl, and K. Ghazi Wakili, An example of deteriorated vacuum insulation panels in a building facade. Energy and Buildings, 2012. 54: p. 278－282

[6] Johansson, P., C.－E. Hagentoft, and A. Sasic Kalagasidis, Retrofitting of a listed brick and wood building using vacuum insulation panels on the exterior of the facade: Measurements and simulations. Energy and Buildings, 2014. 73: p. 92－104.

[7] Fricke, J., et al., Solid conductivity of loaded fibrous insulations. Discussion. ASTM special technical publication, 1990(1030): p. 66－78.

[8] Kim, J. and T. H. Song, Vacuum insulation properties of glass wool and opacified fumed silica under variable pressing load and vacuum level. International Journal of Heat and Mass Transfer, 2013. 64: p. 783－791.

[9] Di, X., et al., Optimization of glass fiber based core materials for vacuum insulation panels with laminated aluminum foils as envelopes. Vacuum, 2013. 97: p. 55－59.

[10] Di, X., et al., Thermal insulation property and service life of vacuum insulation panels with glass fiber chopped strand as core materials. Energy and Buildings, 2014.

[11] EMPA, et al., Study on VIP-components and Panels for Service Life Prediction of VIP in Building Applications (Subtask A). 2005.